SEMI-DEFINITE PROGRAMMING BASED CONVEX OPTIMAL POWER FLOW AND UNIT COMMITMENT METHODOLOGIES OF POWER SYSTEM WITH HIGH PENETRATION OF DISTRIBUTED ENERGY RESOURCES

by

Biswajit Dipan Biswas

A dissertation submitted to the faculty of
The University of North Carolina at Charlotte
in partial fulfillment of the requirements
for the degree of Doctor of Philosophy in
Electrical Engineering

Charlotte

2022

Approved by:

Dr. Sukumar Kamalasadan

Dr. Valentina Cecchi

Dr. Yogendra Kakad

Dr. Rajaram Janardhanam

ABSTRACT

BISWAJIT DIPAN BISWAS. Semi-Definite Programming Based Convex Optimal Power Flow and Unit Commitment Methodologies of Power System with High Penetration of Distributed Energy Resources. (Under the direction of DR. SUKUMAR KAMALASADAN)

The ever-increasing popularity of distributed generation resources and modernization of power system devices is making the power grid operations more complex. Furthermore, the non-convexity of the optimal power flow (OPF) challenges the solver to reach the global optimal solution and affects the overall accuracy of the solution. To overcome this problem, the convex relaxation methods are increasingly adopted to improve the computational efficiency of the solution and reach the global optimal point. New convex optimization methods for Optimal Power Flow and Unit Commitment applications are introduced in this research work. First, a multi-objective OPF formulation for transmission networks is proposed. The objective function includes total generation cost and voltage stability margin. The effect of the weighting factor of the objective functions on the solution has been observed. The formulation is then tested on IEEE 14 bus and IEEE 118 bus systems, and the results are analyzed. Second, a combined UC-OPF formulation is presented based on the mixed-integer semidefinite programming. The UC and OPF consist of separate operating constraints for power system operation. Thus combining the constraints can cover the entire range of power system operations constraints. Since UC is mixed-integer linear programming (MILP) problem and OPF is a convex optimization problem, thus combining the two becomes a MISDP problem. The algorithm is developed and tested using IEEE 14 bus, and IEEE 118 bus systems, and the results were validated. Also, a branch-and-bound (BnB) approach is formulated for the combined UC-OPF problem, and the solutions from the BnB approach are compared and validated with a two-staged MISDP approach. Third, an SDP relaxed OPF formulation is presented for multi-phase unbalanced distribution networks. The approach is based on the branch flow model of the network. The formulation includes detailed modeling of voltage regulators, mutual coupling of the branch impedance matrix, and network switches. The formulation is tested on IEEE 123 bus system and modified 650 bus system, a part of the IEEE 8500 bus network. The solutions were compared with the non-linear power flow solution using the same operating scenario. Due to the increase of power system equipment and distributed generation resources in the distribution network, along with the massive size of the network, the distributed approach to solve the OPF problem has become a significant field of research. An alternating direction method of multipliers(ADMM) based OPF formulation is discussed to solve a large-scale network. For this, the power grid is divided into multiple sub-networks based on geographical position or the location of the regulators then OPF sub-problems are solved for each of the sub-networks iteratively until the global convergence is achieved. The solution is compared with the centralized approach and validated. The algorithm is tested on IEEE 123 bus system and 2500 bus system. The accuracy of the solution in all the cases. It was found that all the methods are accurate, computationally efficient, and provide global optimal solutions.

DEDICATION

This thesis is dedicated to my wife Pushpita, for supporting me and taking care of the family and our child, Nirban, and my parents, whose blessings were with me all the way.

ACKNOWLEDGEMENTS

I would like to express my deepest and most humble gratitude to my advisor, Dr Kamalasadan. His guidance and training shaped who I am today. He is such a genuine mentor who always places his students first. Not just in academic support, his helping hands stretch even in any sort of financial or personal crisis that his students are facing. He showed us the way and give us enough freedom to explore the whole region. Although he always watches our back so that we don't lose our track. Even in the final days of deadlines, he sits with us so that the works can be completed and a refined and polished manuscript can be submitted. He manages his times so well that all his students can get equal attention.

Next, I would like to express my gratitude to other dissertation committee members. Dr Cecchi, Dr Kakad and Dr Rajaram for helping me in refining the dissertation. I'm really thankful to my friends and fellow researchers from our PEISL lab. Whenever I got stuck at any topic, they were always there to help me out. I found an extended family in them.

I enjoyed my time greatly here in ECE department, UNC Charlotte. The administrative officials were very supportive at any cause. It provides an amazing environment for researchers. Thanks to the Graduate School for the GASP which was a major financial support. Even during the pandemic lockdown due to Covid-19, the additional financial aid from the graduate school was noteworthy.

I would like to express my gratitude to my parents for their spiritual support throughout the journey. Staying far away from them was a challenge for all of us, but I carried their prayer and blessing all the time. Same a gratefulness for my parents-in-law, too for their never-ending blessing for my well-being.

Finally, this journey wouldn't have been possible if I didn't have my wife by my side. At a certain point, after our son was born, she halted her career so that we can all stay together as a family. She was a tremendous performer in her field of work and it such a challenging decision for her. Both me and our son will always respect what she sacrificed for the family. Thank you for tolerating me in my worst.

TABLE OF CONTENTS

LIST OF TABLES

LIST OF FIGURES

LIST OF ABBREVIATIONS

N_G Set of generation buses

V_i, δ_i Voltage magnitude and voltage angle of bus i

W,W^m $2n \times 2n$ positive semidefinite matrices

Y_i, Y_{ij} System admittance matrices

δ_{max} Maximum angle deviation

λ,λ^m Current and maximum loading points

ω_1, ω_2 Coefficients of cost and loading margin

$g\left(.\right), h\left(.\right)$ Equality and inequality constraints of OPF

i, j Bus index

$\mathcal{G}$ Graph of transmission system

$r_{g,t}$ Spinning reserve for generator at bus g at time period t; $g \in N_G$

E Set of edges (branches) in G

G_{ij},B_{ij} Conductance and susceptance of transmission line between buses i and j; $(i, j) \in N$

N_G Set of generator buses (nodes) in G

N Set of buses (nodes) in G

$P^G_{g,t}$,$Q^G_{g,t}$ Active and reactive power generation at generator bus g at time period t; $g \in N_G$, $t \in T$

P^{min}_g,P^{max}_g Upper and lower bound of active power generation at bus g; g $\in N_G$

P_n^D,Q_n^D Active and reactive power demand of bus n; $n \in N$

Q_g^{min},Q_g^{max} Upper and lower bound of reactive power generation at bus g; $g \in N_G$

R_t Spinning reserve for the system at time period t; $t \in T$

RU_g,RD_g Ramp up and ramp down limit for generator at bus g; $g \in N_G$

SU_g Startup cost for generator at bus g at time period t; $g \in N_G$

T Set of hourly time periods

t Time period index; $t \in T$

$u_{g,t}$ binary variable for generator status at bus g at time period t; $g \in N_G, t \in T$

UT_g,UD_g Minimum up and down time limit for generator at bus g; $g \in N_G$

V^{min},V^{max} Upper and lower bound of bus voltage magnitude

$v_{g,t}$ binary variable for generator startup command at bus g at time period t; g $\in N_G, t \in T$

V_n Voltage magnitude at bus n; $n \in N$

$w_{g,t}$ binary variable for generator shutdown command at bus g at time period t; g $\in N_G, t \in T$

Y_{ij} Admittance of transmission line between buses i an j; $(i, j) \in N$

CHAPTER 1: INTRODUCTION

The power system is one of the greatest outcomes of scientific advancement in the history of humankind. It is also one of the most complex networks, which comprises numerous generators, transmission lines, and distribution entities that operate relentlessly to deliver the electricity from the source to the consumers. In the conventional topology of the power grid, large-scale generators inject thousands of megawatts of power into the grid through a mesh architecture of high voltage transmission lines that carries the power over a long distance towards the low voltage distribution feeders and eventually to the end of line consumers. The distribution network was designed and operated originally so that the power flow was unidirectional with varying unbalanced loads in different phases.

But now, the power grid is on the edge of entering a new era of modernization due to the ever-increasing popularity of distributed generation resources and controllable loads. Even during the pandemic, due to the Covid-19 scenarios, the annual growth rate of global renewable energy capacity has jumped over 45% in 2020, which is considered to be an "unprecedented boom." This rise includes a 90% rise in world wind capacity followed by a 23% surge in solar power installation. This seems to be the largest annual rate of increase since 1999. The cost of electricity from renewable resources is already competitive with fossil fuels in many markets and is expected to be reduced further. Along with the renewable energy sources, the market of the automobile industry is also seeing a massive change. More than a million plug-in electric vehicles have been sold solely in the US market since 2015. A rise in sales of electric vehicles is shown in Fig. 1.1. This made major automobile manufacturers turn their heads and focus on moving on producing electric vehicles.

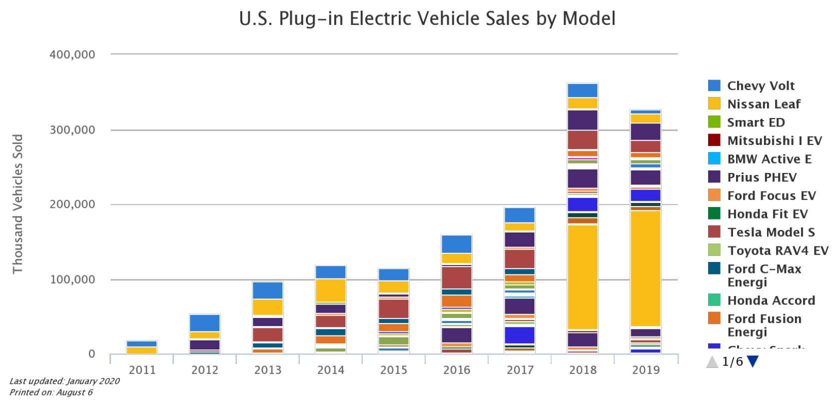

Figure 1.1: Sales of plug-in electric vehicles in the US market.*Source: https://www.anl.gov/esia/light-duty-electric-drive-vehicles-monthly-sales-update

1.1 Challenges Imposed by Distributed Energy Resources

But these renewable sources and energy storage systems as EVs, don't bring only good news. They have their drawbacks too. The most prominent of them is the lack of stability in a generation. Renewable sources are highly intermittent in nature and unpredictable. This characteristic poses a tough challenge in maintaining the balance between supply and demand. Fig 1.2 shows solar electricity generation profile and intermittency for a regular sunny day and an overcast day, respectively. Because of clouds, solar electricity generation can drop as much as 80% in a few minutes and return to an earlier stage once the cloud passes. As a result, the voltage and frequency of the network may experience a severe fluctuation when a large amount of power, whether generation or demand, goes off-line and, the next instant, comes online. According to the ANSI standard, the voltage of a distribution network must always stay within +/-5% of 1 p.u. (0.95 p.u. to 1.05 p.u.). The legacy devices such as voltage regulators and capacitor banks are used in the traditional distribution networks to maintain the bus voltages under the assumption that the voltage change will be slow and predictable along the distance. In such a conventional network, the bus voltage magnitude normally drops with distance from the root node. It is because of the line impedance. In converse, when a DER is connected somewhere in the distribution network, the power injected by the generator causes a spike in the voltage magnitude. If the rise is too high, the network may fail to maintain the standard bus voltage range. Moreover, suppose the generation is significantly higher than the demand. In that case, a reverse power flow will be experienced in the substation node, where the reverse current will flow to the transmission network and interrupt the normal operation of the controlling devices. This vulnerability introduces technical challenges in integrating distributed generation resources in the distribution networks. The challenges include voltage regulation, frequency regulation, grid stability, and power quality. The distribution network can no longer maintain a unidirectional power flow with increased penetration of distributed energy resources. This change in the classical design paradigm asks for new approaches to the operation and protection of the grid to manage the fast change in generation and demand and bi-directional power flow from numerous distributed energy resources.

1.2 Scope of Grid Optimization

From the beginning, the operation of a power distribution network is a very complex problem. Various power system operations run the network stable, such as power flow, economic dispatch, optimal power flow, demand response, unit commitment, and automatic generation control. The network operators perform all these operations to keep the system reliable. This thesis primarily emphasizes Optimal Power Flow (OPF) and Unit Commitment (UC) among these power system operations. Being introduced in the 1960s, the optimal power flow is an optimization problem that consists of control variables such as voltage magnitudes, capacitor bank status, and voltage regulator tap position, subject to physical laws of electrical circuit and network operational constraints. Conventionally, OPF was solved for only transmission networks since it includes multiple sources, not at the distribution level. The power flow was unidirectional, and the network behavior was predictable. But the necessity

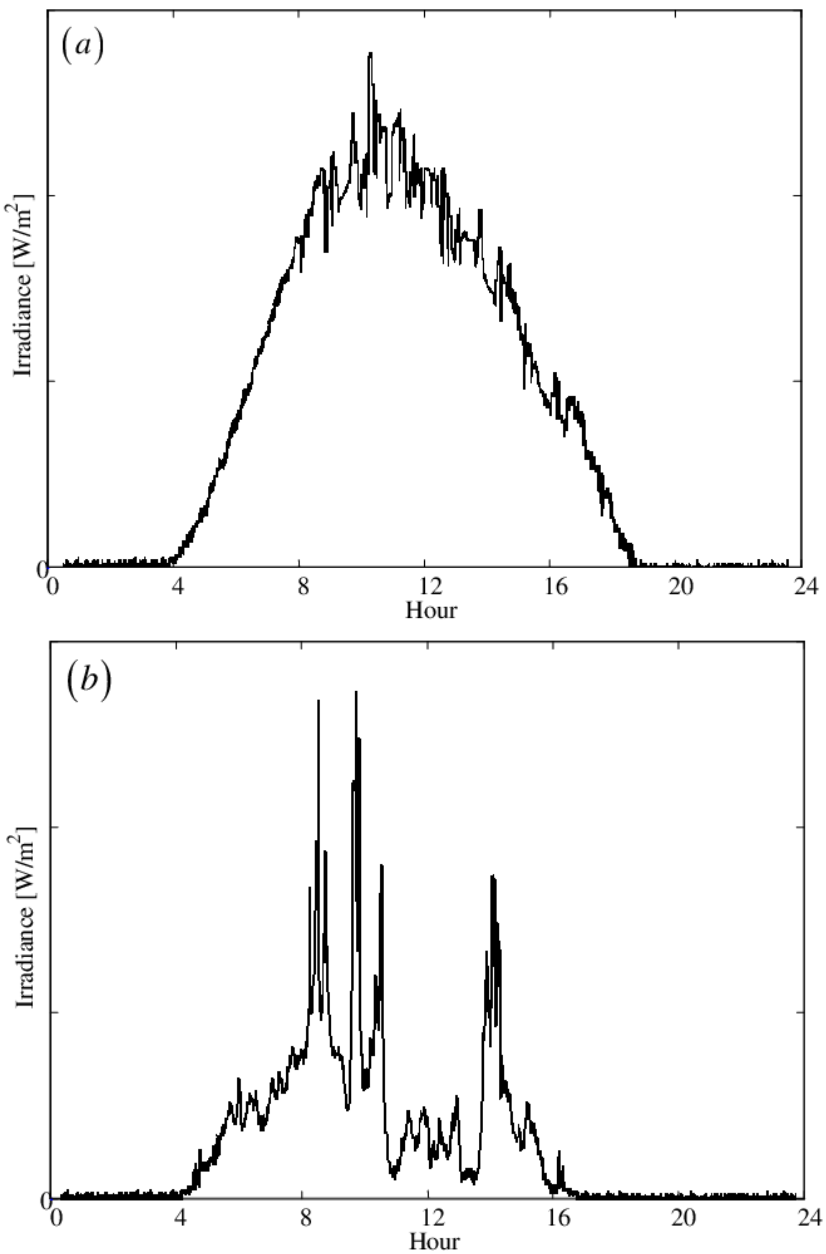

Figure 1.2: PV irradiance profiles on a typical (a) sunny day and (b) cloudy day. *Source: [1]

of solving OPF for distribution networks has become more and more prominent for the following reasons. Firstly, most of the network's losses occur in the distribution grid due to its highly resistive lines. And this loss can be optimized by carefully placing the DERs throughout the networks where they can feed the closely located loads and reducing the long travel of power. By improving the voltage profile of the network, the system loss can be minimized significantly. However, the bottleneck is that this task is beyond the capability of the conventional voltage regulators and shunt capacitors alone. For this problem, the DERs come with a possible solution too. Since the DERs are originally a source of active power, while interconnecting them with the grid, inverters act as the bridge. These inverters are also called smart inverters, where they can provide reactive power support based on the rating. With this reactive power support, the DER can significantly improve the voltage profile of the network. In chapter 3, while formulating the OPF problem for distribution networks with high penetration of DER, the reactive power output is considered the control variable to minimize the objective function value. Then, we also studied the additional benefits the network can achieve when we combined the reactive power support along with the integer control of legacy devices. This thesis aims to identify some key aspects to find the optimal solution to the OPF problem for distribution networks, which are missing in the current works, and improve on those by presenting extensive theoretical analysis and case studies. This also may provide the ground basis for future work.

1.3 Current Research Gaps, Proposed Research, and Main Contributions

Since its introduction, the formulation of various approaches for optimal power flow(OPF) has drawn much interest from power system researchers. There has been a new invention of features for distribution devices that requires further modifications in the OPF formulations. Based on an extensive literature study on existing works of optimal power flow solution methods, the gaps in the research area can be itemized as follows:

- Traditionally, SDP relaxed BIM models are used for transmission networks, and SOCP relaxed BFM models are applied for distribution networks. Knowing that [2] SDP relaxation methods can provide a more accurate solution, the prospect of utilizing the SDP framework for power distribution network optimization is worth exploring.

- In addition to the conventional objective of generation cost minimization, modern power distribution operation seeks solutions for other challenges such as effective voltage regulation, DER hosting maximization, optimal device placement, and cost minimization of the legacy device.

- Challenges associated with approximate modeling (less accurate) and/or accurate modeling (complexity) of the power grid and devices.

- Challenges associated with not having robust optimization solvers that can include mixed-integer variables with semidefinite relaxed problems.

- Major challenges associated with modeling Unit Commitment problem including power system matrices such as line losses and thermal limits.

- Challenges in developing a scalable and accurate model for unbalanced multiphase power distribution systems due to mathematical complexities even though this is the need of the hour.

- Exploring the distributed optimal power flow architecture to solve large and interconnected power grids and seeking solutions to overcome challenges related to timely convergence and optimality conditions.

Based on the limitations found in the existing methods stated above, this thesis finds a way to address those. Initially, in this thesis, we initially proposed SDP relaxed OPF formulations for distribution networks using BIM and BFM models. Then, the BFM-SDP OPF model incorporates the integer control for the legacy devices like voltage regulators and capacitor banks using the MISDP approach. After that, using the MISDP approach, we proposed formulations to combine UC and OPF problems. Then the single-phase BFM-SDP OPF models are extended to unbalanced multiphase networks along with the receding horizon control. Finally, we proposed a distributed and decentralized formulation to solve the OPF for large-scale partitioned networks. There are numerous scopes in the state-of-the-art formulations of distribution system OPF formulation. Chapter 2 will discuss the mathematical preliminaries related to the optimal power flow, such as different power system models, convex relaxation methods, semidefinite programming, and second-order programming. Then the rest of this thesis consists of three chapters. In this section, we will briefly discuss those chapters and portray the contributions of the thesis.

In chapter 3, an SDP relaxed optimal power flow problem for distribution networks is formulated based on bus injection and branch flow model. A bus injection model (BIM) for the distribution network to analyze different objective functions is proposed. The proposed method was studied in IEEE 33 and 123 bus networks. Later in that chapter, another model was proposed for distribution networks based on the branch flow model (BFM). This model presents a novel approach to linearizing the integer control of voltage regulators and a unified approach to the MISDP model. The main contributions can be summarized as follows:

- The alternative BIM-SDP model reduces the computational burden due to the large PSD matrix.
- The BFM-SDP OPF formulation is scalable for larger networks.
- The proposed unified MISDP model can be implemented on standard size distribution networks consisting of legacy devices.

Chapter 4 proposes an approach to solving the combined UC-OPF problem for power systems. We know that both unit commitment and optimal power flow are essential power system operations. However, each of them emphasizes a particular aspect of the grid while another one is not. That's why the combined approach considers all the grid operation aspects for optimal setpoints. Here a two-staged approach is proposed for the problem and compared with a unified method. Later, a branch and bound approach is presented and compared with the previous methods. The contributions from this chapter are:

- The combined UC-OPF formulation includes the active power loss of the network for power balance constraint in UC.
- Developed a combined UC-OPF model without leveraging the rounding of the binary variables as done in the unified formulation.
- The proposed model provides close to global solutions and is scalable for large networks.

Based on the BFM-SDP OPF model proposed in chapter 3 for the balanced single-phase networks, extended work on the formulation of OPF for unbalanced multiphase networks with high penetration of DER is presented in chapter 5. The proposed method is tested for standard IEEE networks such as the IEEE 123 bus system with three different levels of DER penetration and the 650 bus system, which is a part of the IEEE 8500 bus network. The contributions from this chapter's work are:

- The formulation of three-phase BFM-SDP OPF includes mutual coupling of line impedance matrices.
- The three-phase OPF formulation consists of detailed modeling of voltage regulators and switches.
- The three-phase BFM-SDP OPF formulation is scalable for larger networks.

A distributed approach is proposed in chapter 6 to solve optimal power flow for interconnected distribution systems in this chapter. In the case of a very large-scale grid, the centralized approach to solving OPF can be very computationally stressful for the solver. In such a scenario, the whole network can be partitioned into small sub-systems, and they can solve their local OPF problem and communicate the boundary variables to reach convergence. After that, a further extension of this work is presented as the decentralized approach, where the adjacent nodes communicate to achieve convergence and remove the necessity of the central coordinator. Finally, an analysis of the implementation in a real-time simulator is presented to validate the real-world applicability of this model. The main contributions of this work are:

- The distributed OPF formulation makes the partition of the distribution network based on the geographical position or location of voltage regulators.
- The distributed OPF formulation ensures convergence, and the underlying SDP-based OPF formulation guarantees the tightness of the solution.
- The decentralized distributed OPF method removes the necessity of a central coordinator, reducing the complexity of the communication network and the chances of cyber-attacks.

Finally, chapter 7 concludes the dissertation and the pathway for future work.

CHAPTER 2: LITERATURE REVIEW

2.1 Introduction

Optimal power flow is an optimization problem that works on finding an optimal operating point of a power system that minimizes a specific cost function such as generation cost, transmission loss, or stability margin subject to a set of constraints, such as power flow equations, line constraints, voltage constraints. Optimal power flow considers many applications in power systems such as economic dispatch, unit commitment, state estimation, stability and reliability assessment, and demand response. Since the first formulation of OPF in 1962, there has been a great amount of research in this field. [3] An elaborate survey can be found in [4, 5, 6, 7, 8, 9, 10, 11, 12, 13]. The power flow equations are naturally quadratic, meaning the OPF problem can be formulated as a quadratically constrained quadratic program(QCQP). This formulation is non-convex and also NP-hard. Various optimization algorithms and relaxations have been proposed to solve this problem. A widely used approach is linearizing the power flow equation known as DC-OPF. This approach is well explained in [14],[15], [16], [17]. More accurate approximations for linearizing the power flow equations are explored in [18]. Convex relaxation of quadratic programs has been applied to many mathematical problems. Compared to the DC approach of optimal power flow, convex relaxation offers various advantages. Such as, the solution of DC-OPF may not be feasible, so the solution may not satisfy the power flow equations. In that case, some constraints may have to be tightened, reducing the solution's efficiency. Then, after convergence, most nonlinear programs give local optimal solutions. On the other hand, convex optimization provides a globally optimal solution. In the recent research in this area, convex relaxation of a radial distribution system is first proposed [19] as a second-order cone program (SOCP) using a branch flow model. For mesh networks, a semidefinite program (SDP) was first proposed in [20] using the bus injection model. The elaborate formulation of SOCP OPF for the distribution systems [21] using the branch flow model is explained in [22], [23]. The exactness of the solution from this OPF formulation is first studied in [24]. Simplification of SDP relaxation using the graph theory and sparsity is proposed in [25], [26] and analyzed in [27], [28]. Since the first concept of OPF was introduced in 1962, various methodologies have been explored by the researchers, which have been summarized in [29]. Most OPF methodologies focus on minimizing the generation cost. At the same time, there are approaches where optimization emphasizes active power loss, variation in market price, voltage stability index, and reactive power flow. This chapter mainly summarizes various approaches done by the researchers to date in solving the OPF problem. Then based on their advantages and limitations, why convex optimization is more prospective than other methodologies is explained with the respective formulation.

2.2 Power Flow Models

A power system network can be represented as a set of nodes and connecting lines. Let us index the nodes with $i = 1,2,3,...,n$. Node 1 is considered as the reference node or slack bus. The voltage magnitude and angle of the reference node are known. Any network bus i may contain a load or generation or both. The net power injection in node i can be represented by a complex number denoted as s_i, which is equal to the difference between generation and load. The line between two nodes i and j is represented by the impedance of the line z_{ij}. The inverse line impedance will give us the line admittance y_{ij}. Two widely used models to analyze a power system: are the bus injection model and the branch flow model. In the bus injection model, the power system network is represented by an undirected graph G and a set of equations in terms of nodal variables. On the other hand, the branch flow model represents the power network by a directed graph $\bar{G}$ and another set of equations in the form of branch variables. The two models can be used to formulate and analyze power flow problems.

2.2.1 Bus Injection Model

Suppose the power system network is represented by a undirected graph $G = (N,\ E)$, where N = 1,2,3,...,n is set of nodes and $E \subseteq \mathrm{N} \times N$ is the set of lines connecting the nodes. Since this is a undirected graph, so the line $(i, j) \in E$ and $(j, i) \in E$ represents the same line and interchangeable. The admittance matrix Y of the network can be expressed as follows,

$$Y_{ij} = \begin{cases} \sum_{k\sim i} y_{ij}, & \text{if } i = j, \\ -y_{ij}, & \text{if } i \neq j \text{ and } i \sim j, \\ 0, & \text{otherwise.} \end{cases} \tag{2.1}$$

The dimension of Y is $N \times N$, and it is a symmetric matrix. Now, for a node $i \in N$, let V_i be the rectangular expression of the node voltage. Let I_i and S_i be the complex current and apparent power injections on node i from the rest of the network. Then the bus injection model can be expressed with the help of the following Kirchhoff equation, power definition, and power balance equations:

$$I = YV \tag{2.2}$$

$$S = V_i I_i^*$$

$$s_i = \sum_{j:i\tilde{j}} y_{ij}^H V_i (V_i^H - V_j^H)$$

The voltage of the slack bus and connected load in each bus are known for a power flow problem. A set of (V, I, S) is to be calculated, which satisfies the set of equations (2.2) mentioned before.

2.2.2 Branch Flow Model

In this model, the power system network is represented by a connected graph $\bar{G}$ = $(N,\ \bar{E})$. Here $N = 1, 2, 3, ..., n$ is set of nodes and $E \subseteq$ N $\times N$ is the set of lines connecting the nodes where if $(i, j) \in E$, then $(j, i) \notin E$ since this is a directed graph. In this model, the network topology can be represented by the connectivity matrix C_{il}, where

$$C_{ie} = \begin{cases} 1, & \text{if line } e \in E \text{ leaves node } i \in N, \\ -1, & \text{if line } e \in E \text{ enters node } i \in N, \\ 0, & \text{otherwise.} \end{cases} \tag{2.3}$$

Let's assume, $Z = diag(z_{ij}, (i, j) \in E)$ is the $m \times m$ diagonal matrix of impedance of line between nodes i and j. Now, for $i \in N$,V$_i$ is the complex voltage of bus i, $\bar{I_{ij}}$ is the complex current, and $\bar{S_{ij}}$ is the complex power in the sending end flowing through the line between nodes i and j. This branch flow model comprises of following equations in the terms of branch variables $(V, \bar{I_{ij}}, \bar{S_{ij}})$.

$$\begin{aligned} I &= Z^{-1}C^{t}V \\ S_{ij} &= V_i I_{ij}^{*} \\ s_j &= \sum(S_{ij} - z_{ij}|I_{ij}|^2) - \sum S_{jk} \end{aligned} \tag{2.4}$$

To solve a power flow problem using branch flow model, the voltage V_1 at slack bus is given and a set of $(V, \bar{I_{ij}}, \bar{S_{ij}})$ is to be calculated which satisfies (2.4). This model is self-sufficient and does not rely on nodal currents or powers.

2.3 Optimal Power Flow

The objective of optimal power flow is to dispatch the optimal operating point while considering the generation limit constraints for each generator, voltage constraints of buses, and line constraints. The generalized OPF problem can be formulated as [30].

$$Min \sum_{i} z_i \left(x, \lambda, \lambda^m, \Gamma_i\right) \tag{2.5}$$

$$s.t. \begin{cases} h(x, \gamma_i, \lambda_i) = 0 \\ h(x^m, \gamma_i^m, \lambda_i^m) = 0 \\ \underline{a}_i \leq g\left(x, \lambda, \gamma_i\right) \leq \overline{a}_i \\ \underline{a}_i^m \leq g\left(x^m, \lambda^m, \gamma_i^m\right) \leq \overline{a}_i^m \\ \underline{b}_i \leq f(\lambda, \lambda^m) \leq \overline{b}_i \end{cases}$$

The functions $h(.)$ and $g(.)$ represent the problem's equality and inequality constraints, which are bounded by the lower and upper limits of the dependent and independent variables. Here, $x \in N$ denotes the system's dependent variable, the node voltage magnitude. Vector $\gamma \in N_G$ represents the set of independent variables of the system, which is active and reactive power generation at the generator buses. The λ and λ^m stand for the parameter loading factor. Let us assume, in power network, represented by a graph $\bar{G} = (N,\, E)$, the set of generator buses $\Gamma \subseteq N$ and set of lines $\lambda \subseteq E$. Let (V, P_g, Q_g) denote the set of unknown vectors. We can write the classical OPF problem in terms of the V, P_g, and Q_g as follows

$$Min \sum_{i} f_i\left(P_{Gi}\right) \tag{2.6}$$

$$s.t.\begin{cases} P_{Gi} - P_{Di} = \sum Re[V_i(V_i - V_j)^* y_{ij}^*] \\ Q_{Gi} - Q_{Di} = \sum Im[V_i(V_i - V_j)^* y_{ij}^*] \\ P^{min} \leq P_{Gi} \leq P^{max} \\ Q^{min} \leq Q_{Gi} \leq Q^{max} \\ V^{min} \leq |V_i| \leq V^{max} \\ P_{lm}^2 + Q_{lm}^2 \leq |S_{lm}^{max}| \end{cases}$$

where $P^{min}, P^{max}, Q^{min}, Q^{max}, V^{min}, V^{max}, S_{lm}^{max}$ are the given set of parameters for minimum and maximum limit of active power generation, reactive power generation, bus voltage magnitude and line power flows. The objective function in (2.6) can be reformulated in convex form.

2.4 Different Methods for OPF

From the beginning to date, various methods have been utilized to solve the optimal power flow problem. In a high-level view, they can be categorized into two main classes. They are conventional approaches and state-of-the-earth artificial intelligence approaches. In 2.1 and 2.2the popular methodologies, the advantages and limitations of conventional and artificial intelligence approaches are summarized [31].

Table 2.1: Conventional methods to solve OPF

Method	Pioneer	Description	Limitation	Ref.
Gradient Method	Dommel HW	With the help of the penalty function, a nonlinear programming method was developed to optimize generation cost and active power loss.	Largest network that can be solved has 500 buses. Unable to include transformer tap.	[32]
	C.M.Shen et al.	Based on the Lagrange-Kuhn-Tucker condition, proposed an indirect approach to solve.	Includes transformer tap but solves Economic Dispatch	[33]
	O. Alasc et al.	Caarid on the Dommel-Tinney method by integrating outage constraints for a steady-state solution. It	Not applicable for larger systems, and choosing the appropriate gradient size can ensure the solution.	[34]

Newton Method	A.M.H. Rashed	This method utilizes Lagrangian Multipliers and Newton's Method. This method has less oscillation around the solution with the help of the acceleration method.	Largest system this method can solve is the 179 bus system.	[35]
	H.H. Happ	This approach solves the OPF problem with the help of the Jacobian matrix. This method is preferable for online operations.	This method can solve OPF for a power system of most 118 buses.	[36]
Linear Programming	W. Wells	With the simplex method, he designed an economic scheduling method for cost minimization.	The disadvantage of this method is that it cannot be solved in infeasible situations.	[37]

	R.Mota Palomino et al.	This method is formulated using a non-conventional LP approach using a piecewise differentiable penalty function.	This approach is used mostly for contingency-constrained economic dispatch.	[38]
	E. Lobato et al.	This method utilizes a mixed-integer LP approach to optimize transmission line losses and generator reactive power margin.	This methodology is mostly tested on the Spanish power system only.	[39]
Quadratic Programming	G.F.Reid et al.	This method solves OPF in quadratic programming by utilizing Wolde's algorithm.	This method is validated in 5, 14, 30, 57, and 110 bus systems. Not scalable to larger systems.	[40]

	T.C. Giras et al.	This methodology is formulated based on the Quasi-Newton technique and the Han-Powell algorithm. The convergence solution is fast on smaller systems.	Cannot be applicable for larger real-life power systems.	[41]
	A. Berizzi et al.	This approach formulated enhanced security-constrained OPF with FACTS devices and incorporated the Han Powel algorithm. This method solves a nonlinear problem by using the result of successive quadratic problems containing linear constraints.	This approach is applied to the Italian EHV network and 63 bus system.	[42]

Interior Point Method	Momoh, J.A. et al.	This method formulated an extended quadratic interior point method using enhanced initial conditions to solve OPF. The largest system this method verified is the 118 bus system.	This method cannot incorporate contingency constraints.	[43]
	D. Xi-Oying et al.	This paper formulated the interior point branch and cut method using a strict polynomial time algorithm. In this approach, they solved OPF as a mixed integer nonlinear problem.	The largest system it can solve is the 57 bus system.	[44]

	Wei Yan et al.	formulated a novel approach by utilizing the predictor-corrector original dual interior point method. This approach requires less computation time to solve OPF.	This approach cannot be applicable in practical larger systems.	[45]

Table 2.2: Artificial Intelligence methods to solve OPF

Method	Pioneer	Description	Limitation	Ref.
Genetic Algorithm	A. Bakritzs et al.	In this paper proposed two genetic algorithms to solve the economic dispatch problem. This method applies to dynamic programming.	The computation time increases with the increase of generator number in the system	[46]

	M. Usman Aslam et al.	Proposed a method to solve OPF by using a genetic algorithm with optimum non-uniform mutation rate and behavior.	This method is validated in 30 bus systems, not scalable to larger systems.	[47]
Particle Swarm Optimization	Hirotaka Yoshida et al.	This paper formulated a particle swarm optimization to optimize reactive power and voltage var control.	The computation time for a practical larger system is high. Reducing the burden requires parallel computation.	[48]
	L.L. Lai et al.	This paper proposed a method to solve OPF using PSO incorporated with a non-smooth input-output characteristic function.	Largest system this method can solve is IEEE 30 bus system.	[49]

	Bo Yang et al.	Proposed a better PSO with a hiding practicability strategy and neighbor selection procedure to solve OPF. This approach ensures a faster and more accurate solution.	This method can solve OPF for a power system of most 30 buses.	[50]
	Pablo E. Onate and Juan M. Ramirez	In this paper, a novel approach is proposed to solve OPF with security constraints using PSO with reconstruction operators.	This approach can solve most IEEE 39 bus systems.	[51]
	Gonggui Chen et al.	Proposed a newer optimal power flow to minimize reactive power based on a new PSO local random search algorithm.	This method is tested on IEEE 30 bus system and has limitations for larger systems.	[52]

	H C Leung et al.	In this paper, a methodology is formulated to solve OPF with FACTS devices to minimize total cost. In this approach, PSO is incorporated with AC power flow.	This methodology is tested on smaller IEEE 14 bus systems.	[53]

2.5 Convex Relaxations

In the previous section, various methodologies are summarized for solving OPF. Conventional approaches like linear programming or quadratic programming, most of the time, fail to provide the global optimal solutions. On the other hand, state-of-the-earth approaches like genetic algorithms or particle swarm optimization require higher computational power, which is not feasible for real-life larger power systems with thousands of nodes and generators. In that context, convex optimization provides global optimal value for exact relaxations, and this approach can be implemented for practical larger power systems. Moreover, relaxations also help to ensure the feasibility of a problem. If the relaxed problem is infeasible, the original non-convex problem is also infeasible. If the relaxation is exact, the solution to the relaxed convex problem will give the globally optimal value equal to the original non-convex problem. The classification of convex relaxation is illustrated in2.1 [54]. The advantages and disadvantages of different methods of convex relaxations are summarized in 2.3. Among these types of relaxations, semidefinite relaxation for the bus injection model and SOCP relaxation for the branch flow model is explained in the next two sub-sections.

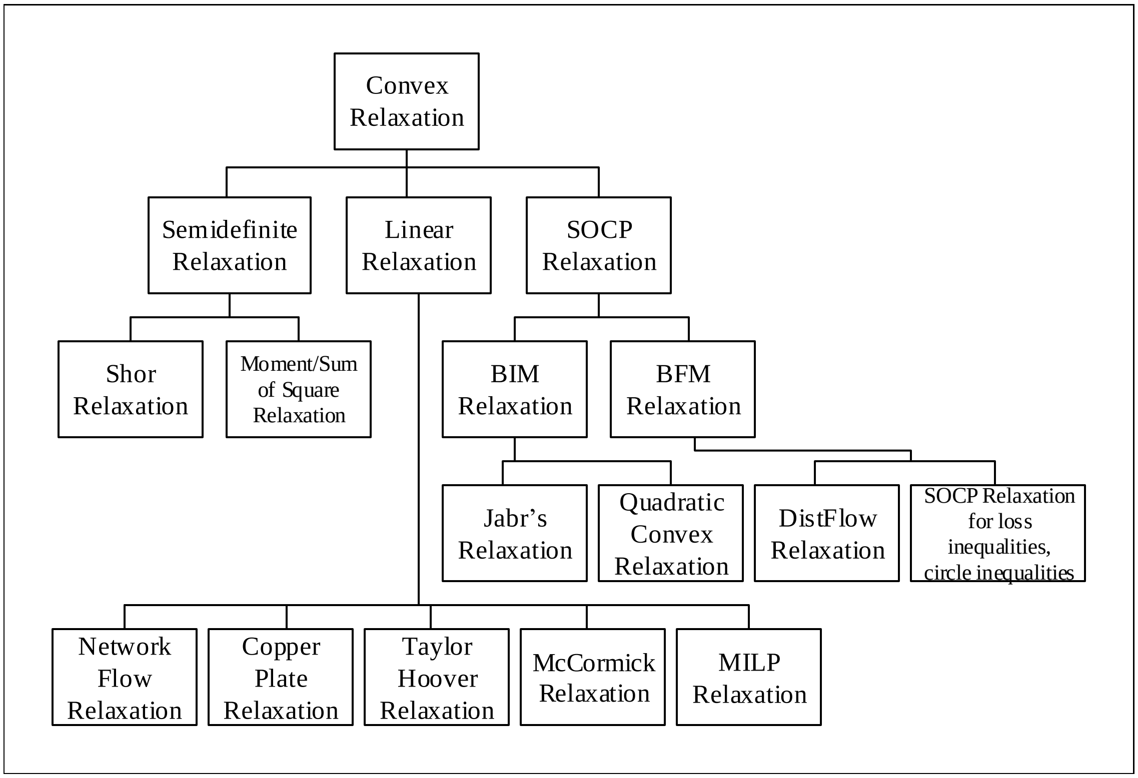

Figure 2.1: Classification of different convex relaxation of OPF problem.

2.5.1 Semi-definite Programming

In this section, the mathematical basis of semidefinite programming will be discussed. Then it will be explored how this can be implemented in power system optimization. Let us consider simple linear programming (LP) example,

$$\text{minimize } c.x$$

$$\text{subject to, } A.x = b$$

$$x \geq 0$$

Here, x is the control variable, and c and A are the parameter matrices. All the equations in objective function and constraints are linear or piecewise linear. Thus, the whole problem is convex. Semidefinite programming is a generalization of linear programming where the inequality constraints are represented by general inequalities which correspond to the cone of positive semidefinite matrices [55, 56]. This is a pure primal form of a semidefinite programming-based optimization problem,

$$\text{Minimize} \quad trace(CX)$$

$$\text{Subject to,} \quad trace(A_i X) = b_i, \;\; for \; i = 1, ..n$$

$$X \succcurlyeq 0$$

Here, $X \in S^n$ is the decision variable; it is also a positive semidefinite matrix. Others, b, C, and A, are symmetric matrices whose values are already known to the model. The feasible set defined by the set of constraints is always convex. The objective function is linear by nature. Thus the whole problem is linear and convex.

There are two main approaches for semidefinite relaxation of the OPF problem. Between them, Shor's relaxation will be explained here. This approach was first introduced [24]. It is evident from the formulation of optimal power flow 2.6 from the rectangular complex voltage phasor representation of power flow equations that it contains quadratic constraints. This makes the OPF problem a non-convex and non-linear problem. In power system analysis, transmission systems are usually modeled using the bus injection method. Due to the less computational burden because of sparsity property, semidefinite relaxation fits best in a mesh network of the transmission system. This method introduces a positive semidefinite matrix W to replace VV^*. After this, all the constraints can be written in the form of linear constraints with respect to W. Let us assume, $e_1, e_2, e_3, ..., e_n$ are the basis vectors, then we can re-write the equations of classical optimal power flow as follows:

$$Min \sum_i f_i\left(P_{Gi}\right) \tag{2.7}$$

$$s.t. \begin{cases} P_i^{min} \leq Tr\{Y_i W\} + \lambda P_{D_i} \leq P_i^{max} \\ Q_i^{min} \leq Tr\{\bar{Y}_i W\} + \lambda Q_{D_i} \leq Q_i^{max} \\ \left(V_i^{min}\right)^2 \leq Tr\{J_i W\} \leq \left(V_i^{max}\right)^2 \\ Tr\{Y_{ij} W\} \leq P_{ij}^{max} \\ Tr\{J_{ij} W\} \leq \triangle\left(V_{ij}\right)^2 \\ W = VV^T \\ W \succcurlyeq 0 \\ rank(W) = 1 \end{cases}$$

In this formulation, the rank-1 constraint is the only non-convex constraint. This constraint is relaxed in the formulation of the SDP relaxed OPF problem. If the solution of this relaxed OPF problem gives a rank-1 W matrix, then the relaxation is considered exact. The exactness of this formulation is an essential criterion because this ensures that the solution for the relaxed SDP-OPF problem will be a solution to the original non-convex OPF problem. Here the relaxation is implemented on real-valued matrices, while a complex-valued Shor relaxation can be formulated using Hermitian matrices [57]. The scope of work to utilize Shor's relaxation for OPF in the transmission system is given below:

- Exploiting the advantages of Shor's relaxation, mixed integer constraints can be introduced in semidefinite programming, and the OPF problem can be solved as a Mixed Integer Semidefinite Program (MISDP).

- Though with the increase in the number of buses in a network n, the number of variables in the PSD constrained matrix increases with a ratio of n^2, by utilizing the chordal sparsity of the network and formulating necessary conditions, this approach can solve the OPF for a network containing thousands of buses [58], [59].

2.5.2 Second Order Cone Programming

The second order cone programming (SOCP) is a branch of convex optimization which has the general form as

$$\begin{aligned}
&\text{Minimize } f(x)\\
&\text{Subject to,}\\
&||A_i x + b_i||_2 \leq c_i x + d_i\\
&Fx = g
\end{aligned}$$

The SOCP relaxation takes place where the nonlinear equation is written in a cone equation in the form of a 2-norm. Then the equality relation between both sides is relaxed to an inequality. A second-order cone is convex by characteristic. In power system analysis, the nonlinear power equation $|VI^*|^2 = SS^*$ can be re-written as a 2-norm, and the optimal power flow problem can be convexified using the SOCP relaxation method. The SOCP formulation introduced convex relaxation of power system optimization before the semidefinite relaxation. Jabr's Relaxation [19] was formulated for the radial network based on the bus injection model. Considering a few assumptions, Jabr's relaxation and Shor's relaxation represent the same relaxed OPF problem for the bus injection model of a network. Applying semidefinite relaxation on a bus injection model has some limitations [60]. Unlike BIM, the branch flow model uses branch variables like line current and line power flow. Here, relaxation of the DistFlow equation [22] approach will focus on the branch flow model of a radial system. Two relaxation stages are applied to convexify the OPF problem in the branch flow model. In the first step, the angle in the variables is relaxed. In the branch flow model, the DistFlow equations are formulated to neglect the voltage angles.

$$Min \ \sum_i f_i\left(P_j\right) \tag{2.8}$$

$$s.t. \begin{cases} P_j = \sum P_{jk} - \sum(P_{ij} - R_{ij}|I_{ij}|^2) + G_j|V_j^2| \\ Q_j = \sum Q_{jk} - \sum(Q_{ij} - X_{ij}|I_{ij}|^2) + B_j|V_j^2| \\ |V_j|^2 = |V_i|^2 - 2(R_{ij}P_{ij} + X_{ij}Q_{ij}) + (R_{ij}^2 + X_{ij}^2)|I_{ij}|^2 \\ |V_i|^2|I_{ij}|^2 = P_{ij}^2 + Q_{ij}^2 \\ P^{min} \leq P_i \leq P^{max} \\ Q^{min} \leq Q_i \leq Q^{max} \\ V^{min} \leq |V_i| \leq V^{max} \end{cases}$$

We can see from the formulation that the equality constraints contain quadratic terms of node voltage and branch current flow. By replacing $|V_i|^2$ and $|I_{ij}|^2$ with v_i and λ_{ij} respectively we can remove the non-linearity. In the second step of relaxation, we write the equation among voltage, line current, and power flow as an inequality constraint. That's how angle and convex relaxation are obtained in second-order conic relaxation.

Finally, the SOCP-OPF takes the form as in2.9.

$$Min \ \sum_{i} f_i \left(P^G\right) \tag{2.9}$$

$$s.t. \begin{cases} P_j^G = \sum P_{jk} - \sum(P_{ij} - R_{ij}\lambda_{ij}) + G_j v_j \\ Q_j^G = \sum Q_{jk} - \sum(Q_{ij} - X_{ij}\lambda_{ij}) + B_j v_j \\ v_j = v_i - 2(R_{ij}P_{ij} + X_{ij}Q_{ij}) + (R_{ij}^2 + X_{ij}^2)\lambda_{ij} \\ v_i + \lambda_{ij} \geq ||2P_{ij}, 2Q_{ij}, \lambda_{ij} - v_i||_2 \\ P^{min} \leq P_i \leq P^{max} \\ Q^{min} \leq Q_i \leq Q^{max} \\ (V^{min})^2 \leq v_i \leq (V^{max})^2 \end{cases}$$

There are a few scopes worth exploring in branch flow relaxation of the SOCP method, which are as follows:

- To extend the work on solving the OPF problem from a smaller single phase to a really large three-phase power network, branch flow SOCP relaxation has more advantages than other approaches, [61]

- In the DistFlow equation of the power system, the voltage angles are neglected. However, exploiting the scope from Jabr's relaxation and QC relaxation, the voltage angles can be included in the problem formulation, which will tighten the relaxation and ensure the minimum gap in the relaxed solution.

- Branch flow relaxation has superior convergence characteristics to the bus injection model [62]. While combining relaxation methods, analyze the conditions to ensure exactness.

Table 2.3: Advantages and Disadvantages of Different Convex Relaxations

	Method	Advantage	Disadvantage	Ref.
Semidefinite Relaxation	Shor's Relaxation	Exact for most common power systems. Ensures global optimal solution Can be extended to three-phase network	Not exact for few power systems. Exactness is not guaranteed for power system optimization other than OPF.	[24]
	Moment Relaxation	Generalizes Shor's relaxation to ensure exactness in cases where it fails.	Computational burden increases with the rise of system size and relaxation order.	[63], [64]
SOCP Relaxation	Jabr's Relaxation	Exact representation of the radial network.	It does not ensure recovering a set of voltage angles that sum to zero or mod of 2π radian for cycles.	[65]
	QC Relaxation	Augments Jabr's relaxation with voltage magnitude and angles variables. Implicitly relax the angle consistency for a cycle, thus applicable for the mesh network. It	Particularly effective when applied to problems with small ranges for voltage magnitude and angle difference between buses.	[66]

	DistFlow Equation Relaxation	Neglect voltage angle, so the exact representation of the radial system. Branch flow relaxation has numerical convergence superiority over bus injection relaxation.	relaxation for the mesh network.	[61]
	Δ inequality, loss inequality, circle inequality relaxation		No known comparison of tightness and computational characteristics relative to other relaxations.	[67], [68]
Linear Relaxation	Network Flow Relaxation	Applicable for systems lined with series impedance with non-negative resistance and reactance.	Systems with three winding transformers may result in negative resistance and reactance.	[69]
	Copper Plate Relaxation	is simpler than the network flow relaxation method.	Neglects power flow equations entirely to form a simple power balance constraint.	[69]

2.6 Summary

Convex relaxation for optimal power flow problem shows an impressive performance in finding the global optimal solution. The scope of work by leveraging semidefinite relaxation (Shor's relaxation) to study bus injection models and SOCP relaxation (Jabr's and DistFlow method) for branch flow model has been discussed. Exploiting the tightness of SDP relaxation in branch flow models, the size of the PSD matrices will be minimized, and thus the computational stress on the solver. Then by adding the mixed integer constraints, the formulation will add a new dimension to the unit commitment problem. On another note, by combining SDP relaxations and the BFM model, the regulator modeling and mutual coupling can be included in the OPF formulation for an unbalanced network, and the scalability can be validated.

CHAPTER 3: SEMIDEFINITE PROGRAMMING FORMULATIONS OF DER INTEGRATED OPF FOR POWER DISTRIBUTION SYSTEMS

3.1 Introduction

In this chapter, an SDP relaxed optimal power flow problem for distribution networks is proposed. A bus injection model (BIM) for the distribution network to analyze different objective functions is presented. The proposed method was studied in IEEE 33 and 123 bus networks. Later in that chapter, another model was proposed for the distribution network based on the branch flow model (BFM). In this model, we proposed a novel approach to linearizing the integer control of voltage regulator and a unified approach to the MISDP model. The main contributions can be summarized as follows:

- The alternative BIM-SDP model reduces the computational burden due to the large PSD matrix.
- The BFM-SDP OPF formulation is scalable for larger networks.
- The proposed unified MISDP model can be implemented on standard size distribution networks consisting of legacy devices.

3.2 Background and Literature Review

In past decades, a significant amount of research has been done on devising formulations to solve the OPF problem for large and realistic networks. One of the most popular trends is to formulate the ACOPF problem in the form of a convex optimization problem. Two major branches of convex OPF formulation are semidefinite programming (SDP) relaxation, which is first proposed in[70], and second-order cone programming (SOCP) relaxation for radial networks, which is first proposed in [65]. The numerical illustration of these convex formulations is discussed in [70, 65] and the exactness of the relaxed model to the original problem is showcased in [71]. The SDP relaxation for OPF formulation has been one of the most active fields due to some advantages of this formulation. It has been proven that if the relaxation is exact, SDP can provide a globally optimal solution [72]. This has been one of the strongest features of SDP relaxation. However, the exact relaxation occurs for some specific cases such as radial networks, under load over satisfaction, and absence of generation lower bounds. But the mathematical advantage of SDP relaxation is that the derivation of Jacobian and Hessian matrices can be avoided for each particular problem. Further simplification of SDP relaxation is made possible by utilizing the sparsity property of the matrices [70, 59, 73, 74].

Initially, OPF has been mostly solved for the transmission networks. However, with the increasing penetration of distributed generations in distribution networks, the necessity of OPF formulation for distribution networks is increasing rapidly. Since most distribution networks are radial, the SDP relaxation can guarantee an exact formulation and thus a globally optimal solution. A branch flow-based model can also be a faster and more popular choice for solving OPF in distribution networks. However, the advantage of the bus injection base model is that the rectangular representation of bus voltages is considered here, conserving the angle information. In BFM models, the angles of the bus voltage and line currents are relaxed. Thus, BIM-SDP can provide a more accurate solution preserving both voltage magnitude and angle. But the conventional BIM-SDP OPF formulation possesses some drawbacks. The dimension of the positive semidefinite (PSD) matrix in conventional BIM-SDP OPF is either n^2 or $2n^2$ depending on the bus voltage representation, where n is the number of buses, and to write each of the constraints, the whole PSD matrix needs to be used. Thus it poses a very high computational burden on the solver.

Later in this chapter, we proposed another formulation of SDP-OPF based on the branch flow model (BFM) for radial networks, including the integer control of various legacy devices. Conventionally, distribution networks include various discrete controllable devices such as load tap changers(LTC) and capacitor banks. These devices only accept integer states such as in LTC; the tap position can vary from {-16, -15,.. to ..+15, +16} or binary states such as capacitor banks where the switches can only be either closed{1} or open {0}. These devices have primarily been used to maintain the system bus voltages between a specific bound. Since the distributed energy resource (DER) penetration keeps increasing daily in a distribution network, the voltage regulation problem has become very complex. Due to the continuous intermittency in the PV profile or load profile, the discrete devices must be operated frequently to maintain the voltage regulated. This process reduces the lifespan of these discrete devices significantly. As a solution, these continuous conventional energy resources and discrete devices need to be operated in coordination.

The conventional OPF problem is a nonlinear, non-convex problem due to the relation of the continuous variables. In addition, control of the discrete devices such as LTC and capacitor bank is a mixed integer problem(MIP). The combined formulation thus takes the form of a mix integer nonlinear problem (MINLP), which is highly complex, computationally heavy, and NP-hard. This means that with the increase of discrete variables, the complexity of the model increases exponentially. That's why, unless some conditions are satisfied, and this problem is not tractable. In [75], for a large network, the MINLP model of the OPF with numerous discrete controls has been solved, but the solution is not guaranteed to be the global optimal, and also the optimality gap is not ensured. Thus, recovering the global optimal solution for the original mixed integer nonlinear opf problem is considered to be a prominent challenge. In previous works, researchers have proposed numerous approaches to handle this problem. One of them is to use penalty function A part of the objective function.

In [76], a penalty function has been used along with the rounding operation of the integer variables to find the solution. In [77], the authors utilized the sensitivity of the objective function to the inequality constraints to solve the problem. Penalty functions are also used tesoler2013penalty to model the discrete variables efficiently, making the model continuous and differentiable. Although, the drawback of using the penalty function is that the solver reaches a sub-optimal solution in most cases. In [78] a hybrid, the method has been proposed where the primal-dual interior point method combines with meta-heuristics to speed up the convergence. Although this approach suffers from the issue of scalability.

The other way to avoid the complexity of the original mixed integer nonlinear problem is to convert the formulation into a linearized or a convex relaxed model. In the linear approximation approach, the power flow equations are converted into linear constraints with few approximations as they are formulated in DC-OPF. Then the combined problem takes the form of a mixed integer linear problem(MILP). The other approach to handling non-linearity is to implement convex relaxation approaches. The advantage of convex relaxed models is that it ensures the global exactness of the modeling with the help of various robust approaches for convex relaxation. There are a few methods for convexifying the original non-convex problem, such as semidefinite programming(SDP) [79, 80], second-order cone programming(SOCP) [81, 81], chordal relaxation, [82]. In semidefinite programming, the nonlinear constraints are relaxed by expressing in terms of a positive semidefinite matrix and relaxing the rank-1 constraint for that matrix. On the other hand, in second-order cone programming, the nonlinear constraint is re-written in terms of a second-order cone and written in the form of an inequality constraint instead of an equality constraint. Then, in the chordal relaxation method, the whole network is expressed in terms of cliques and chords, even with imaginary branches if necessary. Then, semidefinite relaxations can be followed for each clique to model the OPF problem. These different convex relaxation methods have advantages and disadvantages of their own. Such as, the solution of the semidefinite relaxation model is tighter than the second order cone models, although the SDP models put more computational stress on the solver than the SOCP models [83]. On the other hand, it is proven in [84] that, under certain circumstances, both SDP and SOCP relaxed models can recover the global optimal solution of the original model.

In this chapter, an approach is proposed that reduces the computational burden of the BIM-SDP OPF. The major advantage of the proposed approach is that it provides:

- An exact relaxation of original OPF problem for BIM model of radial distribution network using semidefinite programming.
- Quadratic cost function while formulating convex SDP relaxed OPF problem.
- Less computational burden on the solver while guaranteeing a globally optimal solution.
- A scalable OPF formulation of branch flow model using semidefinite relaxation method.
- Includes linearized integer control for the grid legacy devices such as voltage regulators and capacitor banks.

3.3 Problem Formulation

3.3.1 Conventional BIM-SDP Formulation

Let Y_i denote the system admittance matrix, where each entries comprised of two elements, $Y_{ij} = G_{ij} + iB_{ij}$ for each line $(i, j) \in E$ and G_{ij} and B_{ij} are line conductance and susceptance respectively. Now, let e^i stands for the ith standard basis vector in $\mathbb{R}^n$. Now, introducing another matrix $Y = e_i e_i^T \mathbf{Y}$, where T denotes the transpose of the matrix. Now, the matrices required for the power injection constraint can be written as follows:

$$\mathbf{Y}_i = \frac{1}{2}\begin{bmatrix} Re\left(Y_i + Y_i^T\right) & Im\left(Y_i^T - Y_i\right) \\ Im\left(Y_i - Y_i^T\right) & Re\left(Y_i + Y_i^T\right) \end{bmatrix}$$

$$\bar{\mathbf{Y}}_n = -\frac{1}{2}\begin{bmatrix} Im\left(Y_i + Y_i^T\right) & Re\left(Y_i^T - Y_i\right) \\ Re\left(Y_i - Y_i^T\right) & Im\left(Y_i + Y_i^T\right) \end{bmatrix}$$

$$\mathbf{J}_i = \frac{1}{2}\begin{bmatrix} e_i e_i^T & 0 \\ 0 & e_i e_i^T \end{bmatrix}$$

Lets define a vector $V = [V_{1d}, V_{2d}, ..., V_{n,d}, V_{1q}, V_{2q}, ..., V_{n,q}]$ that contains the real and imaginary values of bus voltages. Then a PSD matrix W can be introduced as $\mathbf{W} = VV^T$. With these newly introduced matrices and variable the active and reactive power injections at any bus i will be given by $\mathbf{tr}(\mathbf{Y}_i\mathbf{W})$ and $\mathbf{tr}(\bar{\mathbf{Y}}_i\mathbf{W})$ respectively and the square of the voltage magnitude of bus i will be given by $\mathbf{tr}(\mathbf{J}_i\mathbf{W})$. Here **tr** stands for the *trace*. Then the OPF problem becomes

$$\begin{aligned} Min \;\; \omega_1 \sum_{i \in N_G} &\{C_{i_2}\left(Tr\{Y_i W\} + P_{D_i}\right)^2 \\ &+ C_{i_1}\left(Tr\{Y_i W\} + P_{D_i}\right) + C_{i_0}\} \end{aligned} \tag{3.1}$$

$$s.t. \begin{cases} P_i^{min} \leq Tr\{Y_i W\} + P_{D_i} \leq P_i^{max} \\ Q_i^{min} \leq Tr\{\bar{Y}_i W\} + Q_{D_i} \leq Q_i^{max} \\ (V_i^{min})^2 \leq Tr\{J_i W\} \leq (V_i^{max})^2 \\ Tr\{Y_{ij} W\} \leq P_{ij}^{max} \\ Tr\{J_{ij} W\} \leq \triangle (V_{ij})^2 \\ tan\,(\delta_{max}) \times Tr\{K_{ij} W\} - Tr\{L_{ij} W\} \geq 0 \\ W = VV^T \\ W \succcurlyeq 0 \end{cases}$$

Here $\succcurlyeq 0$ indicates the positive semidefiniteness of the corresponding matrix W. In semidefinite relaxation, another assumption is made. The solution to the problem (10) will be tight and accurate if the rank of the positive semidefinite matrix W is 1. But the rank-1 constraint is non-convex. Thus, this constraint is relaxed to form a convex problem.

3.3.2 Proposed BIM-SDP Formulation

Let the complex voltage phasor of bus i be written in following form $V_i = e_i + if_(i)$ where, $e_i = |V_i|cos\theta_i$, $f_i = |V_i|sin\theta_i$ and $|V_i|^2 = e_i^2 + f_i^2$. Here, θ is the voltage angle of bus i. With this representation, the rectangular formulation of the original OPF problem can be written as follows:

$$Min \sum_i f_i\left(P_{Gi}\right) \tag{3.2}$$

$$s.t. \begin{cases} P_{Gi} - P_{Di} = G_{ii}(e_i^2 + f_i^2) + \sum[G_{ij}(e_ie_j + f_if_j) - \\ B_{ij}(e_if_j - e_jf_i)] \\ Q_{Gi} - Q_{Di} = -B_{ii}(e_i^2 + f_i^2) + \sum[-B_{ij}(e_ie_j + f_if_j) - \\ G_{ij}(e_if_j - e_jf_i)] \\ P^{min} \leq P_{Gi} \leq P^{max} \\ Q^{min} \leq Q_{Gi} \leq Q^{max} \\ V_{min}^2 \leq e_i^2 + f_i^2 \leq V_{max}^2 \\ P_{ij}^2 + Q_{ij}^2 \leq |S_{ij}^{max}| \end{cases}$$

Here the formulation 3.2 is nonconvex quadratic problem and the non-convexity comes from either of the equations: $|V_i|^2 = e_i^2 + f_i^2$, $e_ie_j + f_if_j = |V_i||V_j|cos(\theta_i - \theta_j)$ and $e_if_j - e_jf_i = -|V_i||V_j|sin(\theta_i - \theta_j)$. To overcome this non-linearity, two more variable matrices are introduced as c and s, where the diagonal and off-diagonal elements are defined as $c_{ii} = e_i^2 + f_i^2$, $c_{ij} = e_ie_j + f_if_j$ and $s_{ij} = e_if_j - e_jf_i$. With this new variable set, the formulation 3.2 can be re-written as follows:

$$
\begin{aligned}
& Min \ \sum_i f_i\left(P_{Gi}\right) && (3.3)\\
& s.t. \\
& P_{Gi} - P_{Di} = G_{ii}c_{ii} + \sum[G_{ij}c_{ij} - B_{ij}s_{ij}] \\
& Q_{Gi} - Q_{Di} = -B_{ii}c_{ii} + \sum[-B_{ij}c_{ij} - G_{ij}s_{ij}] \\
& P^{min} \leq P_{Gi} \leq P^{max} \\
& Q^{min} \leq Q_{Gi} \leq Q^{max} \\
& V_{min}^2 \leq c_{ii} \leq V_{max}^2 \\
& P_{ij}^2 + Q_{ij}^2 \leq |S_{ij}^{max}| \\
& c_{ij} = c_{ji}, s_{ij} = -s_{ji} \\
& c_{ij}^2 + s_{ij}^2 = c_{ii}c_{jj}
\end{aligned}
$$

This formulation was proposed by Jabr[65]. This is an exact formulation for power system networks, especially radial ones. Although, this formulation still holds the non-linearity in the last constraint of the formulation4.12. We can convexify this non-convex formulation utilizing the semidefinite programming (SDP) relaxation. That quadratic constraint can be written in the form of a $2 * 2$ matrix for all the lines of the network as follows,

$$
\begin{bmatrix} c_{ii} & c_{ij} + is_{ij} \\ c_{ij} - is_{ij} & c_{jj} \end{bmatrix} \succcurlyeq 0 \tag{3.4}
$$

$$
rank \begin{bmatrix} c_{ii} & c_{ij} + is_{ij} \\ c_{ij} - is_{ij} & c_{jj} \end{bmatrix} = 1 \tag{3.5}
$$

But, equation 3.5 is not convex in nature. Thus, by relaxing 3.5 and replacing the quadratic constraint in 4.12 with 3.5, we can finally write the SDP relaxed convex formulation of BIM-OPF as:

$$Min \sum_{i} f_i\left(P_{Gi}\right) \tag{3.6}$$

$$s.t. \begin{cases} P_{Gi} - P_{Di} = G_{ii}c_{ii} + \sum[G_{ij}c_{ij} - B_{ij}s_{ij})] \\ Q_{Gi} - Q_{Di} = -B_{ii}c_{ii} + \sum[-B_{ij}c_{ij} - G_{ij}s_{ij}] \\ P^{min} \leq P_{Gi} \leq P^{max} \\ Q^{min} \leq Q_{Gi} \leq Q^{max} \\ V_{min}^2 \leq c_{ii} \leq V_{max}^2 \\ P_{ij}^2 + Q_{ij}^2 \leq |S_{ij}^{max}| \\ c_{ij} = c_{ji}, s_{ij} = -s_{ji} \\ \begin{bmatrix} c_{ii} & c_{ij} + is_{ij} \\ c_{ij} - is_{ij} & c_{jj} \end{bmatrix} \succcurlyeq 0 \end{cases}$$

Now, we will test this proposed formulation for IEEE networks of various sizes to test the exactness and scalability of the formulation.

3.3.3 Including Quadratic Cost Function

As shown before, the cost function of active power generation is quadratic, a non-linear equation. While formulating a convex problem for optimal power flow, the objective function has to be convex too. The general expression of the cost function can be written as follows:

$$Cost, f_i(P_{G,i}) = \sum_{i \in N} [C_{2,i}P_{G,i}^2 + C_{1,i}P_{G,i} + C_{0,i}] \tag{3.7}$$

Let's assume we introduce a variable α such as,

$$\alpha_i \geq [C_{2,i}P_{G,i}^2 + C_{1,i}P_{G,i} + C_{0,i}] \tag{3.8}$$

Then, the total generation cost can be minimized by minimizing $\sum_{i \in N} \alpha$. Now, eqn 3.8 can be evolved as follows:

$$\begin{aligned} & 0 \geq C_{2,i}P_{G,i}^2 + C_{1,i}P_{G,i} + C_{0,i} - \alpha_i \\ & \Rightarrow 0 \geq 4C_{2,i}P_{G,i}^2 + 4[C_{1,i}P_{G,i} + C_{0,i} - \alpha_i] \end{aligned} \tag{3.9}$$

Now, introducing two more variables, x, and y, and substituting the following expressions,

$$\begin{aligned} & x = C_{1,i}P_{G,i} + C_{0,i} - \alpha_i \\ & y = C_{2,i}P_{G,i}^2 \\ & Then, \\ & 0 \geq 4y + 4x \\ & \Rightarrow 0 \geq 4y + (1+x)^2 - (1-x)^2 \\ & \Rightarrow (1-x) \geq ||(2\sqrt{y}) + (1+x)||_2 \end{aligned} \tag{3.10}$$

In this approach, the nonlinear quadratic cost function for minimizing generation cost can be written in the form of a cone, and the nonlinear OPF problem becomes a convex optimization problem.

3.3.4 Advantage of Proposed Approach over Conventional Approaches

In conventional BIM-SDP relaxed OPF formulation, a positive semidefinite matrix is formed by multiplying the complex voltage of every node with its conjugate. While building the set of constraints, the whole PSD matrix is used each time, which is not a significant issue for smaller networks. On the contrary, the real-world power networks consist of thousands of buses, making the PSD matrix very large. The solver and the machine go through a massive computational burden while formulating the problem. This makes the whole process very slow; sometimes, the solver can't handle the problem of such dimension. The proposed approach can address the scalability issue effectively. It can solve such systems which can not be solved using available solvers following the conventional SDP-OPF formulation. Moreover, if the network's topology is radial, there will be a high number of zero entries in the PSD matrix, making the matrix poorly conditioned for the solver. Since the proposed solution considers specific entries of the PSD matrix to form the constraints, thus the number of zero entries doesn't cause any trouble for the solver. Another popular approach is to use second-order cone programming(SOCP) formulation for large distribution or transmission networks since SOCP formulation can handle large network problems. But, since we know that the tightness of the SDP formulation is higher than the SOCP, the proposed approach can ensure a more accurate global solution to the problem. In another approach, branch flow models(BFM) seem to perform well with large networks, and test studies show the same trend. Although BFM formulation comprises four variables, bus voltage magnitude squared, line current flow squared, line apparent power flow, and injected power at every bus. Where BIM formulation has only one variable, and less number of variables poses less burden on the solver.

3.4 Convex Relaxation of Optimal Power Flow For Branch Flow Model

3.4.1 Optimal Power Flow Formulation

The optimal power flow formulation as an optimization problem consists of an objective function subject to linear and nonlinear equality and inequality constraints. Considering no loss of generality, for a single-phase radial distribution network, let the adjacent buses of a branch be denoted by i and j. The resistance and reactance of the branch are denoted by R_{ij} and X_{ij}. The impedance and admittance are indicated

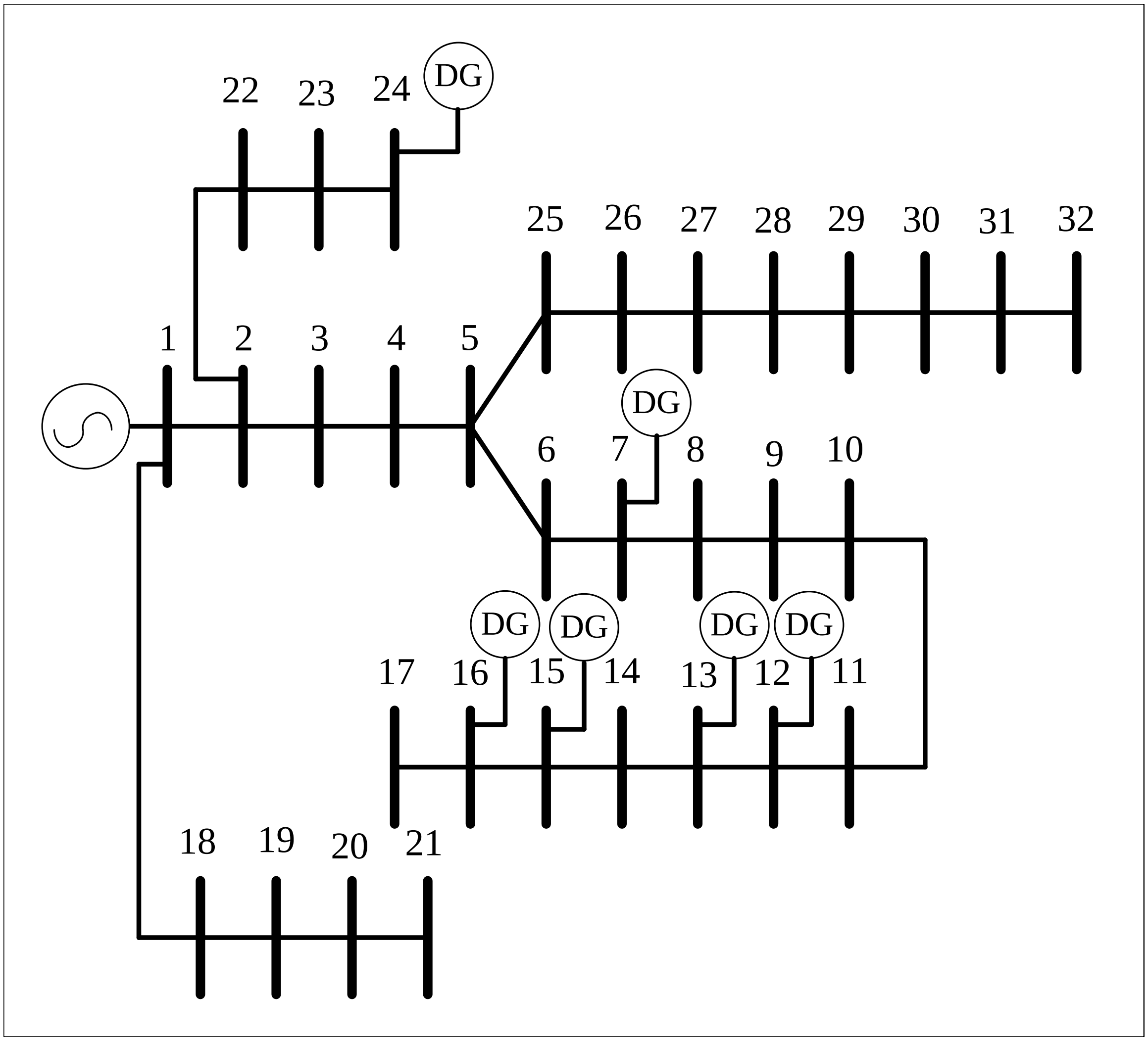

Figure 3.1: Modified 32 bus distribution test system

by z_{ij} and y_{ij}. The real and reactive power flowing through the branch from node i to j are P_{ij} and Q_{ij} and the apparent power $S_{ij} = P_{ij} + jQ_{ij}$. The voltage of node i is denoted by V_i and is bounded by the upper and lower limits $\bar{V}_i$ and $\underline{V}_i$. Similarly, the upper and lower bounds for active and reactive power generation are denoted as $\overline{P}_{G,i}$, $\underline{P}_{G,i}$, $\overline{Q}_{G,i}$ and $\underline{Q}_{G,i}$. With these notations, the original problem formulation of optimal power flow can be stated as:

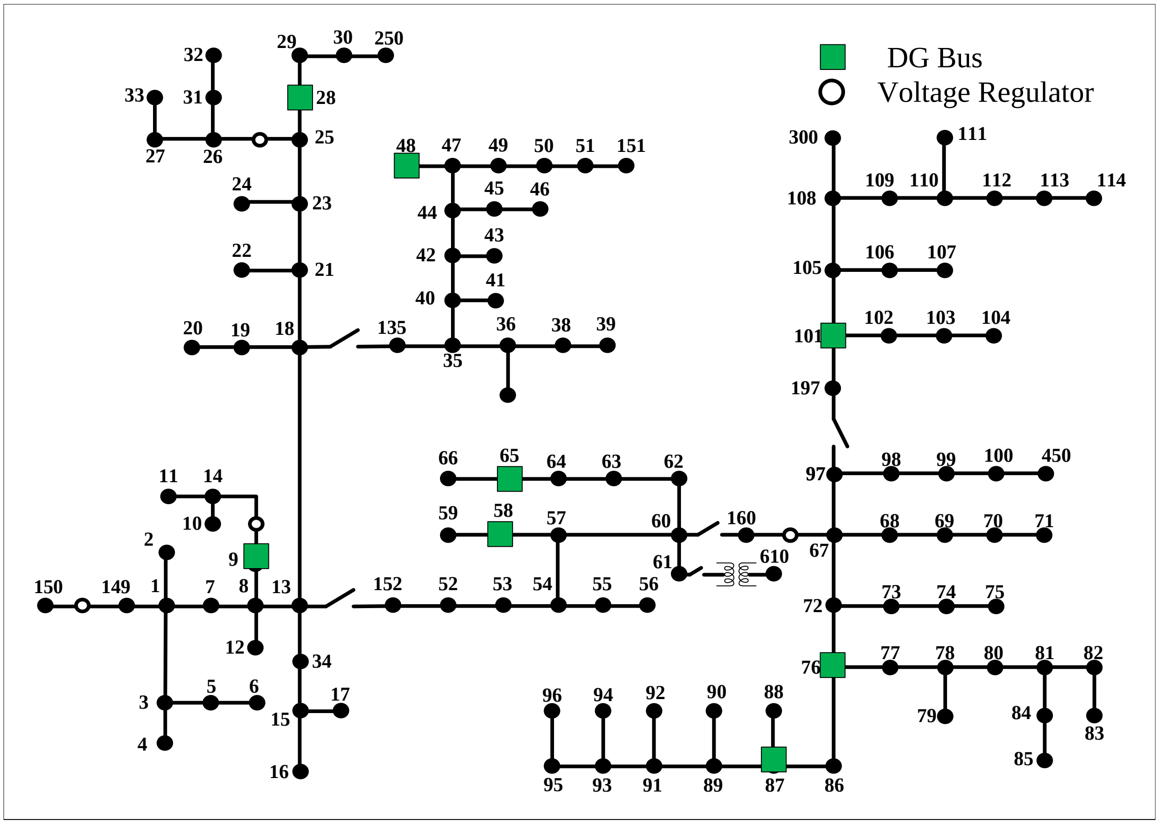

Figure 3.2: IEEE 123 bus distribution test system with 10% DG penetration

$$\text{minimize } f(V, P_G, Q_G) \tag{3.11}$$

subject to,

$$\sum_{j:i\to j} P_{ij} = P_{G,i} - P_{D,i}$$

$$\sum_{j:i\to j} Q_{ij} = Q_{G,i} - Q_{D,i}$$

$$S_{ij} = V_i(V_i^* - V_j^*)y_{ij}^*$$

$$\underline{P}_{G,i} \leq P_{G,i} \leq \overline{P}_{G,i}$$

$$\underline{Q}_{G,i} \leq Q_{G,i} \leq \overline{Q}_{G,i}$$

$$P_{ij}^2 + Q_{ij}^2 \leq \overline{S}_{ij}^2$$

$$\underline{V}_i \leq V_i \overline{V}_i$$

The formulation mentioned above is a nonlinear problem (NLP). If we consider having a tap changer or a voltage regulator in the branch between nodes i and j and include the control of the tap position of the regulator in the formulation. The voltages of the primary and secondary nodes of a regulator are connected as follows:

$$V_{pri} = t_{ij} V_{sec} \tag{3.12}$$

Here, t_{ij} is the tap ratio of the primary and secondary voltages for a specific tap position. The value of tap ratio can be expressed in terms of minimum value of tap ratio t^{min}, tap position, T_{ij} and value of step tap ratio Δt_{ij}.

$$t_{ij} = t^{min} + T_{ij} \Delta t_{ij} \tag{3.13}$$

If we combine 3.12 and 3.13 along with 3.11, the whole problem transforms into a mixed integer non-linear problem. Because the relation in 3.12 is a mixed integer equation, this transformation increases the complexity of the formulation by many times. Although numerous solvers can handle large-scale NLP problems, there are hardly any robust solvers which can solve an MINLP problem for a standard size network OPF problem, including discrete controls of voltage regulators' tap position.

3.4.2 BFM-SDP OPF

In this chapter, we mostly focus on formulating the OPF problem for the distribution systems. Hence the Branch Flow Model of the system is adopted to formulate the OPF problem. Let us assume a graph $G = (N, E)$ represents a radial distribution network where N is the set of all vertices, and E is the set of all branches. The branch flow model comprises the branch variables such as branch current, branch active, and reactive power flow. Let V_i be the voltage of node i, S_{ij} and I_{ij} is the complex power and currently flown through branch $i - j$, then the branch flow model can be stated as follows

$$V_i - V_j = z_{ij} I_{ij}, \forall (i,j) \in E \tag{3.14}$$

$$S_{ij} = V_i I_{ij}^*, \forall (i,j) \in E \tag{3.15}$$

$$\sum_{k:j\to k} S_{jk} - \sum_{i:i\to j} (S_{ij} - z_{ij}|I_{ij}|^2) + y_j^*|V_j|^2 = s_j \tag{3.16}$$

Here, z_{ij} is the branch impedance, and s_j is the injected complex power at node j. The relaxed branch flow model is adopted from this equation by ignoring the angles of the variables. By substituting the expression of current I_{ij} from 3.15 into 3.14 yields $V_i - V_j = z_{ij} S_{ij}^*/V_i^*$. Then taking the square of the magnitudes of this expression derives the equation 3.18 as shown below. In the relaxed model the squared terms of the node voltage and branch current replaces the previous variables as $v_i = |V_i|^2$ and $l_{ij} = |I_{ij}|^2$. The relaxed BFM model is

$$s_j = \sum_{k:j\to k} S_{jk} - \sum_{i:i\to j} (S_{ij} - z_{ij} l_{ij}), \forall j \in E \tag{3.17}$$

$$v_j = v_i - 2(z_{ij}^* S_{ij} + z_{ij} S_{ij}^*) + z_{ij} l_{ij} z_{ij}^*, \forall (i,j) \in E \tag{3.18}$$

$$v_i l_{ij} = |S_{ij}|^2, \forall (i,j) \in E \tag{3.19}$$

The nonlinear equation 3.19 can be expressed in terms of a positive semidefinite matrix as follows:

$$\begin{bmatrix} v_i & S_{ij} \\ S_{ij}^* & l_{ij} \end{bmatrix} \succcurlyeq 0$$
$$rank \begin{bmatrix} v_i & S_{ij} \\ S_{ij}^* & l_{ij} \end{bmatrix} = 1$$

The abovementioned equations still hold the non-convexity due to the rank-1 constraint of the PSD matrix. Relaxing the equation by adopting the semidefinite relaxation (SDR), the BFM-SDP OPF problem is formulated:

$$Min \sum_{i:i\to j} Re\{z_{ij}\}I_{ij} \tag{3.20}$$

$$s.t. \begin{cases} s_j = \sum_{k:j\to k} S_{jk} - \sum_{i:i\to j}(S_{ij} - z_{ij}|l_{ij}|^2) \\ v_j = v_i - (S_{ij}z_{ij}^* + z_{ij}S_{ij}^*) + z_{ij}l_{ij}z_{ij}^* \\ \begin{bmatrix} v_i & S_{ij} \\ S_{ij}^* & l_{ij} \end{bmatrix} \succcurlyeq 0 \\ v_{ref} = V_{ref}V_{ref}^* \\ v^{min} \le v_i \le v^{max} \\ S^{min} \le S_i \le S^{max} \end{cases}$$

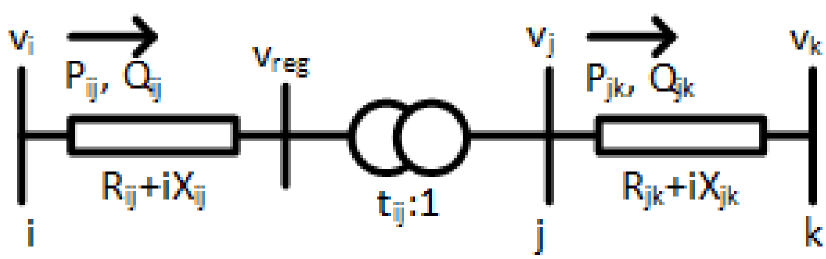

Figure 3.3: A simplified schematic of voltage regulator in the distribution network

3.5 Linearized Model of LTC

Let's assume the branch between bus i and j contains a regulator with a fictitious node depicting the primary of the primary node of the regulator as sketched in Fig. 3.3. Let R_{ij} and X_{ij} stand for the resistance and reactance of the branch before the regulator. Let t_{ij} be the tap ratio of the primary and secondary node voltages. Thus

$$v_{reg} = t_{ij}^2 * v_j \tag{3.21}$$

Here, v_{reg} and v_j are the voltage magnitude squared of the primary and secondary nodes of the regulator. Since all the terms in 3.21 are variables, it becomes a nonlinear constraint, thus making the whole problem non-convex.

To linearize the problem, first, we can write the tap ratio in the following expression:

$$t_{ij} = t_{ij}^{min} + T_{ij}\Delta t_{ij} \tag{3.22}$$

$$\Delta t_{ij} = (t_{ij}^{max} - t_{ij}^{min})/K_{ij} \tag{3.23}$$

where t_{ij}^{max} and t_{ij}^{min} are the maximum and minimum tap ratio and K_{ij} is the total number of tap positions. T_{ij} stands for the integer tap position $\{0, 1, 2, ..., K_{ij}\}$. Here, the LTC is modeled as an ideal LTC with series impedance, where the series impedance of the LTC is modeled as a stable branch in the branch flow model. Now, we can write the T_{ij} with the help of a binary variable $p_{ij,n}$ as shown below:

$$t_{ij} = t_{ij}^{min} + \Delta t_{ij} \sum_{n=0}^{N_{ij}} 2^n p_{ij,n} \tag{3.24}$$

$$\sum_{n=0}^{N_{ij}} 2^n p_{ij,n} \leq K_{ij} \tag{3.25}$$

Here, N_{ij} is the length of the binary representation of K_{ij}. Multiplying both side of 3.24 with v_j and defining new variables $m_{ij} = t_{ij}v_j$ and $x_{ij} = p_{ij,n}u_j$ hereby obtained

$$m_{ij} = t_{ij}^{min}v_j + \Delta t_{ij} \sum_{n=0}^{N_{ij}} 2^n x_{ij,n} \tag{3.26}$$

Now, $x_{ij} = p_{ij,n}u_j$ can be equivalently replaced with the help of big-M method using the following equations

$$0 \leq v_j - x_{ij,n} \leq (1 - p_{ij,n})M \tag{3.27}$$

$$0 \leq x_{ij,n} \leq p_{ij,n}M \tag{3.28}$$

Applying the similar procedure to form $v_{reg} = t_{ij}m_{ij}$ and defining a new variable $y_{ij,n} = p_{ij,n}m_{ij}$

$$v_{reg} = t_{ij}^{min} + \Delta t_{ij} \sum_{n=0}^{N_{ij}} 2^n y_{ij,n} \tag{3.29}$$

$$0 \leq m_{ij} - y_{ij,n} \leq (1 - p_{ij,n})M \tag{3.30}$$

$$0 \leq y_{ij,n} \leq p_{ij,n}M \tag{3.31}$$

With the help of these newly formed equations, the linearized and convexified modeling of the grid legacy device LTC is completed.

3.6 Formulation of the Proposed Mixed Integer OPF Problem

Combining the convexified BFM-SDP OPF problem with operational constraints along with the linearized LTC constraints, the mixed integer SDP OPF model is proposed here:

$$Min \sum_{i:i\to j} Re\{z_{ij}\}I_{ij} \tag{3.32}$$

Subject to

$$s_j = \sum_{k:j\to k} S_{jk} - \sum_{i:i\to j}(S_{ij} - z_{ij}|l_{ij}|^2) \tag{3.33}$$

$$v_j = v_i - (S_{ij}z_{ij}^* + z_{ij}S_{ij}^*) + z_{ij}l_{ij}z_{ij}^* \tag{3.34}$$

$$\begin{bmatrix} v_i & S_{ij} \\ S_{ij}^* & l_{ij} \end{bmatrix} \succcurlyeq 0 \tag{3.35}$$

$$v_{ref} = V_{ref}V_{ref}^* \tag{3.36}$$

$$v^{min} \leq v_i \leq v^{max} \tag{3.37}$$

$$S^{min} \leq S_i \leq S^{max} \tag{3.38}$$

(3.25) – (3.31)

As mentioned earlier, the formulation of optimal power flow problem is evolved based on various types of objective functions. In this study, we consider two different objective functions. The most popular objective function used in OPF formulation is to minimize line losses, as shown in 3.32. Let denote this active power loss function as C_1,

$$C_1 = \sum_{i:i \to j} Re\{z_{ij}\} I_{ij} \tag{3.39}$$

Next, we consider another objective function to minimize the voltage deviation of each bus from a nominal value. In this case, the objective function is combined with the loss minimization since it is proven that convex relaxation is not exact for objective functions which are not monotonously increasing. Since the voltage deviation minimization is not a monotonously increasing function, in SDP or SOCP relaxed formulation, combining the deviation with a gradually increasing function like line losses is advised. This objective function is denoted as C_2,

$$C_2 = C_1 + \sum_{i:i \in N} |v_i - v_{set}|$$

Since the $abs()$ function is a non-convex one, we need further modification to make the model convex for this objective function. This objective is achieved by implementing the epigraph model of convex relaxation. In this approach, another auxiliary variable, e_i is introduced where,

$$e_i \geq |v_i - v_{set}| \tag{3.40}$$

So, if $\sum_{i \in N} e_i$ is minimized, the voltage deviation will be minimized, and a few additional constraints will be added to the existing MISDP-OPF as shown below.

$$v_i - v_{set} \leq e_i \tag{3.41}$$

$$v_{set} - v_i \leq e_i \tag{3.42}$$

$$e_i \geq 0 \tag{3.43}$$

Thus the problem for combined minimization of line loss and voltage deviation is as follows:

$$Min\ C_2 \tag{3.44}$$

$$s.t.$$

$$(23) - (28), (15) - (21), (31) - (33)$$

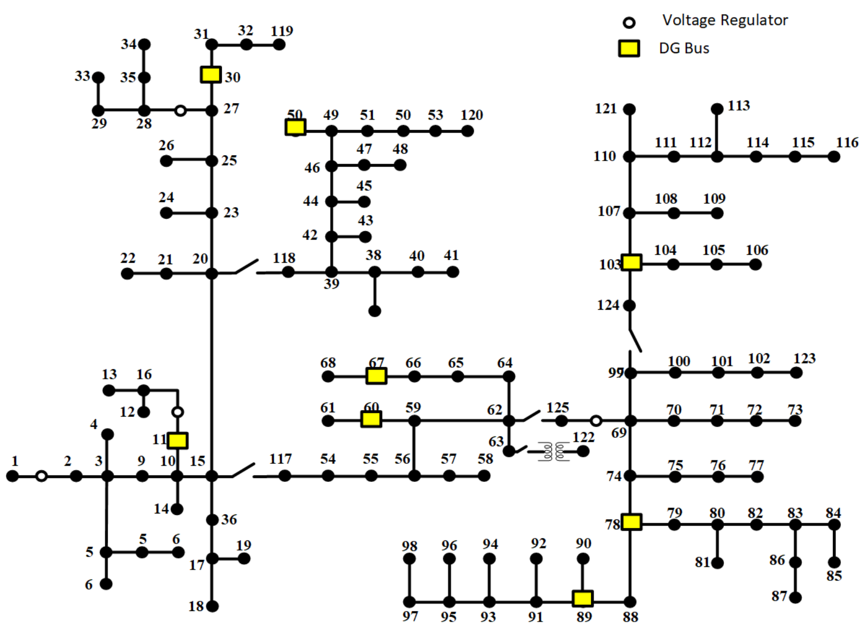

Figure 3.4: Modified IEEE 123 bus system with DERs.

3.7 Case Studies

This section tests the proposed approach on different IEEE power system networks. The formulation is implemented in the MATLAB platform using the YALMIP toolbox for optimization. The solver used to solve the SDP-relaxed OPF is MOSEK. All the simulations are performed on a windows computer with a 2.5GHz Intel Core i5 processor and 16GB of memory. For test models, in this paper, modified IEEE 32 bus system and IEEE 123 bus system are evaluated to prove the scalability of the proposed formulation. The single-line diagrams of the modified 32 bus system are shown in Fig.3.1 with the DG buses marked. There are 6 distributed generators on buses 7,12,13,15,16, and 24. Fig.3.2 shows the network topology and DG locations of the IEEE 123 bus distribution system with 10% DG penetration. The installed DG locations are 9, 28, 48, 58, 65, 76, 87, and 101. Four shunt capacitors are connected at bus 85, 90, 92, and 94 capacity 200, 16.67, 16.67, and 16.67 KVAR.

3.7.1 Result Analysis from Alternative SDP-OPF Formulation

Fig.3.5 shows the voltage magnitude profile comparison of optimal power flow solution from the different formulations of modified 32 bus system, The same for the 123 bus system with 10% and 30% DG penetration are shown in Fig. 3.6 and 3.7. Table 3.1 shows the computational time consumed by the solver to solve the OPF problem in different approaches. We can see that conventional BIM-SDP formulation takes the longest time among the approaches. The proposed CS-SDP formulation is faster than the conventional BIM-SDP and nonlinear approach, but it's seen that BFM-SDP is the fastest among the formulations. From the figures, we can see that, for the smaller system such as the modified 32 bus network, the profiles from nonlinear formulation, conventional BIM-SDP formulation, and proposed CS-SDP formulation are the same. Although, for a larger system, such as IEEE 123 bus network with 10% and 30% DG penetration, the conventional BIM-SDP OPF problem cannot be solved by the solver due to out-of-memory storage error. Thus, the BFM-SDP approach's solution is compared with a nonlinear formulation using MATPOWER. In this comparison, we can see a difference in voltage profile between the BFM-SDP approach and CS-SDP approach, although the profiles are almost the same in the nonlinear approach and CS-SDP approach.

This statement is also validated by the result comparison shown in Table 3.2. In this

Table 3.1: Computational time to solve OPF for test systems in different formulations

Formulations	Solver Time (s)	
	32 bus	123 bus
NLPOPF(Matpower)	0.67	1.67
BIM-SDP OPF	2.3149	N/A
BFM-SDP OPF	0.3021	0.3067
CS-SDP OPF	0.3219	0.3654

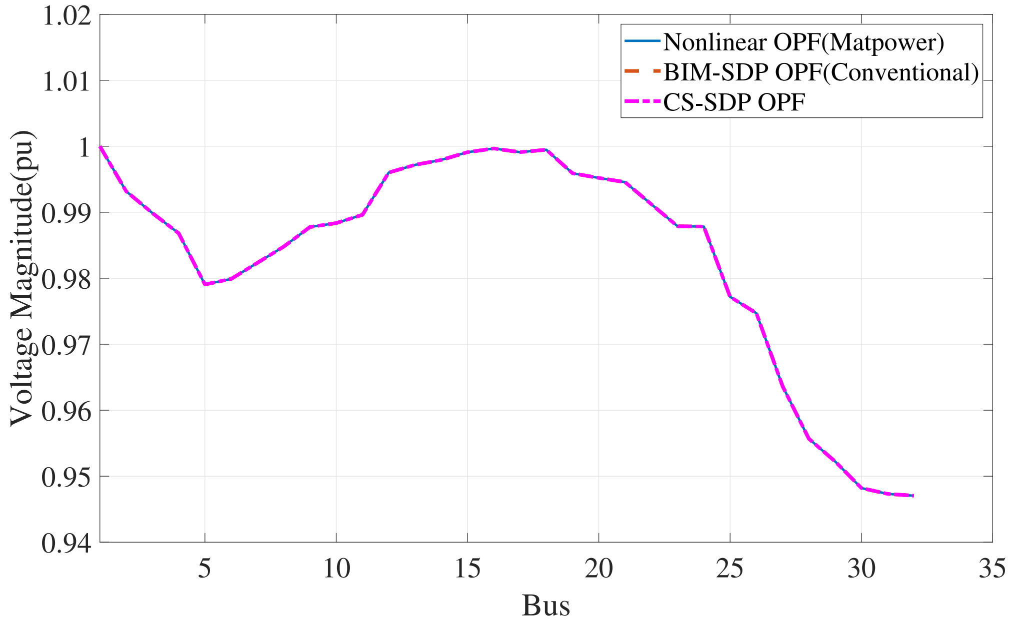

Figure 3.5: Voltage profile comparison of modified 32 bus system among different OPF formulations

table, we can see that the difference in values of active and reactive power dispatch from the substation in the nonlinear approach and proposed CS-SDP approach is negligible where there is a small difference between the BFM-SDP approach and CS-SDP approach. Albeit, for smaller networks, the solutions from nonlinear formulation, conventional BIM-SDP OPF, and CS-SDP OPF are the same.

3.7.2 Result Analysis from MISDP-OPF Formulation

In the case studies for branch flow models, the performance of the proposed MISDP OPF solution is tested on a single-phase representation of the IEEE 123-node system. The existing unbalanced system extracts the positive sequence representation using

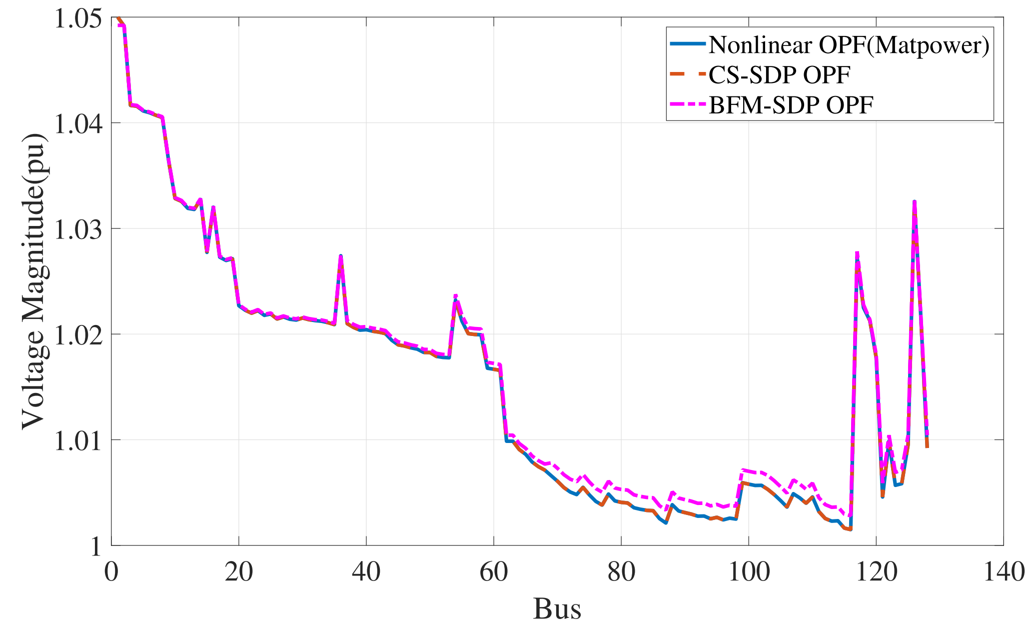

Figure 3.6: Voltage profile comparison of IEEE 123 bus system with 10% DG penetration among different OPF formulations

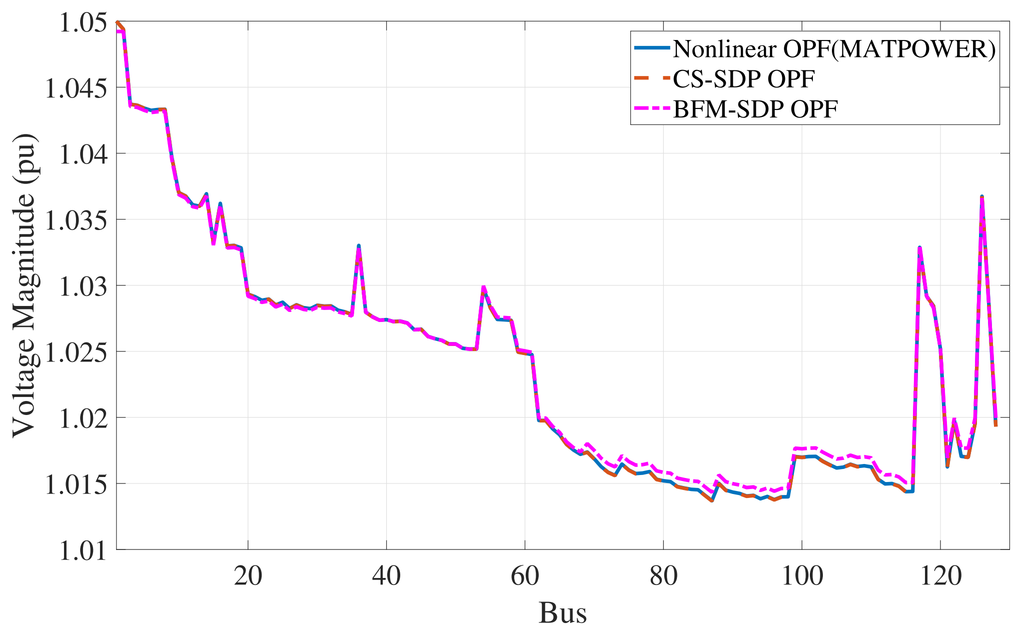

Figure 3.7: Voltage profile comparison of IEEE 123 bus system with 30% DG penetration among different OPF formulations

the OpenDSS software. The connected active and reactive loads are scaled down by one-third factor. The single-line diagram of the network with LTC and DER locations

Table 3.2: substation active and reactive power generation and active power line loss comparison table

	Psub(MW)	Qsub(MVAR)	Ploss(MW)
	Modified 32 bus		
NLPOPF	2.0274	1.4971	0.0674
BIM-SDP OPF	2.0274	1.4969	0.0674
CS-SDP OPF	2.0274	1.4969	0.0674
	IEEE 123 bus system 10% DG		
NLPOPF	0.9239	0.5099	0.0189
BFM-SDP OPF	0.9238	0.5068	0.0188
CS-SDP OPF	0.9239	0.5098	0.0189
	IEEE 123 bus system 30% DG		
NLPOPF	0.7299	0.3703	0.0114
BFM-SDP OPF	0.7297	0.3679	0.0113
CS-SDP OPF	0.7299	0.3699	0.0114

Table 3.3: Tap Position Comparison

123 node system with 10% DER			
	MISDP	MISOCP	MINLP
Tap Position	-1, 0, -7	-3, -1, -6	-1, -2, 1
Psub(KW)	920.93	920.992	927
Qsub(KVAR)	254.334	250.93	510.5
Ploss(KW)	16.0034	16.0023	22.0734
Time(s)	11.2	1.08	25
Gap(pu)	4.14e-15	7.75e-07	

is shown in Fig. 3.2. The active power capacity of the DERs is considered the same as the active demand of the respective buses. The DERs are considered operating at a 0.83 power factor, meaning the apparent power rating of each DER is 1.2 times the active power rating. All the delta-connected loads are considered to be wye-connected for ease of computation. All the LTCs are considered to be operating from -16 to 16 tap positions. For the binary representation of the tap position, a 6-bit representation has been used. To solve the optimization problem CUTSDP solver in the YALMIP optimization tool has been selected due to the scarcity of available solvers for MISDP problems.

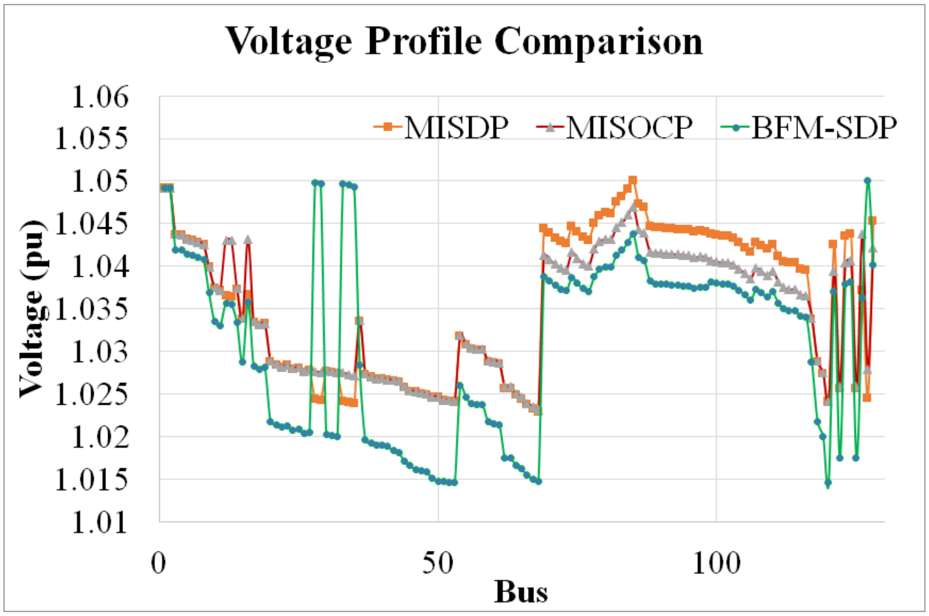

Figure 3.8: Voltage profile comparison with 10% DERs.

3.7.2.1 Loss Minimization

In the first case, we solved the objective function of loss minimization. The same objective function is solved using the proposed MISDP approach, and solutions are compared with those from MISOCP and MINLP. Fig 3.8 shows the voltage profiles from MISDP, MISOCP, and BFM-SDP OPF using the tap positions from the MISDP approach. Table 3.3 shows the comparison of the numerical results. From the table, we can see that, even though the numerical solutions such as dispatched active and reactive power from the substation are very close. However, the tap positions and the bus voltages deviate from one approach to another.

3.7.2.2 Combined Loss and Voltage Deviation Minimization

After minimizing the line losses in the distribution network, the next case was selected a multi-objective model where both the voltage deviation and line losses are to be minimized. The voltage deviation minimization objective function is not a monotonically increasing function. As a result, the solver can not always guarantee

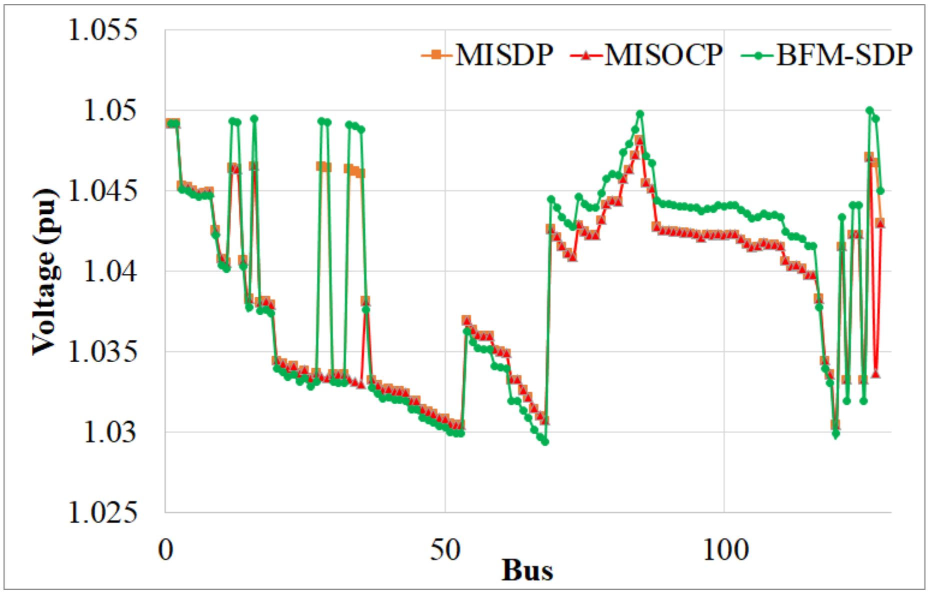

Figure 3.9: Voltage profile comparison with 30% DERs.

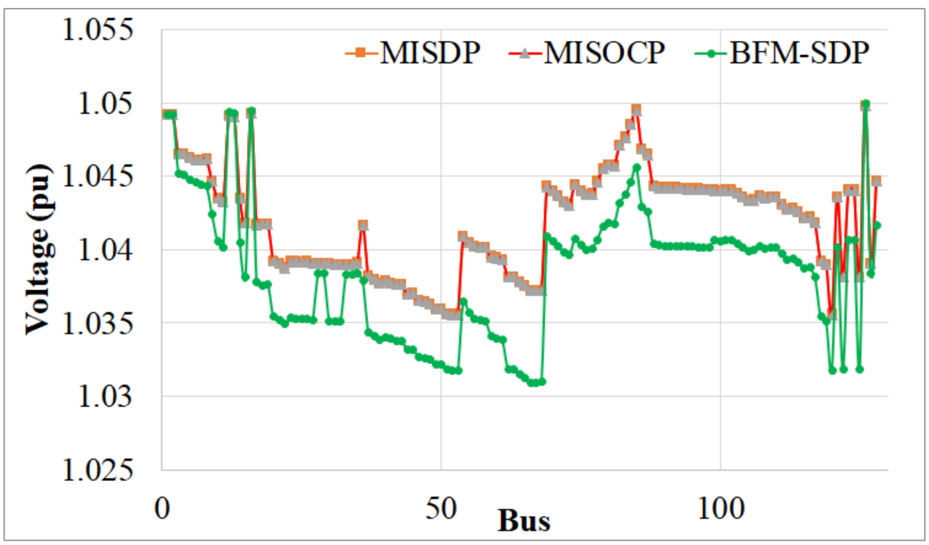

Figure 3.10: Voltage profile comparison with 50% DERs.

the global optimal solution. That's why it is combined with the loss minimization objective to increase the objective function monotonically. On top of that, since this is a combination of multiple functions, weighting factors have been used to set the priorities for each function. It has been experienced that if the higher priority is assigned to the voltage deviation function, the solver converges to a local optimal point, resulting in a higher optimality gap. After few trial and error, the weight factors found for the global optimal point is $w_1 = 0.9$ and $w_2 = 0.1$, where w_1 is the weighting factor for loss minimization function and w_2 is the weighting factor for the voltage deviation function. Using the formulation mentioned in 3.44 and the weighting factors mentioned, the proposed MISDP problem is solved by the CutSDP solver for IEEE 123 bus network with different DER penetration levels. The voltage profiles and numerical solutions are summarized. It was mentioned in the literature study that there is a number of robust and reliable MISOCP solvers available commercially which can solve large-scale MISOCP problems with a minimum optimality gap. In that regard, the solution we achieved from the proposed MISDP model is compared with the same from the MISOCP model. To solve the MISOCP models, Gurobi has been used as the solver. The voltage profile and numerical solutions from the MISOCP model are also showcased in Fig 3.8, 3.9, 3.10 and Table 3.3, 3.4, 3.5 along with the MISDP solution. From those figures and tables, we can confirm that they align exactly with each other, which validates the global optimality and tightness of the proposed MISDP model. However, the computational time of MISDP is significantly higher than the MISOCP models, which solely depends on the solvers. And it is widely known that SDP problems are computationally more expensive than SOCP problems.

3.7.3 Contributions of active, reactive power support and regulator control in loss minimization

Some test cases were conducted to analyze the contribution of active and reactive power support and the voltage regulator control in the formulation of optimal power flow. Here, the optimal power flow for a distribution network for a specific load profile is solved. Then the substation active power, reactive power dispatches, and the network line losses are compared. The profiles are shown in Fig 3.11. The figure shows that introducing active power support from the DERs improves the system

Table 3.4: Tap Position Comparison

123 node system with 30% DER		
	MISDP	MISOCP
Tap Position	-3,-5,-4	-3,-1,-4
Psub(KW)	728.8389	728.8389
Qsub(KVAR)	147.219	146.423
Ploss(KW)	10.066	10.068
Time(s)	29.4	1.42
Gap(pu)	9.13e-7	7.46e-7

losses. But the reactive power support can reduce the line losses further. And finally, the voltage regulator control can reduce the losses even more. Here, the test studies were conducted on the IEEE 123 bus system with 10% DER penetration, and we've noticed the improvement in loss minimization with the regulator control is much less. But for a real-world network scale, the loss reduction will be a significant scale.

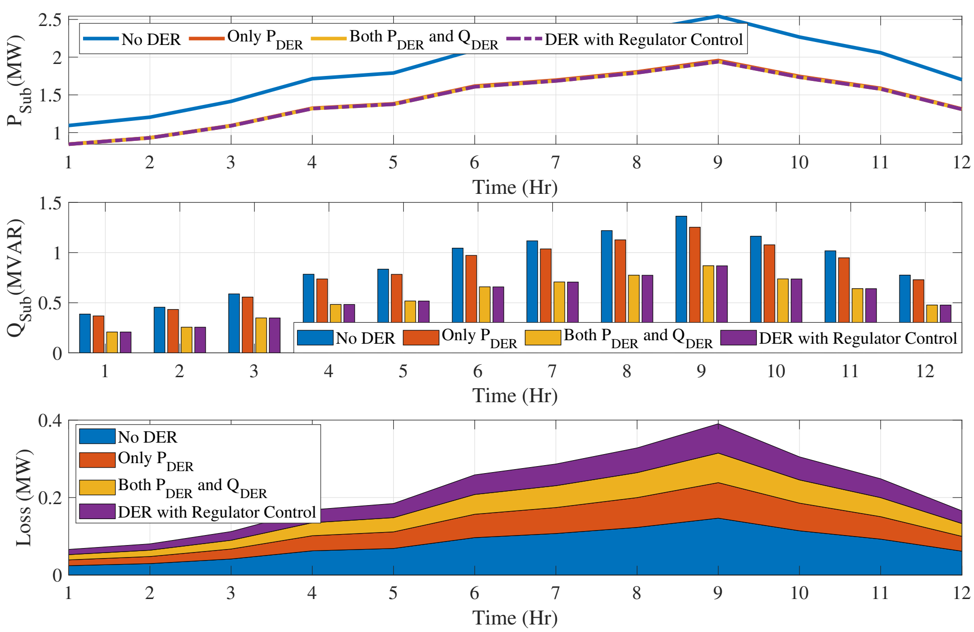

Figure 3.11: substation active, reactive power, and system line loss profile comparison for without DER, with active power only, with active and reactive power support, and with regulator tap control.

Table 3.5: Tap Position Comparison

123 node system with 50% DER		
	MISDP	MISOCP
Tap Position	-3,-1,-3	-3,-1,-3
Psub(KW)	518.513	518.517
Qsub(KVAR)	90.833	91.323
Ploss(KW)	5.1882	5.1892
Time(s)	28.3	1.14
Gap(pu)	1.02e-06	6.23e-07

3.8 Summary

Conventional SDP-based OPF formulations for the bus injection models of power systems impose major computational burden for the off the shelf solvers. The computational stress increases exponentially with the size of the network. That's why, the conventional approach does not scale up to the real-world networks. The proposed alternative BIM-SDP OPF approach reduces the complexity by relating the matrix entries rather than the whole matrix for the constraint formulation. In the case studies, the proposed model scaled up for larger networks with conclusive accuracy. On the other hand, the BFM-SDP OPF is also an exact formulation and converges to the global optimal solution. Based on the BFM-SDP OPF, the integer control of the legacy devices can also be included in the formulation. This algorithm can be used for different objectives by choosing from various cost functions.

CHAPTER 4: MIXED INTEGER SEMIDEFINITE PROGRAMMING FORMULATION MODEL UNIT COMMITMENT OPF APPLICATION

4.1 Introduction

This chapter discusses the Mixed Integer SemiDefinite Program(MISDP) based on combined UCOPF formulation. Unit Commitment (UC) is an essential model in the power system to optimally schedule the generating resources over a horizon of time considering the load changes and various other factors. UC is a non-convex problem, which also includes discrete variables. Since the beginning of UC formulation [85], many types of research have explored different paths to formulate UC as a Mixed Integer Linear Programming (MILP) problem without network constraints [86, 87, 88]. Various types of research have been conducted over time for the formulation of this problem that represents the power network in DC form with or without considering active power losses [89, 90]. Generator scheduling using such models ignores reactive power dispatch, which should be considered. Various methodologies have been applied to solve UC problems, such as Dynamic Programming[91, 92], Branch & Bound (B&B) method [93], and Lagrangian Relaxation Method [94]. Each approach has its drawbacks, such as B&B and genetic algorithm approaches are not computationally efficient. One of the basic properties of the UC problem formulation is that it considers mostly linear constraints. Also, it overlooks the losses in the system and other line constraints. Those constraints are very crucial to getting the correct optimal solution. OPF is another important model for power grid operations that consider the power flow and balance constraints for specific nodes along with other line constraints. However, OPF is another non-convex, non-linear problem and NP-hard in nature [95, 96, 71]. As a result, the combined formulation of UC with OPF is complicated to solve and poses higher stress for the solver[97]. There are few works where the UC-OPF problem is solved in MINLP form [98, 99, 100]. Albeit the formulation for the smaller system may be possible, the scalability of the MINLP version is an issue. Nasri et al.[101] and Fu et al. [99] did extensive work on UC formulation, including AC network and security constraints using Bender's Decomposition method. To convexify the non-convex OPF problem, various relaxation methods are utilized. SDP relaxations have been studied to provide more exact solutions for mesh networks in transmission systems than the second-order cone programming (SOCP) relaxation. Though SDP relaxed problem puts an additional computational burden on the solver than the SOCP problems, one major advantage is that SDP relaxed model contains the bus voltage angle while SOCP models mostly do not. SDP relaxed OPF formulations include rectangular representations of power flow equations [71, 102] or a polar representation of the bus voltages [73].

In this chapter, a two-stage approach UC-OPF formulation is proposed as a combination of the MILP UC problem and SDP OPF formulation. Comparisons with unified MISDP UC-OPF formulation have been presented to show the advantage of the two-staged approach. The contributions of this chapter are threefold. The approach develops a combined UC-OPF model a) without leveraging the rounding of the binary variables as done in the unified formulation, b) Includes the active power loss of the network for power balance constraint in UC, c) Provides close to global solutions and scalable. The rest of the chapter is organized as follows. Section 4.2 discusses UC-OPF preliminaries. Conventional unified and proposed two-staged UC-OPF formulation is described in Section 4.3. The numerical studies and comparison are showcased in Section 4.4, and conclusions and future work are discussed in section 4.5.

4.2 UC-OPF Preliminaries

This section will discuss the essential variables and parameters of unit commitment and optimal power flow. Also, this section will elaborate on the constraints that formulate the problem of unit commitment and OPF.

4.2.1 UC Constraints

The objective of UC is to determine a day-ahead schedule to minimize the power system operation cost while supplying the demand and satisfying other constraints. The UC constraints are briefly explained next.

4.2.1.1 Power Balance

The power balance equation without considering losses can be represented as

$$\sum_{g=1}^{N_G} P_{g,t}^{G} - \sum_{n=1}^{N} P_{n,t}^{D} = 0 \tag{4.1}$$

4.2.1.2 Spinning Reserve

The utility must operate in a way that it should be able to accommodate the largest generator of the system. That means there should be some generating resources that are online but unloaded, and they can respond quickly in case of a loss of any generator. The spinning reserve constraint is

$$\begin{aligned}
& r_{g,t} \leq RU_g \\
& \sum_{g=1}^{G} r_{g,t} = R_t \\
& \sum_{n=1}^{N} P_{n,t}^{D} + R_t - \sum_{g=1}^{G} u_{g,t} P_g^{max} = 0
\end{aligned} \tag{4.2}$$

4.2.1.3 Minimum start-up and shut-down time of units

The minimum up and down time can be formulated as [103].

$$\sum_{i=t-UT_g+1}^{t} v_{g,i} \leq u_{g,t}; \forall g \in N_G, \forall t \in [UT_g + 1, T] \tag{4.3}$$

$$\sum_{i=t-DT_g+1}^{t} w_{g,i} \leq 1 - u_{g,t}; \forall g \in N_G, \forall t \in [DT_g + 1, T] \tag{4.4}$$

4.2.1.4 Ramping up and Ramping Down

Further, the ramp-rate constraints can be represented as

$$P_{g,t} - P_{g,t-1} \leq RU_g; \forall g \in N_G \tag{4.5}$$

$$P_{g,t-1} - P_{g,t} \leq RD_g; \forall g \in N_G \tag{4.6}$$

4.2.1.5 Active and Reactive Power Generation Limit

The active and reactive power generation of the generating units are constrained by the following boundaries,

$$P_g^{min} \leq P_{g,t} \leq P_g^{max}; \forall g \in N_G \tag{4.7}$$

$$Q_g^{min} \leq Q_{g,t} \leq Q_g^{max}; \forall g \in N_G \tag{4.8}$$

4.2.1.6 Voltage Boundary

The voltage magnitude of all the buses of the network is bounded by the following constraint,

$$V^{min} \leq V_n \leq V^{max}; \forall n \in N \tag{4.9}$$

4.2.2 Power Flow Constraints

Let us assume, G $= (N, E)$ represents an undirected graph as the power transmission network where N is the set of buses, and E is the set of branches. Let, V_i is the voltage of bus $i \in N$. The power balance of the power network represents the equality of total incoming power and outgoing power. If, P_i^G, Q_i^G, P_i^D, Q_i^D denotes the active and reactive power generation and active and reactive power demand of bus $i \in N_G$ and y_{ij} denotes the admittance of line between bus i and j, then the power balance for the bus i can be written as shown below:

$$P_i^G - P_i^D = \sum_{i \neq j}^{N} Re[V_i(V_i - V_j)^* y_{ij}^*] \tag{4.10}$$

$$Q_i^G - Q_i^D = \sum_{i \neq j}^{N} Im[V_i(V_i - V_j)^* y_{ij}^*] \tag{4.11}$$

Here, * denotes the complex conjugate of the parameter.

Let $Y \in$C$^{N \times N}$ be the admittance matrix of the network, where y_{ij} represents the admittance for the line segment between bus i and j. Here, $Y_{ij} = G_{ij} + iB_{ij}$ where, G and B represents the conductance and susceptance matrices. Also, $G_{ii} = g_{ii} - \sum_{i \neq j} G_{ij}$ and $B_{ii} = b_{ijj} - \sum_{i \neq j} B_{ij}$ where, g_{ii} and b_{ii} are shunt conductance and susceptance of bus i. Now, the bus voltage, V_i can be written in it's rectangular form as, $V_i = a_i + ib_i$ and similarly, $|V_i|^2 = a_i^2 + b_i^2$ represents the voltage magnitude squared for that specific bus. With these notations, the power balance equations can be written as follows:

$$\begin{aligned} P_i^G - P_i^G = G_{ii}(a_i^2 + b_i^2) + & \sum [G_{ij}(a_i a_j + b_i b_j) \\ & - B_{ij}(a_i b_j - a_j b_i)] \end{aligned} \tag{4.12}$$

$$\begin{aligned} Q_i^G - Q_i^D = -B_{ii}(a_i^2 + b_i^2) + & \sum [-B_{ij}(a_i a_j + b_i b_j) \\ & - G_{ij}(a_i b_j - a_j b_i)] \end{aligned} \tag{4.13}$$

Here, this rectangular formulation of the power balance equation formulates the OPF as a nonlinear and non-convex problem. Non-linearity is coming in the following expressions of variables, $(a_i^2+b_i^2)$, $(a_ia_j+b_ib_j)$ and $(a_ib_j-a_jb_i)$. To get rid of this non-linearity, following new variables are introduced as, $c_{ii}=(a_i^2+b_i^2)$, $c_{ij}=(a_ia_j+b_ib_j)$ and $d_{ij}=(a_ib_j-a_jb_i)$. The newly introduced variables are related to each other through the following equation, $c_{ij}^2+d_{ij}^2=c_{ii}c_{jj}$. The updated formulation of power balance constraints then becomes

$$P_i^G - P_i^D = G_{ii}c_{ii} + \sum[G_{ij}c_{ij} - B_{ij}d_{ij}] \tag{4.14}$$

$$Q_i^D - Q_i^D = -B_{ii}c_{ii} + \sum[-B_{ij}c_{ij} - G_{ij}d_{ij}] \tag{4.15}$$

where the matrix variables c_{ii}, c_{ij} and d_{ij} are related to each other as $c_{ij}=c_{ji}, d_{ij}=-d_{ji}, c_{ij}^2+d_{ij}^2=c_{ii}c_{jj}$. If a Hermitian matrix Z is introduced, such as, $Z=VV^*$, then all the variables c_{ii}, c_{ij} and d_{ij} can be mapped into Z as shown in equation 4.23

$$P_i^G - P_i^D = G_{ii}c_{ii} + \sum[G_{ij}c_{ij} - B_{ij}d_{ij}] \tag{4.16}$$

$$Q_i^G - Q_i^D = -B_{ii}c_{ii} + \sum[-B_{ij}c_{ij} - G_{ij}d_{ij}] \tag{4.17}$$

$$P^{min} \leq P_{Gi} \leq P^{max} \tag{4.18}$$

$$Q^{min} \leq Q_{Gi} \leq Q^{max} \tag{4.19}$$

$$(V^{min})^2 \leq c_{ii} \leq (V^{max})^2 \tag{4.20}$$

$$c_{ij} = c_{ji} \tag{4.21}$$

$$d_{ij} = -d_{ji} \tag{4.22}$$

$$Z = \begin{bmatrix} c_{ii} & (c_{ij}+id_{ij}) \\ (c_{ij}-id_{ij}) & c_{jj} \end{bmatrix} \tag{4.23}$$

$$Z \geq 0 \tag{4.24}$$

4.3 UC-OPF Formulations

In the following sub-sections, the mathematical formulations of the unified approach to the UC-OPF problem and, later, the proposed two-staged UC-OPF problem is derived in detail.

4.3.1 Unified UC-OPF Formulation

Combined UC-OPF formulation can be written in the MISDP form as in 4.2-4.9, 4.16 - 4.24. In this approach, the problem consists of both a mixed integer problem and a convex optimization problem. Currently, there aren't many mature MISDP solvers that can solve large-scale complex MISDP problems, that's why in this unified approach, the binary variables are initialized as continuous variables, and once the problem is solved then, with the help of rounding, the values of unit-commitment variables, the ultimate solution is achieved. The formulation of the unified UC-OPF problem is as follows:

$$\text{Min}: \sum_{t=1}^{T}\sum_{g=1}^{N_G}(u_{g,t}f(P_{g,t}^{G}) + v_{g,t}SU_g) \tag{4.25}$$

Here, $f(P_g^G)$ represents the generating cost function. The other cost associated is the start-up cost of the generator SU_g. The constraints are,

$$P_{i,t}^G - P_{i,t}^D = G_{ii}c_{ii,t} + \sum[G_{ij}c_{ij,t} - B_{ij}d_{ij,t}] \tag{4.26}$$

$$Q_{i,t}^G - Q_{i,t}^D = -B_{ii}c_{ii,t} + \sum[-B_{ij}c_{ij,t} - G_{ij}d_{ij,t}] \tag{4.27}$$

$$u_{i,t}P_i^{min} \leq P_{i,t}^G \leq u_{i,t}P_i^{max}; \forall i \in G \tag{4.28}$$

$$u_{i,t}Q_i^{min} \leq Q_{i,t}^G \leq u_{i,t}Q_i^{max}; \forall i \in G \tag{4.29}$$

$$\sum_{n=1}^{N} P_n^D + R_t - \sum_{g=1}^{N_G} u_{g,t}P_g^{max} = 0 \tag{4.30}$$

$$P_{g,t}^G - P_{g,t-1}^G \leq RU_g; \forall g \in N_G \tag{4.31}$$

$$P_{g,t-1}^G - P_{g,t}^G \leq RD_g; \forall g \in N_G \tag{4.32}$$

$$\sum_{i=t-UT_g+1}^{t} v_{g,i} \leq u_{g,t}; \forall g \in N_G, \forall t \in [UT_g + 1, T] \tag{4.33}$$

$$\sum_{i=t-DT_g+1}^{t} w_{g,i} \leq 1 - u_{g,t}; \forall g \in N_G, \forall t \in [UD_g + 1, T] \tag{4.34}$$

$$u_{i,t}, v_{i,t}, w_{i,t} \in \{0, 1\} \tag{4.35}$$

$$c_{ij} = c_{ji} \tag{4.36}$$

$$d_{ij} = -d_{ji} \tag{4.37}$$

$$Z = \begin{bmatrix} c_{ii} & (c_{ij} + id_{ij}) \\ (c_{ij} - id_{ij}) & c_{jj} \end{bmatrix} \tag{4.38}$$

$$Z \succcurlyeq 0 \tag{4.39}$$

$$(V^{min})^2 \leq c_{ii} \leq (V^{max})^2; \forall i \in N \tag{4.40}$$

In the MISDP UC problem, the variables u, v, w are binary variables, but since there are not enough mature solvers to solve large-scale MISDP problems, the binary variables are relaxed to continuous variables. Then, a rounding-off approach is applied to obtain an integer solution. When the problem 4.25 - 4.3.1 is solved, the values of the variable u, v, and w are converted to binary values using the rounding operation. Then, those binary values solve the OPF problem to get the generation setpoints.

4.3.2 Two-staged UC-OPF Formulation

To solve integer recovery as mentioned above, in this chapter, initially, the value of $Ploss_t$ is an estimated system loss. Once the OPF problem is solved for the given generator status, actual power loss is calculated. In the next iteration, while the UC problem is to be formulated, that loss is updated in the power balance equation. This iterative process is continued until the generator commitment status remains the same for two successive iterations. The whole process is portrayed in the flow chart in Fig. 4.1:

Algorithm 1 Proposed Two-staged UC-OPF

```
Initialize network parameters.
Initialize P_{loss,1} as 5% of P_D.
Use 4.1 - 4.9 to formulate UC problem.
From the solution, use the generator status value to identify the active generator
Use 4.16 - 4.24 to formulate OPF problem.
After convergence calculate P_{loss}, 2.
if (P_{loss,1} = P_{loss,2}) then
    Update the solution to dispatch generator
else
    Update P^{k+1}_{loss,1} = P^{k}_{loss,2}
end if
```

The MILP UC problem in the two-staged approach can be formulated as,

$$\text{Min}: \sum_{t=1}^{T}\sum_{g=1}^{N_G}(u_{g,t}f(P^G_{g,t}) + v_{g,t}SU_g) \tag{4.41}$$

$$\text{Subject to}:$$

$$\text{Constraints}: (4.28) - (4.35)$$

$$\sum_{n=1}^{N} P^D_n - \sum_{g=1}^{N_G} P^G_{g,t} + Ploss_t = 0; \forall g \in N_G \tag{4.42}$$

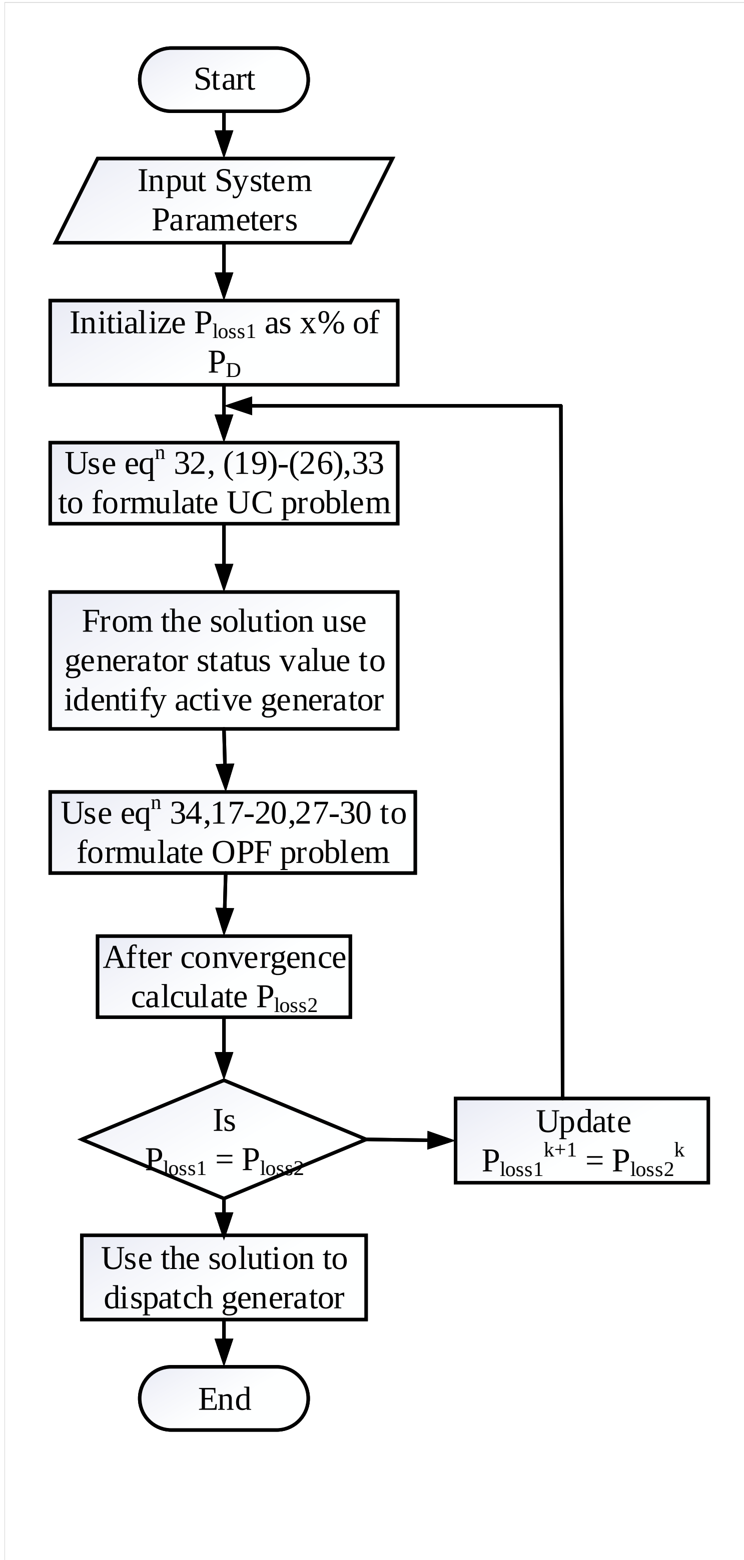

Figure 4.1: Flow chart for the two-staged approach of UC-OPF formulation.

If $u^*_{g,t}$ is obtained from UC solution, then using $u^*_{g,t}$ as parameter, OPF in two-stage formulation is modeled as,

$$\text{Min}: \sum_{t=1}^{T}\sum_{g=1}^{N_G} u^*_{g,t}\, f(P^G_{g,t}) \tag{4.43}$$

$$\text{Subject to}:$$

$$\text{Constraints}: (4.26)-(4.29), (4.36)-(4.40)$$

4.3.3 Unified Branch and Bound Formulation

Since the unified formulation of UC-OPF is a MISDP problem that only a few solvers can handle on a small scale, we've proposed a branch and bound method where the integer variable will be initialized as a continuous variable and solve the whole problem as an SDP model. Once converged, the value of the generator status variables will be extracted. Then using the following approach, the branch and bound methods are formulated.

4.3.3.1 Branch

The generator status value, u, most likely be a real number and does not satisfy the constraint to be an integer. Then, a u_i is selected; let's assume the largest generator's status that does not meet the integer constraint and includes the following constraints,

$$\tilde{u} \leq [u]$$

$$\tilde{u} \geq [u] + 1$$

Here, $\tilde{u_i}$ is the biggest number that does not exceeds u_i

4.3.3.2 Bound

Once a branch is created, each subproblem will be considered a branch, and the result will be noted. The minimum value of the objective functions of all the sub-problems will be regarded as the new lower bound. In this way, further down the tree, branches will be created. For all the sub-problems, the minimum value of the objective functions, where the integer constraint of the generator status variable is satisfied, will be considered the new upper bound of the objective function value.
The result section further describes the implementation of this proposed branch and bound method.

4.4 Numerical Case Studies

The proposed two-stage approach to solving the combined UC-OPF problem is implemented in YALMIP, an optimization toolbox for MATLAB. The simulations are conducted on modified IEEE 6 bus network, IEEE 14 bus, and IEEE 118 bus test networks. The simulation is performed on a Dell laptop with a 2.5GHz Core i5 processor and 16 GB RAM, running a 64bit Windows-10 operating system. To test the approach, test systems of three different sizes were selected. For IEEE 6 bus system, there are 3 generators at buses 1, 2, and 3 of capacity 200MW, 150MW, 800MW respectively, and 3 load buses. A load profile is generated for 24 hours and used to solve the problem. The maximum capacity of the generation is 1150 MW. IEEE 14 bus network contains 5 generators and 11 loads. A 24-hour load profile is also generated based on standard benchmark load conditions. The base voltage of the system is 230 kV. IEEE 118 bus network consists of 19 generators, 35 synchronous condensers, 177 lines, 9 transformers, and 91 loads.

4.4.1 UC-OPF for 6 bus system

The UC-OPF problem for the 6 bus system is solved using unified and two-staged approaches. The generators' parameters are given in Table 4.1. In a unified approach,

Table 4.1: UC Parameters Limits for 6 Bus System

Constraints	Gen 1	Gen 2	Gen 3
Ramping Up (MW)	55	50	20
Ramping Down (MW)	55	50	20
Minimum Up Time (Hr)	4	2	1
Minimum Down Time (Hr)	4	3	1

Table 4.2: UCOPF Solution for 6 Bus System

Parameters	Unified MISDP	Two-staged MISDP	BnB
Total Pgen (MW)	5174.474	5174.127	5170.15
Total Ploss (MW)	22.0738	21.7274	17.749
Total Cost	84795.32	86602.04	80210.08

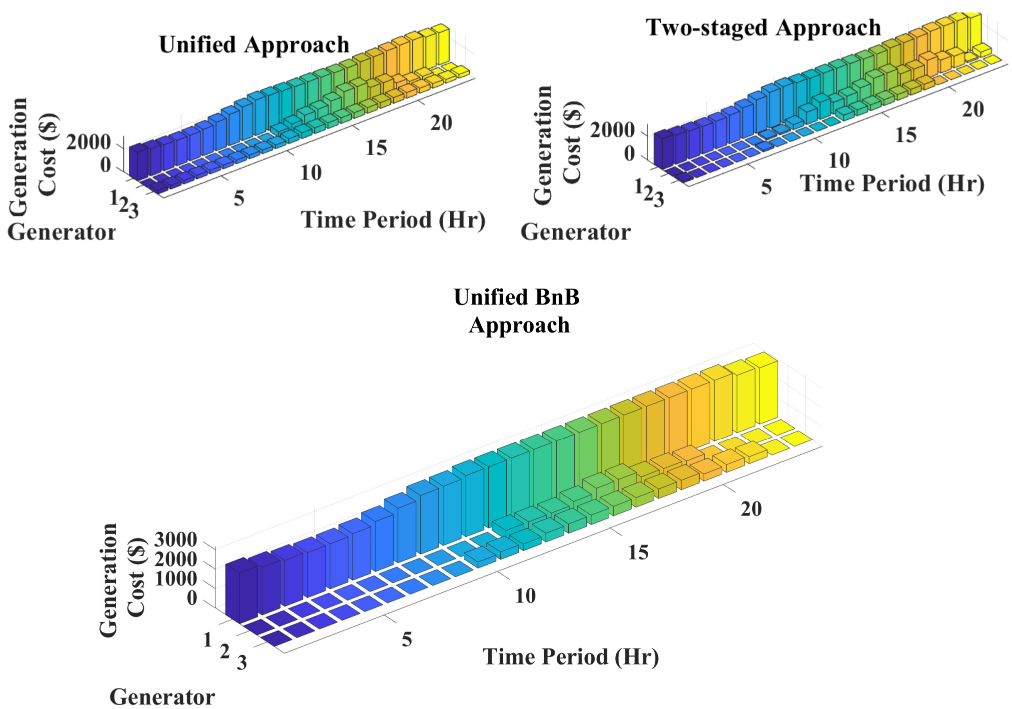

Figure 4.2: Generator status comparison of 6 bus systems for unified, two-staged, and unified BnB approaches.

the binary variables are initially defined as continuous variables. Once the problem is solved, the value of those variables is compared with a threshold value to perform the rounding-off operation. Then the feasibility is checked by solving the OPF problem. The total cost of this approach for 1-day is \$84,795.32. For the two-stage approach,

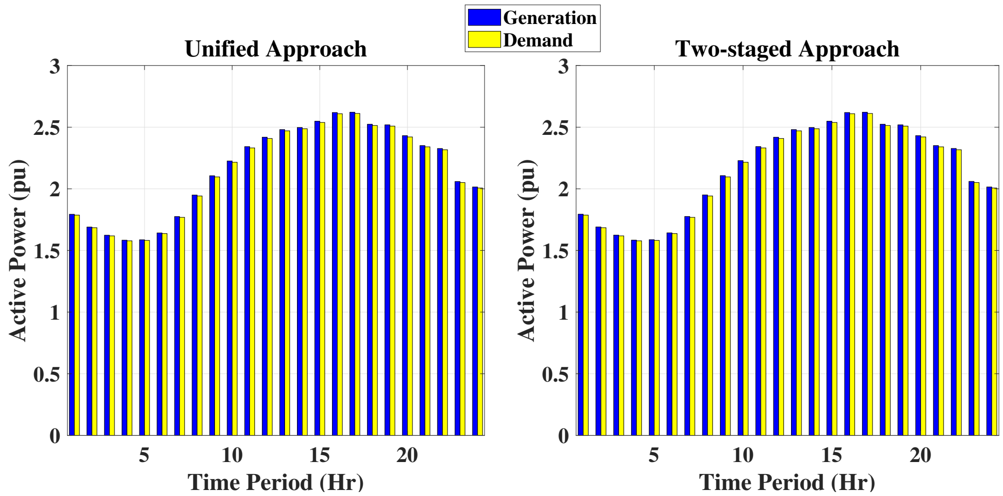

Figure 4.3: Total demand and generation comparison of 6 bus systems for a 24-hr time horizon.

the total generation cost for the day is $86,602.04, which can be seen as higher than the unified approach. The total cost of the unified BnB approach is $80,210.08. However, the total active power loss in the two-staged approach is 21.73 MW, which is lower than the 22.07 MW from the unified approach but more than the unified BnB method, 17.749 MW (see Table 4.2). The generators' status comparison from both approaches is shown in Fig. 4.2. The voltage profile comparison between the two approaches for the time of maximum and minimum loading is shown in Fig. 4.7. The total demand and generation comparison on an hourly basis is shown in Fig. 4.3. The total generation from the proposed approach for each time was compared with the same from the unified approach. The maximum error was 0.038%. The way the branches are created and bounds are updated in the proposed BnB method is shown in Fig4.4.

4.4.2 UC-OPF for IEEE 14 bus system

In the case of the IEEE 14 bus system, the total generation cost and system active power loss is less in the unified approach than in the two-staged approach. The comparison is given in Table 4.4. The generator UC parameter data are shown in Table 4.3. From the numerical solutions in this table, we can see the contrast of

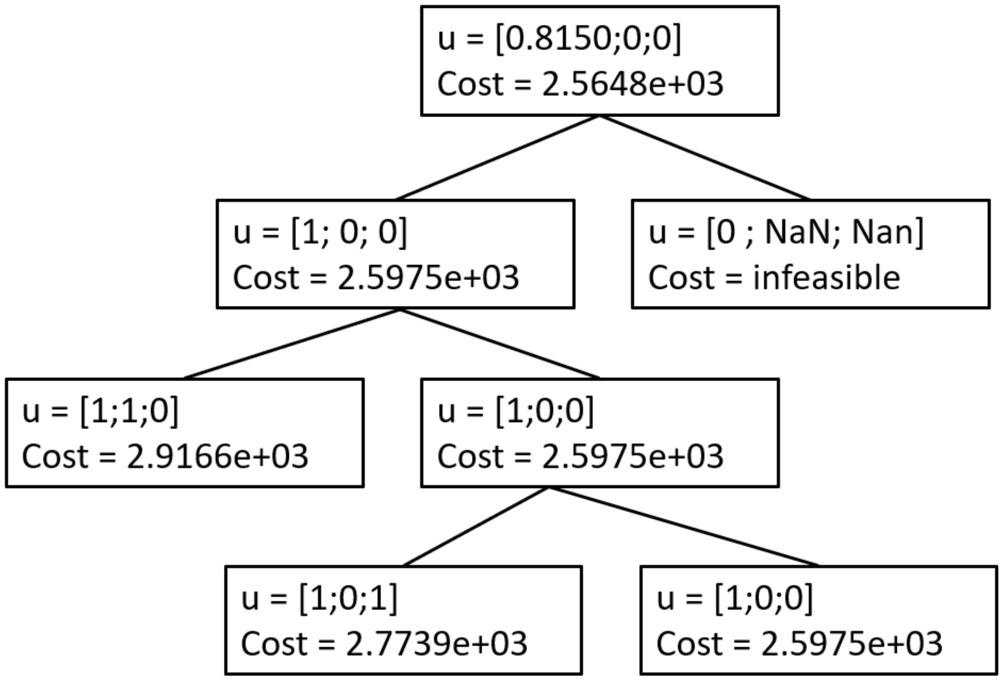

Figure 4.4: Solution process for BnB method for 6 bus networks.

improvement of results observed in the 6bus network using the unified BnB method. The generators' status in Fig. 4.5, in the unified approach, all the generators have been committed, as the value of the generator status variable was higher than the threshold value for all instances, While in the two-staged approach, the cheap generators (e.g., G1, G2) have been committed for all the time and costly generators (e.g., G3, G4, and G5) are offline for some periods following the minimum uptime. The voltage profile comparison for the maximum and minimum loading time is shown in Fig. 4.7. The demand and generation profile comparison for the test case is shown in Fig. 4.6. The maximum error for the total active power generation comparison between the approaches was 0.014%.

4.4.3 UC-OPF for IEEE 118 bus system

For a large system like the modified IEEE 118 bus network, the unified approach was not solvable as the number of constraints and variables are large. So, here only the solution from the two-staged approach is presented. This problem is also formulated

Table 4.3: UC Parameters Limit Value for IEEE 14 Bus System

Constraints	Gen 1	Gen 2	Gen 3	Gen 4	Gen 5
Ramping Up (MW)	55	50	50	40	30
Ramping Down (MW)	55	50	50	40	30
Minimum Up Time (Hr)	4	2	1	2	1
Minimum Down Time (Hr)	4	2	1	2	1

Table 4.4: UCOPF Solution for IEEE14 Bus System

Parameters	Unified MISDP	Two-staged MISDP	BnB
Total Pgen (MW)	3898.189	3898.48	3910.029
Total Ploss (MW)	90.8890	91.183	102.7289
Total Cost	77963.775	77969.67	78200.58

for a 24-hr time horizon with a maximum load of around 6,800 MW, and the solver could easily solve the problem. The generators' cost coefficients for the system are available in [104]. The total demand and generation profile for the whole time horizon of the network is shown in Fig. 4.8. The solution has Pgen (MW) = 132396.31, Ploss (MW) = 4135.41 and Generation cost ($) is 4135.41.

Table 4.5: UCOPF Solution for IEEE118 Bus System Using two-staged Approach

Parameters	Two-staged UCOPF
Pgen (MW)	132396.31
Ploss (MW)	4135.41
Generation Cost ($)	83541

4.5 Summary

In this chapter, a two-stage approach for UC-OPF formulation is proposed. The approach is scalable, accurate with respect to optimal solutions, and feasible. For example, due to the lack of availability of mature solvers, the unified UC-OPF problem in the MISDP form cannot be solved for larger systems, i.e., IEEE 118 bus network, where the two-staged approach was able to solve and is scalable for larger networks.

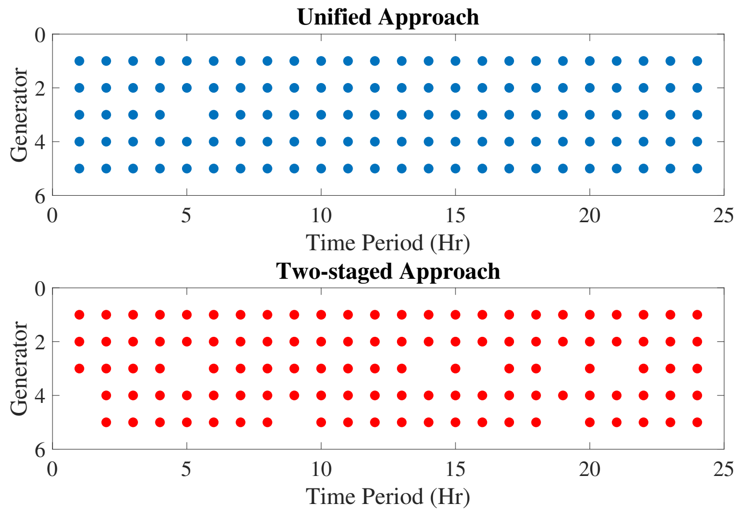

Figure 4.5: Generator status comparison of IEEE 14 bus system for unified and two-staged approaches.

Table 4.6: Generator Cost Coefficients

Bus	Cost Coeff. ($/MWh)	Bus	Cost Coeff. ($/MWh)	Bus	Cost Coeff. ($/MWh)
1	10	42	10	80	0.21
4	10	46	3.45	85	10
6	10	49	0.47	87	7.14
8	10	54	1.72	89	0.16
10	0.22	55	10	90	10
12	1.05	56	10	91	10
15	10	59	0.61	92	10
18	10	61	0.59	99	10
19	10	62	10	100	0.38
24	10	65	0.25	103	2
25	0.43	66	0.25	104	10
26	0.31	69	0.19	105	10
27	10	70	10	107	10
31	5.88	72	10	110	10
32	10	73	10	111	2.17
34	10	74	10	112	10
36	10	76	10	113	10
40	10	77	10	116	10

The solution from the two-staged approach may not be the most economical (we have seen up to a 2% difference compared to the unified approach), but the scheduling of the generating units is feasible. Future work includes extending to integrating

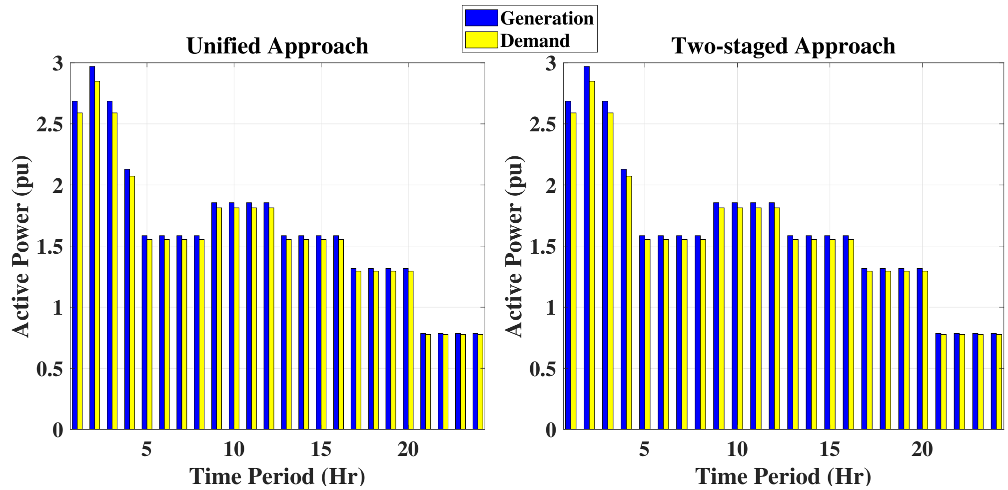

Figure 4.6: Total demand and total generation comparison of IEEE 14 bus system for 24-hr time horizon.

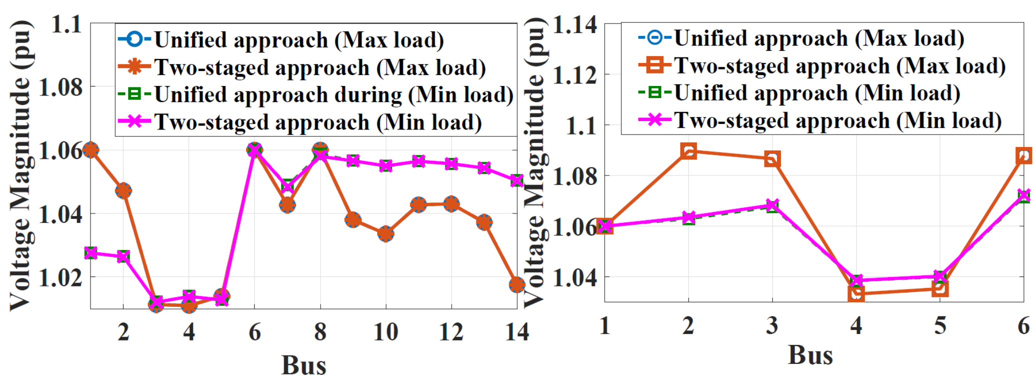

Figure 4.7: Voltage profile comparison for maximum and minimum loading hours in 6 and IEEE 14 bus systems.

contingency scenarios and tighter network constraints. Also, the computational time can be reduced significantly by leveraging the matrix sparsity for larger networks.

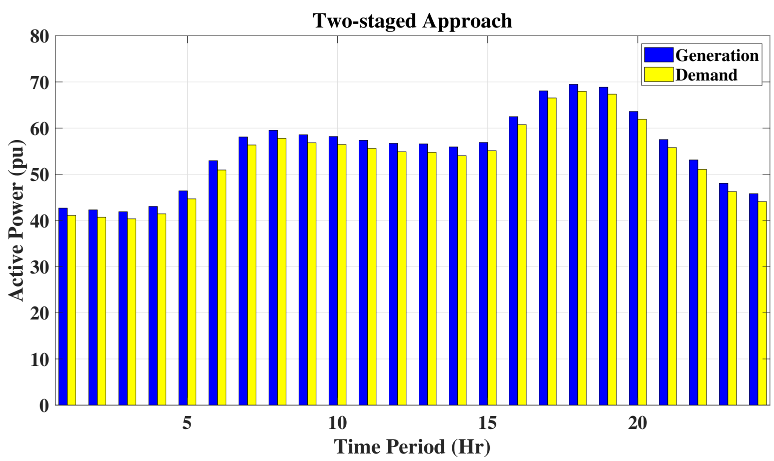

Figure 4.8: Total demand and total generation comparison of IEEE 118 bus system for 24-hr time horizon.

CHAPTER 5: SEMIDEFINITE PROGRAMMING FORMULATIONS OF DER INTEGRATED OPF FOR THREE PHASE POWER DISTRIBUTION SYSTEMS

5.1 Introduction

This chapter discusses optimal power flow for multiphase unbalanced distribution networks. In general, the distribution systems are highly unbalanced due to the unbalanced property of connected loads and the configuration of distribution lines. The numerous generating resources make the system more unbalanced. Thus, the assumption of the nearly balanced voltage of the phases cannot ensure the exactness of the formulation. Also, the mutual coupling of the distribution lines contributes to the unbalanced property. The R/X ratio of the distribution branches is also meager, and the active power losses through the branches cannot be neglected. These complexities make the original ACOPF problem a large numerical burden for the existing nonlinear solvers.

A widely supported approach for this hardship of ACOPF is to solve the convexified OPF problem. It offers several advantages to the problem. It is well proven that if the relaxation is exact, then the optimal solution will be the same as the global optimal solution of the original problem. A commonly adopted approach to convexify the OPF problems is semidefinite relaxation. It is first proposed in [105] how to formulate the OPF problem as a semidefinite program for single-phase power systems. The assumptions and conditions under which the relaxation is exact are discussed and studied in [71]. Later, in [65] it shows how to formulate the OPF problem in a more solver-friendly way in terms of a second order cone problem. [81, 106] did an extensive survey of the various convex relaxation methods of OPF for single-phase distribution networks.

OPF formulation for multiphase networks using the semidefinite relaxation method was first proposed in [80]. Later in [61], it proposed a more stable formulation of OPF for multiphase distribution networks using the branch flow model. This model was based on the Wye-connected load in distribution systems, albeit both Wye and Delta-connected loads can be present in distribution networks. Later in [107], they proposed another updated formulation based on the branch flow model and semidefinite programming, which includes both Wye and Delta connections in distribution networks. In both of those publications, they did not consider the on-load tap changer(OLTC) or voltage regulators of the network. Those formulations were proved to be very exact, and the solutions were very close to the global optimal solution. Since the OLTC and voltage regulators are essential components of distribution networks, it is necessary to have an exact formulation that includes voltage regulators, transformers, and the different connections and mutual coupling of real-world distribution networks.

5.2 Standard Power Flow Model of Multiphase Unbalanced Power System

Conventionally distribution networks are comprised of buses and lines. These buses and lines are multiphased in existing networks, and the network topology is radial. Usually, distribution networks are unbalanced since the total load connected to each phase of the bus change with time. The root node of the distribution system is called the substation bus, and the voltage magnitude of the substation bus is kept constant all the time. The substation bus voltage's phase angle is considered 0. Let $N = \{1, 2, 3, ..., n\}$ denotes the set of buses where bus 1 is the substation bus. Now, assume (i, j) denotes a distribution line connecting bus i and j where both buses are members of N. Let E represent the set of all the lines of the network. The direction of the current flow through the lines can be expressed interchangeably; for example, $i \rightarrow j$ can also be written as $j \rightarrow i$.

Since our focus is on the unbalanced multiphase distribution networks, let a,b, and c denote the three phases of the power system, and Φ_i stands for the phases of bus $i \in N$, and Φ_{ij} denotes the phases of branch between buses (i, j). Let the complex voltage of bus $i \in N$ is denoted by V^{ϕ} where $\phi \in \Phi$ is the set of phases of that bus. Let, I_i^{ϕ} is the complex current injection at bus $i \in N$ and s_i^{ϕ} represents the injected complex power at bus $i \in N$. Then, for the branch parameters, let, $I_{i,j}^{\phi}$ denotes the currents flown through each phase in line from i to j and $S_{i,j}^{\phi}$ denotes the apparent power flown through each phase of the line $i \rightarrow j$. Let, $z_{i,j}$ is the impedance matrix of line (i, j) and the admittance matrix is defined by $y_{i,j} = z_{i,j}^{-1}$. In terms of these variables, the power flow equations can be written for a distribution network as follows:

$$I_{ij} = y_{ij}(V_i^{\phi_{ij}} - V_j^{\phi_{ij}}), i \sim j \tag{5.1}$$

$$I_i = \sum_{j:i\sim j} I_{ij}^{\phi_{ij}}, i \in N \tag{5.2}$$

$$s_i = diag(V_i I_i^H), i \in N \tag{5.3}$$

5.3 Optimal Power Flow for Unbalanced System

Optimal power flow determines the power generation from the sources that minimize the objective function value. Different objective functions are based on preference, such as generation cost minimization, line loss minimization, PV hosting maximization, and voltage deviation minimization. In this chapter, our concern is to minimize the line active power loss with the help of distributed generation resources by solving OPF. Since the line loss is a function of line current, we can write the objective functions as follows:

$$Minimize \sum_{j:i\sim j\in N} f(I_{ij})$$

Optimal power flow is an optimization problem. Thus it contains an objective function, equality constraints, and inequality constraints. The power balance equation of the power flow is considered the equality constraint of OPF. Other equality constraints can be included depending on the extension of the formulation of OPF. In the previous section, replacing the injected current with branch current and branch power flow, we can write the power balance equation as shown below:

$$s_i = \sum_{j:i\sim j} diag[V_i^{\phi_{ij}}(V_i^{\phi_{ij}} - V_j^{\phi_{ij}})^H y_{ij}^H]^{\phi_i} \tag{5.4}$$

Along with this equality constraint, some boundary inequality constraints are needed to be added to define the upper and lower bound for the variables used in the formulation. The general bounds are for the injected or generated power for each bus and the complex voltage of each bus.

$$s_i^{min} \leq s_i \leq s_i^{max} \tag{5.5}$$

$$V_1 = V_1^{ref} \tag{5.6}$$

$$V_i^{min} \leq V_i \leq V_i^{max} \tag{5.7}$$

In summary, the OPF problem can be stated as follows,

$$Minimize \sum_{j:i\sim j\in N} f(I_{ij}) \tag{5.8}$$

Subject to,

(5.4) – (5.7)

5.3.1 BFM-SDP OPF Formulation

The power systems can be modeled in various approaches; the most powerful ones are Bus Injection Model (BIM) and Branch Flow Model (BFM). For radial networks, BFM model is more numerically stable since in this approach the subtraction of $(V_i^{\phi_{ij}} - V_j^{\phi_{ij}})$ can be avoided. This subtraction may make the model ill-conditioned if the difference in voltage values is minimal. The branch flow model is expressed in terms of the following equations,

1. Ohm's law:

$$V_i^{\phi_{ij}} - V_j^{\phi_{ij}} = z_{ij} I_{ij}^{\phi_{ij}} \tag{5.9}$$

2. Variable definition:

$$l_{ij} = I_{ij}^{\phi_{ij}} I_{ij}^{\phi_{ij} H}, S_{ij} = V_i^{\phi_{ij}} I_{ij}^H \tag{5.10}$$

3. Power balance:

$$\sum_{i:i \to j} diag(S_{ij} - z_{ij} l_{ij})^{\phi_j} + s_j = \sum_{k:j \to k} diag(S_{jk})^{\phi_j} \tag{5.11}$$

Here, the injected power at bus i can be defined as the difference of power generated at bus i and total load demand at bus i, i.e., $s_i = s_{G,i} - s_{D,i}, i \in N$.

Since the equation (5.10) is nonlinear, the whole optimization problem is non-convex. This non-convexity can be resolved by using the semidefinite programming relaxation approach. Let us introduce another variable v_i such that, $v_i = V_i V_i^H$. Then, the equation (5.9) can be written as:

$$V_j^{\phi_{ij}} = V_i^{\phi_{ij}} - z_{ij} I_{ij}^{\phi_{ij}}$$

Now, multiplying both sides of the equation by their Hermitian transpose, we obtain,

$$v_j = v_i^{\phi_{ij}} - (S_{ij} z_{ij}^H + z_{ij} S_{ij}^H) + z_{ij} l_{ij} z_{ij}^H \tag{5.12}$$

Furthermore, if we multiply the equation (5.10) with their hermitian transpose, we get

$$S_{ij} S_{ij}^H = V_i^{\phi_{ij}} (V_i^{\phi_{ij}})^H I_{ij}^H I_{ij} \tag{5.13}$$

$$S_{ij} S_{ij}^H = v_i^{\phi_{ij}} l_{ij}$$

Equation (5.13) can be written as a positive semidefinite matrix that can hold the rank-1 property.

$$\begin{bmatrix} v_i^{\phi_{ij}} & S_{ij} \\ S_{ij}^H & l_{ij} \end{bmatrix} = \begin{bmatrix} V_i^{\phi_{ij}} \\ I_{ij} \end{bmatrix} \begin{bmatrix} V_i^{\phi_{ij}} \\ I_{ij} \end{bmatrix}^H \tag{5.14}$$

With the help of these equations, another equivalent formulation of BFM optimal power flow for the unbalanced radial network can be written as follows:

$$\text{Minimize} f(l_{ij}) \tag{5.15a}$$

Subject to,

$$v_j = v_i^{\phi_{ij}} - (S_{ij} z_{ij}^H + z_{ij} S_{ij}^H) + z_{ij} l_{ij} z_{ij}^H \tag{5.15b}$$

$$\sum_{i:i \to j} diag(S_{ij} - z_{ij} l_{ij})^{\phi_j} + s_j = \sum_{k:j \to k} diag(S_{jk})^{\phi_j} \tag{5.15c}$$

$$v_1 = V_1^{ref} (V_1^{ref})^H \tag{5.15d}$$

$$V_i^{min} \leq diag(v_i) \leq V_i^{max} \tag{5.15e}$$

$$s_i^{min} \leq s_i \leq s_i^{max} \tag{5.15f}$$

$$\begin{bmatrix} v_i^{\phi_{ij}} & S_{ij} \\ S_{ij}^H & l_{jj} \end{bmatrix} \succcurlyeq 0 \tag{5.15g}$$

$$rank \begin{bmatrix} v_i^{\phi_{ij}} & S_{ij} \\ S_{ij}^H & l_{ij} \end{bmatrix} = 1 \tag{5.15h}$$

The rank-1 constraint in the above formulation is non-convex. Thus, a semidefinite relaxation can be obtained by relaxing the constraint (5.15h). Therefore, the BFM-SDP relaxed OPF formulation for an unbalanced distribution network can be written in the form as follows:

$$\text{Minimize} \sum_{j:i\sim j} (z_{ij} l_{ij}) \tag{5.16}$$

Subject to,

$$v_j = v_i^{\phi_{ij}} - (S_{ij} z_{ij}^H + z_{ij} S_{ij}^H) + z_{ij} l_{ij} z_{ij}^H$$

$$\sum_{i:i\to j} diag(S_{ij} - z_{ij} l_{ij})^{\phi_j} + s_j = \sum_{k:j\to k} diag(S_{jk})^{\phi_j}$$

$$v_1 = V_1^{ref} (V_1^{ref})^H$$

$$V_i^{min} \leq diag(v_i) \leq V_i^{max}$$

$$s_i^{min} \leq s_i \leq s_i^{max}$$

$$\begin{bmatrix} v_i^{\phi_{ij}} & S_{ij} \\ S_{ij}^H & l_{ij} \end{bmatrix} \succcurlyeq 0$$

5.3.2 Regulator Modelling

A significant part of the modern power distribution networks is the step voltage regulators, which are tap-changing transformers. The acceptable range of operation for distribution voltages is given by the American National Standards Institute (ANSI). In an unbalanced system, three-phase lines and three single-phase regulators are installed. The voltages of the primary and secondary sides of the regulators are related through ratios, and it is shown below:

$$ratio = [r_a, r_b, r_c]^T \tag{5.17}$$

$$[V_a^{sec}, V_b^{sec}, V_c^{sec}]^T = [r_a V_a^{pri}, r_b V_b^{pri}, r_c V_c^{pri}]^T$$

where,

$$r_a = 1 + 0.00625 * Tap_a$$

$$r_b = 1 + 0.00625 * Tap_b \tag{5.18}$$

$$r_c = 1 + 0.00625 * Tap_c$$

In the formulation, the voltage regulator in the line can be visualized in Fig. 5.1

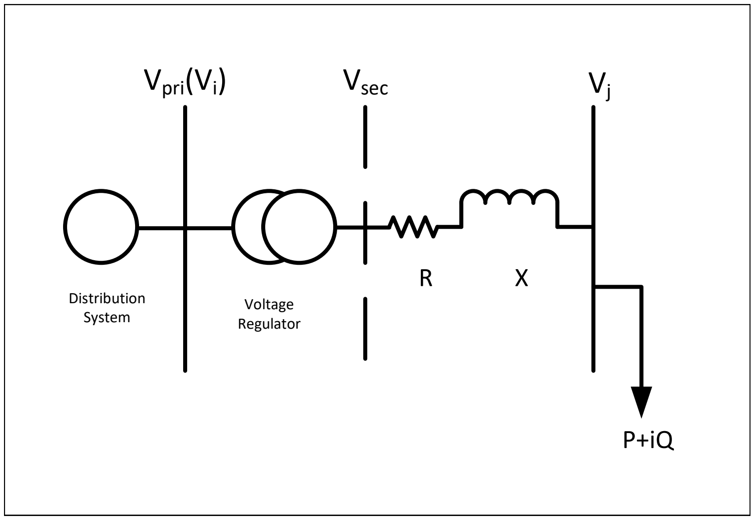

Figure 5.1: A simplified schematic of voltage regulator in the distribution network

In the formulation of the branch flow model, we mentioned that the voltage of both ends of a branch is expressed through equation (5.15b). But if the branch contains a regulator, we need further modification in the equation. The voltage of the load end will be calculated in two steps. First, we calculate the secondary voltage of the regulator using equation (5.17). Then the voltage of the load side of the branch will be calculated using (5.15b), and the secondary voltage will be considered as the source side voltage of the branch. In this regard, the voltage equation for regulator branches can be written as follows:

$$v_j = v_i^{\phi_{ij}} * ratio - (S_{ij} z_{ij}^H + z_{ij} S_{ij}^H) + z_{ij} l_{ij} z_{ij}^H$$

5.3.3 Modelling Switches

In power distribution network topology, switches play a very significant role. Since, in most cases, distribution networks are radial, to ensure reliability and redundancy, switches are used to supply the power to the customer if the primary supply line is compromised. But the resistance and reactance value of the conductor of the switch is meager. That's why while solving for the voltage drop and power balance constraint for the switch, there is a possibility of a high feasibility gap. Which causes the solution to deviate from the global solution. In this formulation, while constructing the branch constraints, the line loss is ignored in the case of switches to overcome that issue. Thus the voltages of both terminals of switches stay the same.

5.3.4 Modelling Mutual Coupling of Branches

The impedance matrix significantly differs while formulating the power flow equations for multiphase systems. Since radial distribution systems are unbalanced, the mutual coupling of the branch impedance matrices plays a significant role in power flow. While formulating the power balance constraints, in other approaches, it is not easy to include the mutual impedance. Because not always a matrix can be included in the constraint as a whole. For example, it is impossible to have a matrix while writing the cone equation in SOCP formulation. But in SDP formulation, the total impedance matrix can be considered while building the power flow or power balance constraints. That's why the proposed method can ensure more exactness in the formulation.

5.4 Case Studies

To implement the three-phase OPF formulation for the unbalanced radial distribution systems, we have chosen IEEE 123 bus system. The nominal operating voltage is 4.16KV. The network contains unbalanced loads with constant impedance, current and power, underground and overhead lines, online tap changer, voltage regulators, multiple switches, and shut capacitors. A simple single-line diagram of the IEEE 123 bus network is shown in Fig. 5.2. Four capacitor banks are connected to buses 83, 88, 90, and 92. Among them, the capacitor bank at bus 83 has three phases, and the rest are single phases. There is an OLTC connected between buses 1 and 2, and 3 more voltage regulators are situated between buses 9-14, 25-26, and 160-67. There are 6 Normally Closed switches connected between buses 13-152, 18-135, 60-160, 61-611, 97-197, and 150-149.

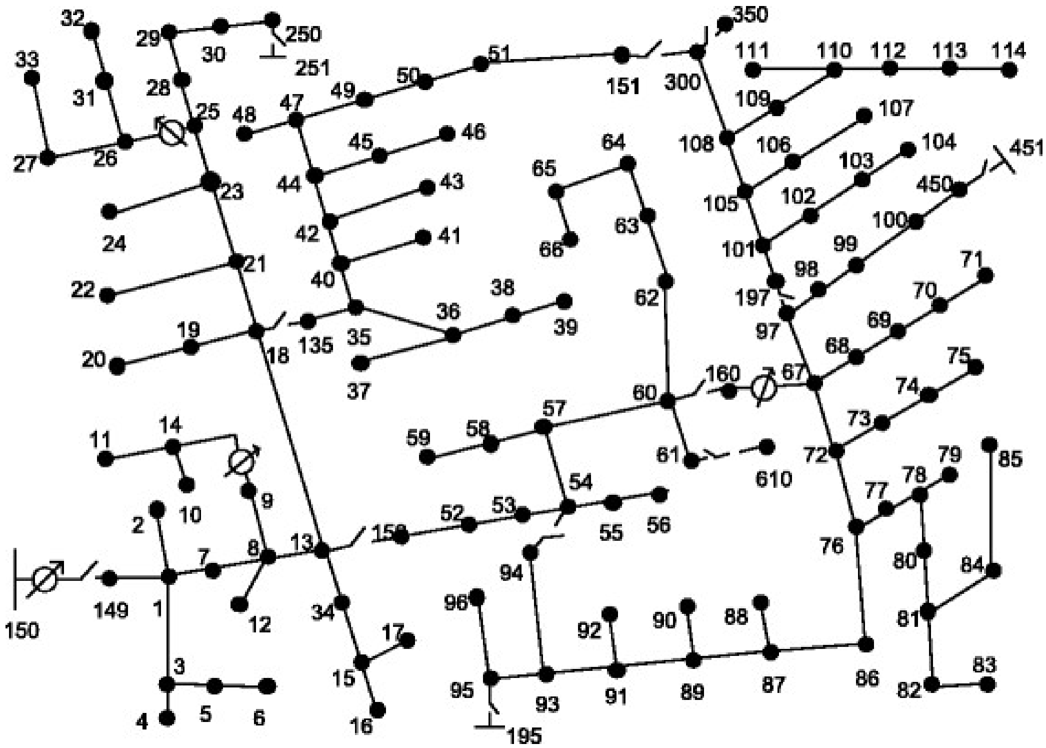

Figure 5.2: A single line representation of the IEEE 123 bus system.

To test the three-phase OPF formulation, first, the approach was tested on the base case scenario. Where all the DGs are made inactive, thus it is only the substation that will dispatch the active and reactive power demanded by the connected loads. Later, the nonlinear power flow was solved for the same case. Since solving the OPF without any DGs and objective function is similar to the power flow analysis, the results from both approaches should match if the formulation is exact. The comparison of the voltage profile from both approaches is shown in Fig 5.4.

Table 5.1: Result comparison for IEEE 123 bus system base case

	$P_{sub,A}$ (KW)	$Q_{sub,A}$ (KVar)	$P_{sub,B}$ (KW)	$Q_{sub,B}$ (KVar)	$P_{sub,C}$ (KW)	$Q_{sub,C}$ (KVar)
Power Flow	1463.86	582.1	963.48	343.68	1193.15	398.9
OPF	1471.6	633.3	921	299.2	1193.2	431.1

Since the approach provided a definitive solution for the IEEE 123 bus system, we tried it on a modified 650 bus system. It is a part of the IEEE 8500 bus system. It

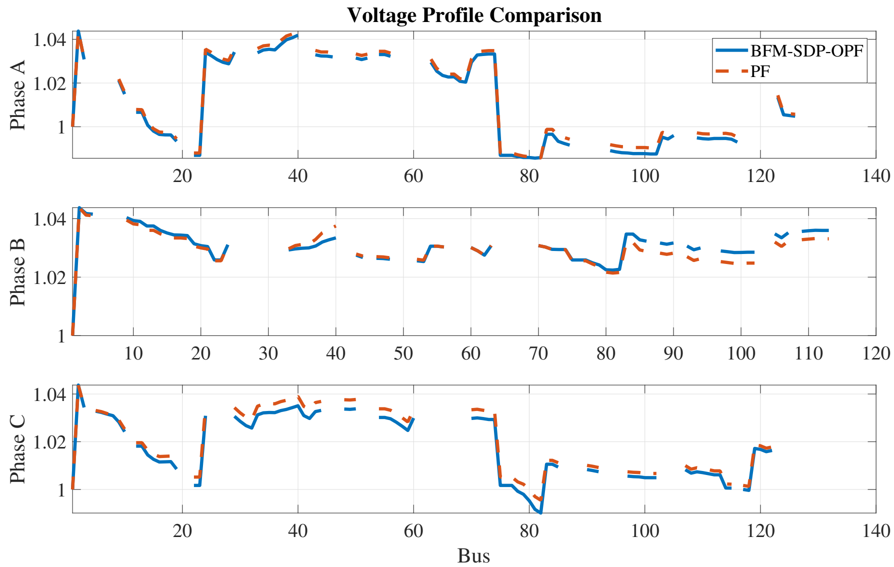

Figure 5.3: Voltage profile comparison of BFM-SDP OPF and nonlinear PF for the base case

contains 647 buses and 646 branches. All the branches of this network are three-phase lines. The nominal voltage is 7.2KV, and the base MVA is 25MVA. The voltage of the root node is considered to be 1.05 pu. The network has four voltage regulators: bus 219-218, 344-343, 234-233, and 3-4. Similar to the IEEE 123 bus system test case, the OPF formulation was tested for the base case where all the DGs are considered to be turned off and then simulated the OPF for the objective function of loss minimization. Thus the result will be similar to the power flow solution. The comparison of voltage magnitude profile comparison between the base case OPF and nonlinear power flow solution is shown below:

Table 5.2: Result comparison for modified 650 bus system base case

	PsubA (MW)	QsubA (MVar)	PsubB (MW)	QsubB (MVar)	PsubC (MW)	QsubC (MVar)
Power Flow	4.1492	2.5637	3.9920	3.2753	3.7744	-1.0413
OPF	4.1643	1.2073	3.9737	-6.250	3.7713	9.1973

Next, we can consider the 10% DG penetration for the system where in some buses, DGs are connected. The capacity of the DGs is considered to be equal to the

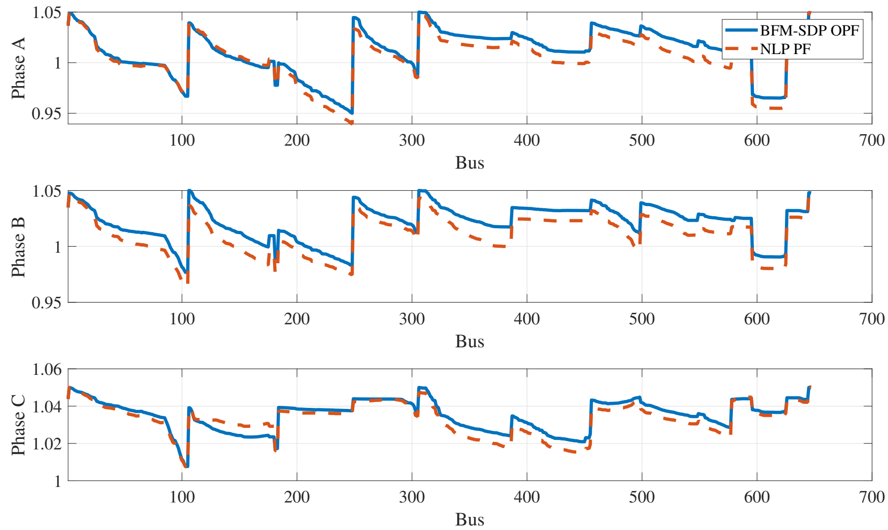

Figure 5.4: Voltage profile comparison of BFM-SDP OPF and nonlinear PF for 650 Bus network base case.

connected active power load to the bus. The reactive power capacity of the DG is considered to be 48.43% of the active power capacity. Then in a similar approach, the BFM-SDP OPF is solved using the proposed approach, and for the exact dispatch of the DGs, the nonlinear power flow is solved, and all the solutions are compared to test the exactness of the proposed approach. The comparison of the voltage profiles is shown in Fig 5.5. The numerical solution values are summarised in Table 5.3. The percentage error of node voltages from BFM-SDP OPF and power flow is shown in Fig 5.6. The PSD matrices' rank represents the solution's accuracy for the BFM-SDP OPF. The rank is calculated based on the ratio of the first two eigenvalues of those matrices. The ratio values are presented in Fig 5.7. Finally, the computational time consumed by the solver for solving OPF and the power flow of the test systems are summarised in table 5.4

5.4.1 Receding Horizon Control for Unbalanced BFM-SDP OPF

Once the proposed formulation of optimal power flow for an unbalanced multiphase distribution network was validated for individual timestamps, the next step was to

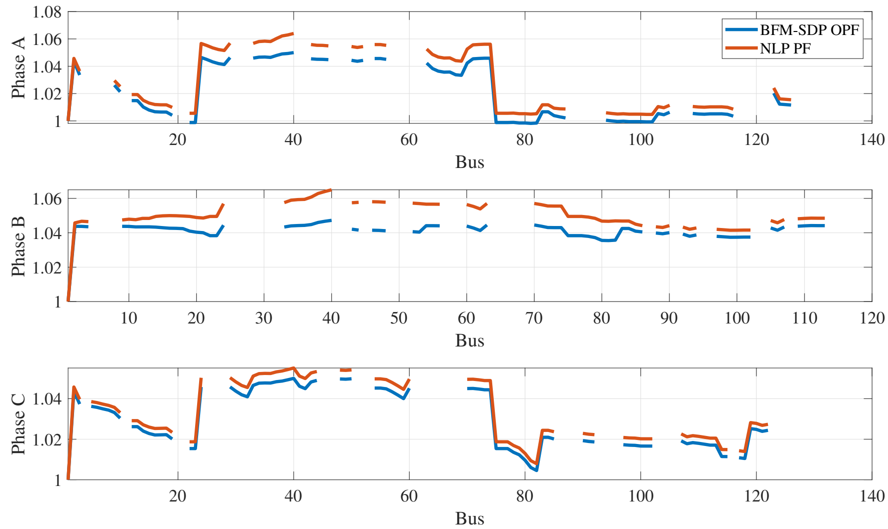

Figure 5.5: Voltage profile comparison of BFM-SDP OPF and nonlinear PF for IEEE 123 Bus network with 10% DG penetration case.

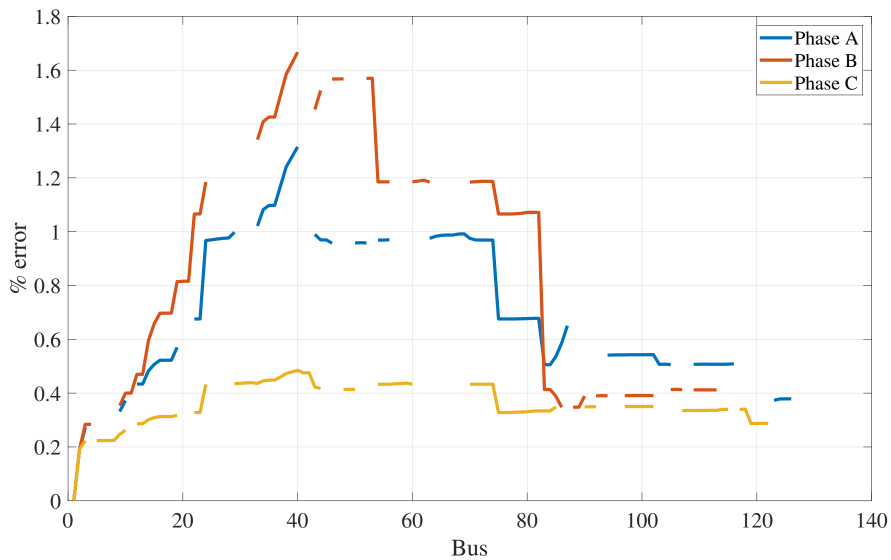

Figure 5.6: Percentage error of voltage profiles for three phases for 10% DG penetration case.

Table 5.3: Result comparison for IEEE 123 bus system with 10% DG penetration case

	PsubA (KW)	QsubA (KVar)	PsubB (KW)	QsubB (KVar)	PsubC (KW)	QsubC (KVar)
Power Flow	1037.4	407.6	586	72.1	815.1	227.7
OPF	1089.0	490.0	586.5	194.7	814.9	272.1

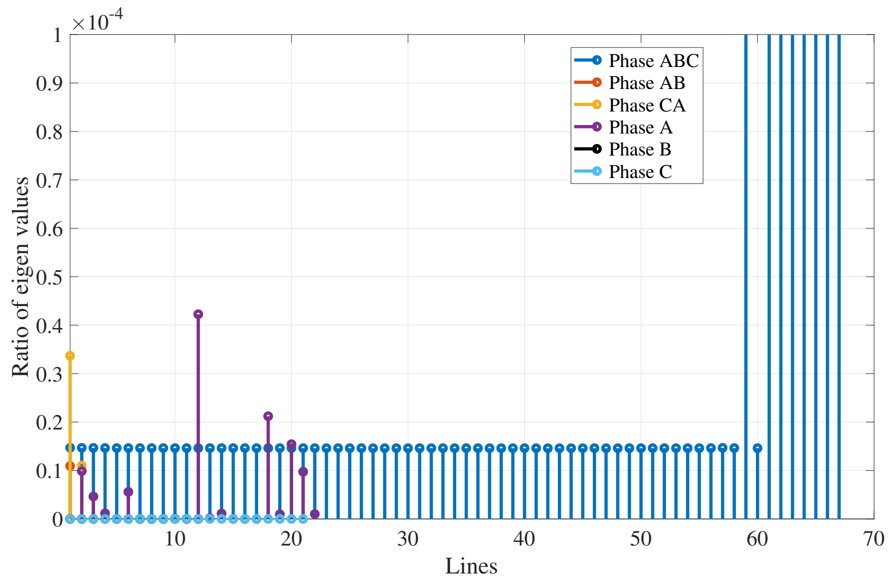

Figure 5.7: ratio of first two eigenvalues of PSD matrix for each branch represents the matrix's rank.

Table 5.4: Computational time to solve OPF for test systems in different formulations

Formulations	Solver Time (s)	
	123 bus	650 bus
NLP-PF(Current Injection)	0.5089	21.41
BFM-SDP OPF	0.5291	2.3167

implement for multi-period approach for receding horizon control (RHC). Receding horizon control is used to forecast dispatches in the day ahead approach. In this approach, the time horizon for a whole time window is moving forward, and the optimization problem is solved in each. The concept of receding horizon control is depicted in Fig 5.8. The advantage of receding horizon control is that it can be considered in solving the problem if some changes or adjustments occur at any time

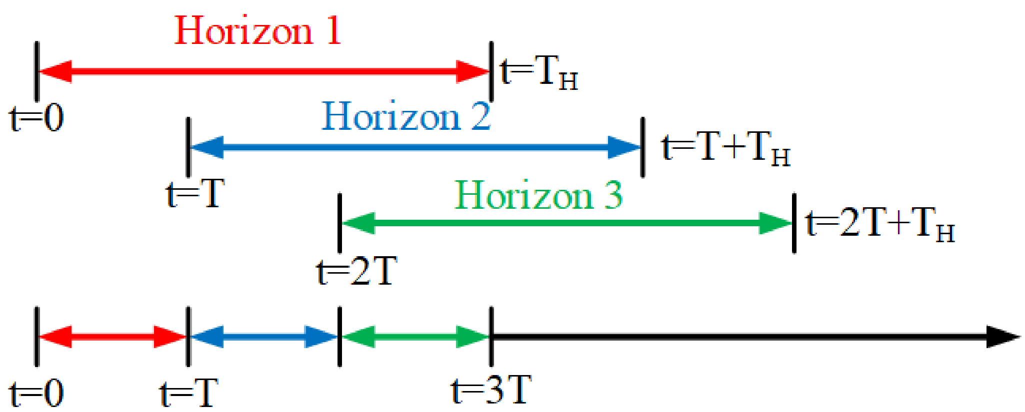

Figure 5.8: Concept of moving time horizon in receding horizon control method.

window. This removes the necessity to solve the whole issue for the total time. The implementation of RCC using the proposed BFM-SDP OPF proves the scalability of the method. In Fig 5.9 we have shown the substation active and reactive power dispatch profiles for a period of 12 hours. For this case, 10% DER penetration of the network was considered. The substation power from OPF is compared with the power flow results for the same DER setpoints. The comparison shows the exactness of the solution. We can see that, except for some hours, the active and reactive power dispatch is almost similar to the power flow solution. In this simulation, a moving horizon of 6 hours was considered, moving forward through the time window.

5.5 Summary

The proposed formulation for unbalanced radial distribution networks includes voltage regulator modeling, line switches, and mutual coupling in the branch impedance matrix. The relaxation is considered to be exact, and the solutions are conclusive considering the comparison with the power flow solution for similar operating conditions. The implementation of receding horizon control using the proposed method opens up the scope of integration of different inter-temporal constraint to the OPF problem.

[a]

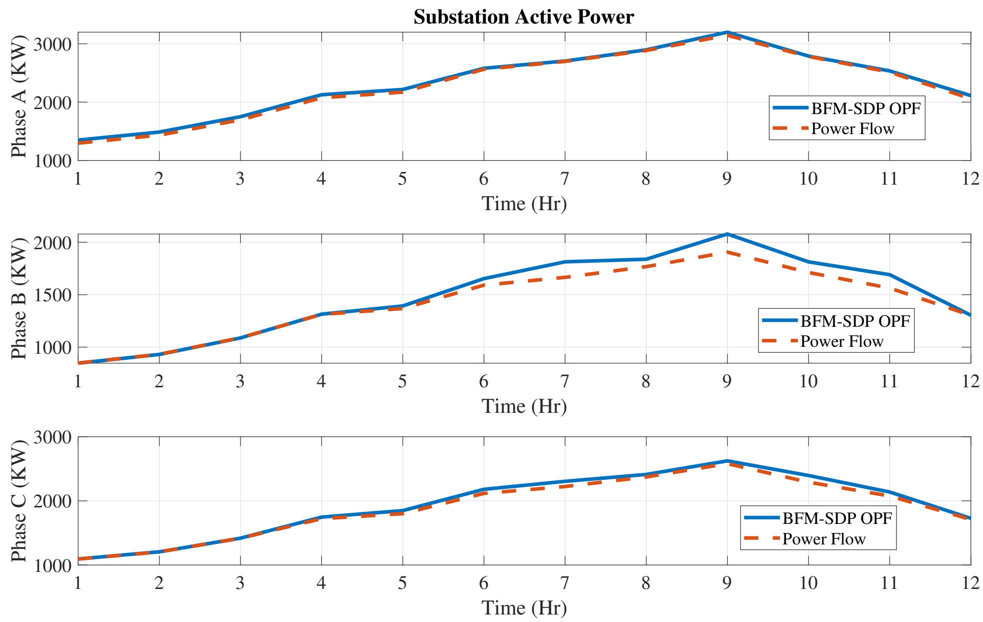

[b]

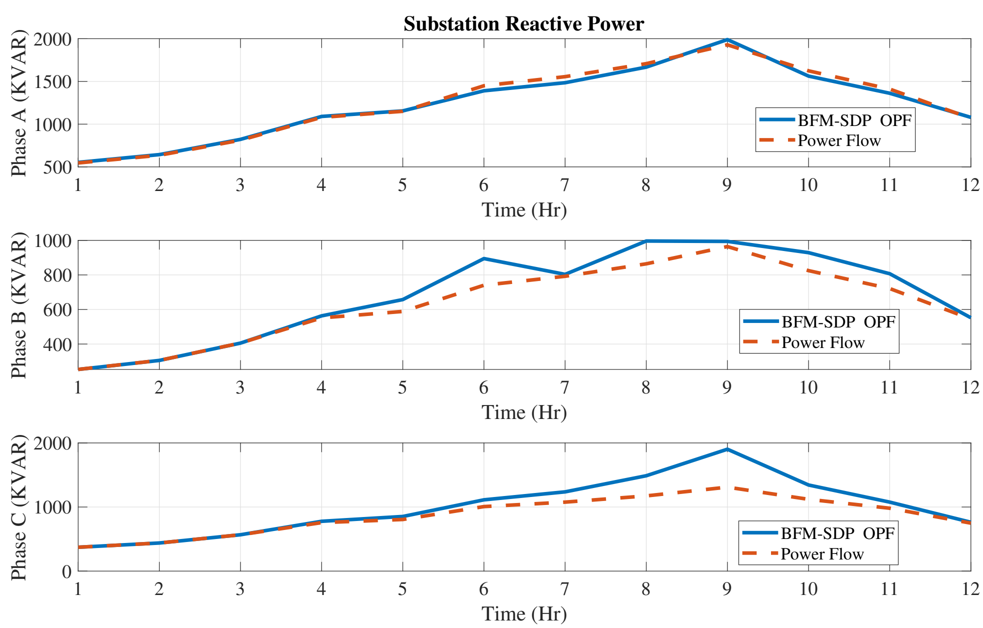

Figure 5.9: Active and reactive power dispatch from substation compared with the power flow solution with similar DER support to check the tightness of solution.

CHAPTER 6: ADMM BASED DISTRIBUTED OPTIMIZATION FOR DER INTEGRATED POWER DISTRIBUTION SYSTEM

6.1 Introduction

This chapter presents the formulation of distributed optimal power flow for large distribution networks based on ADMM and SDP relaxation. The objective of OPF is to minimize or maximize a cost function such as minimizing the generation cost, line losses, or maximizing voltage stability, DG generation. Numerous economic operations of power systems such as economic dispatch, unit commitment, demand response, and volt-var control are designed around OPF. Since the first approach to solve the OPF problem was proposed by J. Carpentier in 1962 [3], many approaches have been proposed by researchers to solve the problem. Detailed survey literature on different formulations of OPF and the evolution of the problem formulation can be found in [4, 5, 6, 7, 8, 9, 10, 11, 12, 13]. The original alternating current optimal power flow (AC-OPF) problem is a non-linear, non-convex optimization problem. Different relaxation methods have been explored to handle the non-convexity of the problem. Semidefinite programming (SDP), second-order cone programming (SOCP), and chordal relaxation are the most popular. Initially bus injection models (BIM) of transmission networks utilized both SDP relaxation [65, 108, 102] and SOCP relaxation [109, 110] for OPF formulation. Since these are the relaxed model of the original problem, the formulation is said to be exact if the solution of the original problem can be recovered from the relaxed model. However, radial network modeling requires additional considerations for exact modeling.

Another aspect of the conventional OPF formulations is that they are primarily centralized operations. This means the original network is formulated as one single problem and solved as one model. However, as the distributed generation is becoming more and more popular in today's power system, it increases the total number of variables in the formulation, thus increasing the problem's difficulty level [111]. So, OPF formulation of real-world distribution networks with thousands of nodes and high DG penetration is complicated to solve with a centralized approach. Thus there is a real need to solve distributed formulation of the OPF problem for the future distribution grid. In that regard, various distributed approaches have been proposed by different researchers. The generalized approach breaks down the OPF problem into subproblems that can be solved simultaneously. There are distributed formulations based on the AC non-convex OPF problem as in [112, 113] which used the method of multipliers. Tesun2013fully the formulation leveraged ADMM for distributed optimization, but the main disadvantage of such formulation is that it does not guarantee convergence. On the other hand, the distributed formulation of the convexified OPF problem ensures convergence; primarily, ADMM-based convex methods combine the benefits of the dual decomposition [114].

In this chapter, an approach has been proposed where a radial system is divided into multiple regions. This division can be based on different criteria such as geographical location, the position of the SVR, placement of the transformer, or switches. In this approach, two main aspects are significant: intra-regional optimization and inter-regional coordination. The intra-regional optimization model has been formulated by utilizing the SDP relaxed branch flow model, and the inter-regional coordination is implemented with the help of ADMM. The main contributions of this chapter are as follows. This approach provides a simplified architecture to implement the distributed formulation of the OPF problem for the radial distribution network. It identifies the consensus region for the split network and implements ADMM to solve the OPF problem in a fully distributed approach. All the regional OPF problems are parallelizable and computationally cheaper than other distributed OPF counterparts.

The rest of the chapter is organized in the following order. Section II describes the mathematical preliminaries regarding the ADMM and OPF problem formulation. Section III describes the proposed distributed OPF formulation based on ADMM; system description and numerical case studies are discussed in section IV. Finally, section V concludes the chapter and briefly discusses the future extension of this work.

6.2 Mathematical Preliminaries

ADMM is an algorithm that leverages the better convergence properties of the method of multipliers to solve constrained optimization problems. Assume a problem in the following form,

$$\begin{aligned} &Min\ f(x) + g(y) \\ &s.t. Ax + By = c \end{aligned} \tag{6.1}$$

Here, $x \in$ and $y \in$ are the variables and A and B are parameter matrices. The augmented Lagrangian equation of this problem can be written as:

$$\begin{aligned} &L_\rho(x, z, \beta) = f(x) + g(y) + \beta^T(Ax + By - c) \\ &+ \frac{\rho}{2}||Ax + By - c||_2^2 \end{aligned} \tag{6.2}$$

ADMM solves the problem in three updation steps. First, x is updated with fixed y, then y is solved with updated x from the previous step, and in the final step, β is updated from fixed values of x and y. These steps are as follows.

$$x^{k+1} := \arg\min_{x}\{f(x) + (\beta^k)^T(Ax + By^k - c) \tag{6.3}$$

$$+ \frac{\rho}{2}||Ax + By^k - c||_2^2\}$$

$$y^{k+1} := \arg\min_{y}\{g(y) + (\beta^k)^T(Ax^{k+1} + By - c) \tag{6.4}$$

$$+ \frac{\rho}{2}||Ax^{k+1} + By - c||_2^2\}$$

$$\beta^{k+1} := \beta^k + \rho(Ax^{k+1} + By^{k+1} - c) \tag{6.5}$$

Here $\rho > 0$ is the penalty factor, and β is the vector of lagrangian multipliers. The convergence of the ADMM depends on the following criterion,

$$\lim_{k\to\infty}(Ax^{k+1} + By^{k+1} - c) = 0$$

6.2.1 Consensus Optimization via ADMM

If the objective function of the ADMM problem consists of N terms, then the problem takes a new form, known as consensus ADMM. This form of the objective function may represent minimizing the loss function of an individual area of the distribution system or minimizing the line losses of a region of a large distribution network. The problem can be written as

$$Min \sum_{i=1}^{N} f(x) \tag{6.6}$$

$$s.t. x_i - y = 0$$

Here, x_i is the local variable, and y is the global variable, where the objective is to converge all the local variables to the global value. In our application, the objective is to minimize the line power loss in the network. The branch flow model formulation variables are bus voltage magnitude, line current, and active and reactive line power flow. Thus in the consensus formulation, the constraint would be to converge the bus voltage and line power flow of certain buses and lines between the regions observed from each region. Section 6.3 discusses the definition of these local and global variables, where the ADMM-based OPF problem is formulated. The augmented Lagrangian function for this scenario can be written as,

$$L_\rho(\mathbf{x}, y, \beta) = \sum_{i=1}^{N}(f(x_i) + \beta^T(x_i - y) + \frac{\rho}{2}||x_i - y||_2^2)$$

The local variables x_i and the global variable y are updated using the following steps,

$$x_i^{k+1} := \arg\min_x \{f(x_i) + (\beta^k)^T(x_i - y^k) + \frac{\rho}{2}||x_i - y^k||_2^2\} \tag{6.7}$$

$$y^{k+1} := \frac{1}{n}\sum_{i=1}^{N}(x_i^{k+1}) \tag{6.8}$$

$$\beta^{k+1} := \beta^k + \rho(x_i^{k+1} - y^{k+1}) \tag{6.9}$$

We propose a consensus ADMM approach to solve the OPF problem of a large distributed network where all the regions solve their OPF problem for a constraint set and a global variable y. This iterative updating process continues till the error reduces below the threshold value.

6.3 ADMM Based OPF Formulation

In the distributed approach to solving the OPF of a power network, consider that the network is divided into multiple areas. Among them, one is the master network, and the others are the sub-networks. There are communication links established between master and sub-networks to exchange information. As shown in Figure 6.1, let us assume the whole network is divided into 3 regions, where nodes $1, ...5$ belong to the master network, nodes $6, ..., 8$ belong to sub-network 1, and nodes $9, ...12$

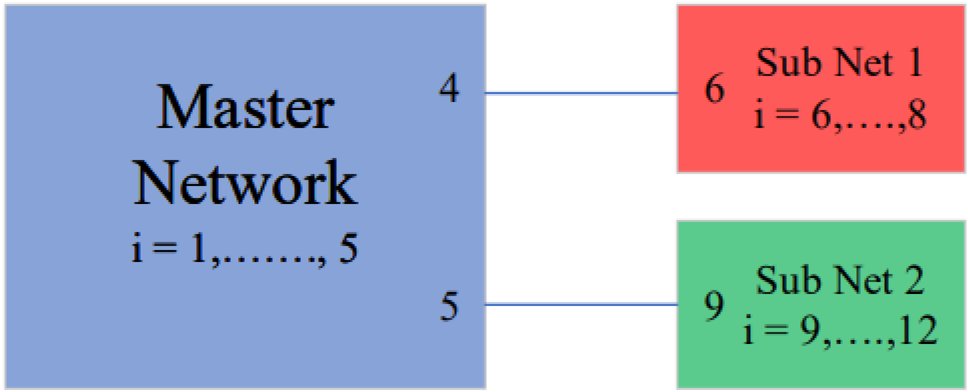

Figure 6.1: A distribution system divided into three regions

belongs to sub-network 2. Also, the branches between $4-6$ shared by both master network and sub-network 1 and $5-9$ shared by master network and sub-network 2. Basically the area covered by branches $4-6$ and $5-9$ is the consensus area and the variables $P_{4-6}, P_{5-9}, Q_{4-6}, Q_{5-9}, V_4, V_5, V_6, V_9$ represents the global variable Z. Each area will solve the OPF problem of its region in parallel and assign the values. Next, the global variable will be updated based on values calculated by each local iteration. Then consensus will be achieved considering the preset threshold value.

6.3.1 Decentralized ADMM by Substituting Lagrange Multiplier

The consensus ADMM, as well as the original formulation of ADMM, does not ensure a fully decentralized formation. The local variable and Lagrange multiplier update using (6.3) and (6.5) can be performed locally. However, updating the global variables using (6.4) for overlapping regions requires executing a central controller. By replacing the global variable y and Lagrange multiplier β, it is possible to formulate a fully decentralized model. For that purpose, a new local variable vector w is introduced for area a corresponding to the Lagrange multiplier β_i,

$$w_a^k := y_a^k - \beta_a^k/\rho \tag{6.10}$$

Further, leveraging the features of radial distribution networks, ADMM can be reformulated for any local problem as

$$x_a^{k+1} := \arg\min_x \{f(x_a) + \frac{\rho}{2}||x_a - w^k||_2^2\} \tag{6.11}$$

$$w_a^k := w_a^k + x_a^{k+1} - \frac{x_a^{k+1} + x_b^{k+1}}{2} \tag{6.12}$$

6.3.2 Auto Tuning of Penalty Parameter by Residual Balancing

The convergence of ADMM based OPF problem is mathematically proven, although the speed to convergence depends significantly on the choice of penalty parameter. One way to accelerate the ADMM convergence is to vary the penalty parameter depending on the residual values from each iteration. Various approaches have been proposed by the researchers to implement a self-tuning penalty parameter model. Most of those approaches require a central controller to look at the residual values and update the penalty parameter. In the decentralized approach, the penalty parameter for each area can be updated based on the local primal and dual residual values. So central coordination is not required anymore. The penalty parameter tuning can be performed as

$$\rho_i^{k+1} = \begin{cases} \frac{\rho_i^k}{1+\tau}, & \text{if } ||r_i^k||_2 \leq \mu||d_i^k||_2, \\ (1+\tau)\rho_i^k, & \text{if } ||d_i^k||_2 \leq \mu||r_i^k||_2, \\ \rho_i^k, & \text{otherwise.} \end{cases} \tag{6.13}$$

where μ and τ are parameters whose values are usually selected as $\mu = 0.1$ and $\tau = 1.0$.

6.3.3 Accelerated ADMM Method

In the accelerated ADMM approach, additional steps are included to update the global variable y^{k+1} and Lagrange multiplier β^{k+1} as follows

$$\hat{y}_i^{k+1} = \alpha^k.y^{k+1} + (1-\alpha^k).y^k \tag{6.14}$$

$$\hat{\beta^{k+1}} = \alpha^k.\beta^{k+1} + (1-\alpha^k).\beta^k \tag{6.15}$$

$$\alpha^k = \begin{cases} 1 + \frac{\gamma^k - 1}{\gamma^{k+1}}, & if \frac{max(||r^k||_2, ||s^k||_2)}{max(||r^{k-1}||_2, ||s^{k-1}||_2)} \leq 1 \\ 1, & otherwise \end{cases} \tag{6.16}$$

where $\gamma = [1 + \sqrt{1 + 4(\gamma^{k-1})^2)}]/2$ for $k > 1$. Here r and s stand for the primal and dual residuals.

6.3.4 BFM-SDP OPF

In this chapter, we mostly focus on formulating the OPF problem for the distribution systems. Hence the Branch Flow Model of the system is adopted to formulate the OPF problem. Let us assume a graph $G = (N, E)$ represents a radial distribution network where N is the set of all vertices, and E is the set of all branches. The branch flow model comprises branch variables such as branch current, branch active, and reactive power flow. Let V_i be the voltage of node i, S_{ij} and I_{ij} is the complex power and currently flown through branch $i - j$, then the branch flow model can be stated as follows

$$V_i - V_j = z_{ij} I_{ij}, \forall (i,j) \in E \tag{6.17}$$

$$S_{ij} = V_i I_{ij}^*, \forall (i,j) \in E \tag{6.18}$$

$$\sum_{k:j \to k} S_{jk} - \sum_{i:i \to j} (S_{ij} - z_{ij}|I_{ij}|^2) + y_j^* |V_j|^2 = s_j \tag{6.19}$$

Here, z_{ij} is the branch impedance, and s_j is the injected complex power at node j. The relaxed branch flow model is adopted from this equation by ignoring the angles of the variables. By substituting the expression of current I_{ij} from (6.18) into (6.17) yields $V_i - V_j = z_{ij}S_{ij}^*/V_i^*$. Then taking the square of the magnitudes of this expression derives the equation (6.21) as shown below. In the relaxed model the squared terms of the node voltage and branch current replaces the previous variables as $v_i = |V_i|^2$ and $l_{ij} = |I_{ij}|^2$. The relaxed BFM model is

$$s_j = \sum_{k:j\to k} S_{jk} - \sum_{i:i\to j} (S_{ij} - z_{ij}l_{ij}) + y_j v_j, \forall j \in E \tag{6.20}$$

$$v_j = v_i - 2(z_{ij}^* S_{ij} + z_{ij}S_{ij}^*) + z_{ij}l_{ij}z_{ij}^*, \forall (i,j) \in E \tag{6.21}$$

$$l_{ij} = \frac{|S_{ij}|^2}{v_i}, \forall (i,j) \in E \tag{6.22}$$

The non-linear equation (6.22) can be expressed in terms of a positive semidefinite matrix as follows:

$$\begin{bmatrix} v_i & S_{ij} \\ S_{ij}^* & \lambda_{ij} \end{bmatrix} \succcurlyeq 0$$

$$rank \begin{bmatrix} v_i & S_{ij} \\ S_{ij}^* & \lambda_{ij} \end{bmatrix} = 1$$

The abovementioned equations still hold the non-convexity due to the rank-1 constraint of the PSD matrix. Relaxing the equation by adopting the semidefinite relaxation (SDR), the BFM-SDP OPF problem is formulated:

$$Min \sum_{i:i\rightarrow j} z_{ij} I_{ij} \tag{6.23}$$

$$s.t. \begin{cases} s_j = \sum_{k:j\rightarrow k} S_{jk} - \sum_{i:i\rightarrow j}(S_{ij} - z_{ij}|l_{ij}|^2) + y_j v_j \\ v_j = v_i - (S_{ij} z_{ij}^* + z_{ij} S_{ij}^*) + z_{ij}\lambda_{ij} z_{ij}^* \\ \begin{bmatrix} v_i & S_{ij} \\ S_{ij}^* & \lambda_{ij} \end{bmatrix} \geq 0 \\ v_{ref} = V_{ref} V_{ref}^* \\ v^{min} \leq v_i \leq v^{max} \\ S^{min} \leq S_i \leq S^{max} \end{cases}$$

6.3.5 Implementing Consensus ADMM Based BFM-SDP-OPF

The distributed problem can be formulated for each region based on the consensus ADMM and the BFM-SDP OPF formulation. Before that, the global variable z can be defined as, $y^{'=[P_{mn}Q_{mn}P_{lt}Q_{lt}V_m V_l]}$. The augmented OPF problem for each region can be formulated as follows. For the master network, all the nodes, as shown in Fig.6.1 along with the consensus region nodes, are considered to formulate the augmented

OPF problem.

$$Min \sum_{i:i\to j} z_{ij}I_{ij} + (\beta_1^k)^T(x_1 - y_1^k) + \frac{\rho}{2}||x_1 - y_1^k||_2^2 \tag{6.24}$$

$$s.t. \begin{cases} s_j = \sum_{k:j\to k} S_{jk} - \sum_{i:i\to j}(S_{ij} - z_{ij}|l_{ij}|^2) + y_j v_j \\ v_j = v_i - (S_{ij}z_{ij}^* + z_{ij}S_{ij}^*) + z_{ij}\lambda_{ij}z_{ij}^* \\ \begin{bmatrix} v_i & S_{ij} \\ S_{ij}^* & \lambda_{ij} \end{bmatrix} \geq 0 \\ v_{ref} = V_{ref}V_{ref}^* \\ v^{min} \leq v_i \leq v^{max} \\ S^{min} \leq S_i \leq S^{max} \end{cases}$$

where $y_1 = y$

Similarly, for sub-network 1, the augmented OPF problem can be formulated with updated y as follows

$$y_2 = \Big[P_{mn}, Q_{mn}, V_m\Big]^T$$

The augmented Lagrangian objective function for sub-network 1 is as follows:

$$Min \sum_{i:i\to j} z_{ij}I_{ij} + (\beta_2^k)^T(x_2 - y_2^k) + \frac{\rho}{2}||x_2 - y_2^k||_2^2 \tag{6.25}$$

Further, for sub-network 2, the augmented OPF problem can be formulated with updated y as follows,

$$y_3 = \Big[P_{lt}, Q_{lt}, V_l\Big]^T$$

With the objective function as

$$Min \sum_{i:i \to j} z_{ij} I_{ij} + (\beta_3^k)^T (x_3 - y_3^k) + \frac{\rho}{2} ||x_3 - y_3^k||_2^2 \tag{6.26}$$

Once all the regions have done solving for the variable $\mathbf{x}$ then, the global variable y is updated using Eq. (8) as,

$$\begin{aligned} y(1,3,5) &= 0.5 * [y_1(1,3,5) + y_2] \\ y(2,4,6) &= 0.5 * [y_1(2,4,6) + y_3] \end{aligned} \tag{6.27}$$

The primal and dual residual of the formulation are denoted as follows,

$$\begin{aligned} r^k &= ||x^k - y^k||_2 \\ s^k &= \rho ||y^k - y^{k-1}||_2 \end{aligned} \tag{6.28}$$

After that, the dual variable is updated using Eq. 6.38. Finally, the error is calculated as,

$$error^k = \left\| \begin{matrix} r^k \\ s^{k-1} \end{matrix} \right\|^2 \tag{6.29}$$

The error threshold cut-off value is $10e^{-4}$. A global consensus is achieved if the error value becomes less than the threshold.

6.3.6 Proposed Decentralized-SDP(D-SDP) OPF in ADMM Framework

6.3.6.1 Local OPF Problem for Each Area

-Based on the BFM-SDP model described in the previous sub-section, the local OPF problem for each area can be formulated. For example, let's consider the network topology shown in Fig 6.1 where the whole network is partitioned into three local areas. The network partitioning can be done based on different aspects such as geographical location, voltage regulator position, or location of the network switches. Lets assume the set of buses of the local areas are denoted as $N_1 = \{1-5, 6, 9\}$, $N_2 = \{4, 6-8\}$, $N_3 = \{5, 9-12\}$. Now the set of adjoining buses are $N_1 \cap N_2 = \{4, 6\}$, $N_1 \cap N_3 = \{5, 9\}$. Then the local OPF problems for each of these areas can be written as follows:

Local OPF 1

$$Min \sum_{i:i\to j}^{N_1} z_{ij} I_{ij}$$

Local OPF 2

$$Min \sum_{i:i\to j}^{N_2} z_{ij} I_{ij}$$

Local OPF 2

$$Min \sum_{i:i\to j}^{N_3} z_{ij} I_{ij}$$

subject to

(25) - (30)

6.3.6.2 Distributed Formulation of OPF

Since all the local OPF problems are part of the global OPF for the whole network, they need to communicate with each other to achieve the global optimal solution. To do so, the objective functions of the local OPF problem are modified to the form of an augmented lagrangian where the difference between local variable and global variables are included along with the Lagrange multiplier and penalty parameters.

The updated objective functions are as follows:

$$Min \sum_{i:i\to j}^{N_1} z_{ij}I_{ij} + (\beta_1^k)^T(x_1 - y_1^k) + \frac{\rho}{2}||x_1 - y_1^k||_2^2 \tag{6.30}$$

$$Min \sum_{i:i\to j}^{N_2} z_{ij}I_{ij} + (\beta_2^k)^T(x_2 - y_2^k) + \frac{\rho}{2}||x_2 - y_2^k||_2^2 \tag{6.31}$$

$$Min \sum_{i:i\to j}^{N_3} z_{ij}I_{ij} + (\beta_3^k)^T(x_3 - y_3^k) + \frac{\rho}{2}||x_3 - y_3^k||_2^2 \tag{6.32}$$

Here, x_1, x_2, x_3 denotes the set of local variable, $y_1 = \{v_4, v_5, v_6, v_9, P_{4,6}, Q_{4,6}, P_{5,9}, Q_{5,9}\}$, $y_2 = \{v_4, v_6, P_{4,6}, Q_{4,6}\}$ and $y_3 = \{v_5, v_9, P_{5,9}, Q_{5,9}\}$ are the set of global consensus variables. These global variables are needed to be updated in a separate step once the central coordinator receives the information from local areas. Then, the Lagrange multipliers β_1, β_2 and β_3 are updated. In the objective functions, k denotes the number of iterations, and ρ stands for the penalty parameter. The $||.||_2$ denotes the second norm of the variables.

6.3.6.3 Decentralization of the Distributed Model

In the fully decentralized proposed ADMM approach, the main contributions when compared to the state-of-the-art are a) relaxing the global variable and introducing an auxiliary local variable and b) introducing the convex model in the ADMM framework, The combined formulation takes the form as

$$x_i^{k+1} := \arg\min_x \{f(x_i) + \frac{\rho}{2}||x_i - w^k||_2^2\} \tag{6.33}$$

$$w_i^{k+1} := w_i^k + x_i^{k+1} - \frac{x_i^k + x_j^k}{2} \tag{6.34}$$

For a generic network, as shown in Fig.6.1, the detailed implementation of the proposed approach is explained below. The boundary bus i which is shared by adjoining areas 1 and 2 will have it's variables denoted as $x_{1,i}$ and $x_{2,i}$. For the network in example, $x_{1,4} = x_{2,4} = y_4$, $x_{1,6} = x_{2,6} = y_6$, $x_{1,5} = x_{3,5} = y_5$ and $x_{1,9} = x_{3,9} = y_9$. Now, to implement the decentralized approach, a local auxiliary variable is introduced to replace the global variable as

$$\begin{aligned}
w_{1,4} &= y_4 - \frac{\beta_{1,4}}{\rho} & \qquad w_{1,6} &= y_6 - \frac{\beta_{1,6}}{\rho} \\
w_{2,4} &= y_4 - \frac{\beta_{2,4}}{\rho} & \qquad w_{2,6} &= y_6 - \frac{\beta_{2,6}}{\rho} \\
w_{1,5} &= y_5 - \frac{\beta_{1,5}}{\rho} & \qquad w_{1,9} &= y_9 - \frac{\beta_{1,9}}{\rho} \\
w_{3,5} &= y_5 - \frac{\beta_{3,5}}{\rho} & \qquad w_{3,9} &= y_9 - \frac{\beta_{3,9}}{\rho}
\end{aligned}$$

With the help of these local auxiliary variables, the update equation for area 1 can be written as,

$$x_{1,i}^{k+1} := \arg\min_{x}\{f(x_{1,i}) + \frac{\rho}{2} \sum_{j \in N_1 \cap N_2 \cap N_3} ||x_{1,j} - w_{1,j}^k||_2^2\} \tag{6.35}$$

$$w_{1,j}^{k+1} := w_{1,j}^k + x_{2,j}^{k+1} - \frac{x_{1,j}^k + x_{2,j}^k}{2}; j \in N_1 \cap N_2 \cap N_3 \tag{6.36}$$

Here, the variable vectors can be expressed as, $x_1 = \{v_4, v_6, P_{4,6}, Q_{4,6}, v_5, v_9, P_{5,9}, Q_{5,9}\}$ and $w_1^k = \{\hat{v}_4^k, \hat{v}_6^k, \hat{P}_{4,6}^k, \hat{Q}_{4,6}^k, \hat{v}_5^k, \hat{v}_9^k, \hat{P}_{5,9}^k, \hat{Q}_{5,9}^k\}$. Then the local OPF problem for area 1 will take the form as shown below:

$$Min \sum_{i:i\to j} z_{1,ij} I_{1,ij} + \frac{\rho_1}{2}[(x_1 - w_1^k)^2] \tag{6.37}$$

subject to

(25) - (30)

Once the OPF is solved, the local auxiliary variable w_1^{k+1} is updated using (36), and then the residuals are calculated for area 1 using the following equations:

$$r_1^k = ||(x_{1,j}^k - x_{2,j}^k)/2|| \tag{6.38}$$

$$d_1^k = ||((x_{1,j}^k + x_{2,j}^k) - (x_{1,j}^{k-1} + x_{2,j}^{k-1}))/2|| \tag{6.39}$$

The convergence is assumed to be achieved once all the residuals are calculated and $max(r^k, d^k) \leq \epsilon$. The error threshold cutoff value is $10e^{-4}$.

6.3.6.4 Auto Tuning of Penalty Parameter

If the convergence is not reached for the subproblem, then the penalty parameter is updated using 6.40 based on the primal and dual residual ratio.

$$\rho_i^{k+1} = \begin{cases} \frac{\rho_i^k}{1+\tau}, & \text{if } ||r_i^k||_2 \leq \mu||d_i^k||_2, \\ (1+\tau)\rho_i^k, & \text{if } ||d_i^k||_2 \leq \mu||r_i^k||_2, \\ \rho_i^k, & \text{otherwise.} \end{cases} \tag{6.40}$$

Here the value of ρ, τ, and μ are initialized at the beginning of the algorithm. The update of the penalty parameter based on the relativity between the primal and dual residual speeds up the convergence process. Since the penalty parameter update depends only on the local residual, the decentralized approach stays operational without the requirement of a central coordinator.

Algorithm 2 Proposed Distributed OPF

```
Input network data.
Initialize y ← {1, 0}
Initialize ρ and β for ADMM formulation.
while (error^k ≥ 10^-4) do
    Update x_1 for region 1 using (6.24)
    Update x_2 for region 2 using (6.25)
    Update x_3 for region 3 using (6.26)
    Update y using (6.27)
    Update β for each region using (6.9)
    Calculate primal and dual residual using (6.38)
    error ← max(r^k, d^k)
end while
```

Algorithm 3 Proposed D-SDP ADMM

```
Initialize β ← rand, y ← {1, 0} and ρ ← 10 for each subsystem.
Initialize μ ← 0.1 and τ ← 1
Initialize the error ← 100.
Solve local OPF for each subsystem using objective function as (6.11).
All the adjacent subsystems share the solution for consensus variables.
Update the local auxiliary variables using (6.12).
Broadcast the updated local auxiliary variables to the adjacent subsystems.
Calculate the local primal and dual residuals, r_a, d_a in all subsystems.
error ← max(r_a^{k+1}, d_a^{k+1})
if (error ≥ 1e^-4) then
    Update the penalty parameter in each subsystem using (6.13)
end if
```

6.4 Result and Analysis

To test the scalability of the proposed approach, a large distribution network such as a modified IEEE 123 bus system is utilized. The existing network is three-phase and unbalanced. For this approach, the single-phase version is used, which is the positive sequence equivalent of the existing network. The system operates at 4.16KV. The total load connected to the system is 1163.3KW and 640KVAR. Some further modifications were also done. Some distributed generation (DG) plants are introduced into the system. The capacity of the DG generation is 10% of the total connected load. The maximum active power generation capacity of the DG plants is considered equal to the active power demand of the respective bus. And the KVA rating of the DG plants is considered 120% of the active power rating. The plants' upper and lower bound for the reactive power generation capacity are calculated.

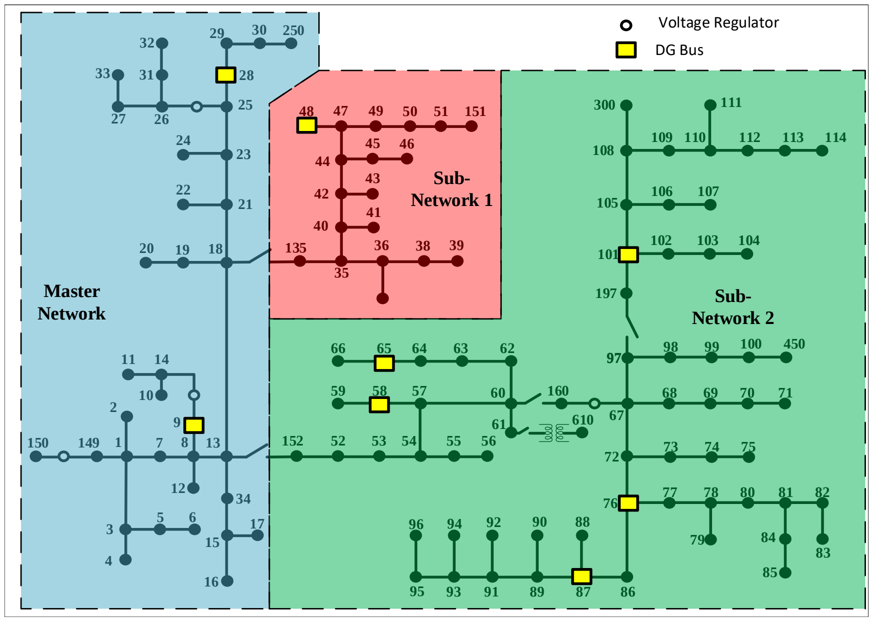

Figure 6.2: Modified IEEE 123 bus system with 10% DG penetration

Then the whole network is divided into three regions. There are switches between nodes 20-118 and 15-117. The partitions are made on the location of those two switches. The area containing substation node 1 is considered the master network. This area is marked with a blue line in the figure. Next, the area enclosed by the red line is considered sub-network 1. This is connected to the master network through the switch between 20-118. Finally, the rest of the network is considered sub-network 2, connected to the master network through the switch at 15-117 and marked by a green line in the figure. A single-line diagram of the network along with the DG plant's location in all three regions is shown in Fig.6.2.

In this case study, different scenarios were run for different values of penalty factor ρ. It is known that primal and dual residual values, as well as the convergence speed, depend greatly on the value of the penalty factor. A higher-valued penalty factor increases dual variables; on the other hand, primal residual increases for smaller

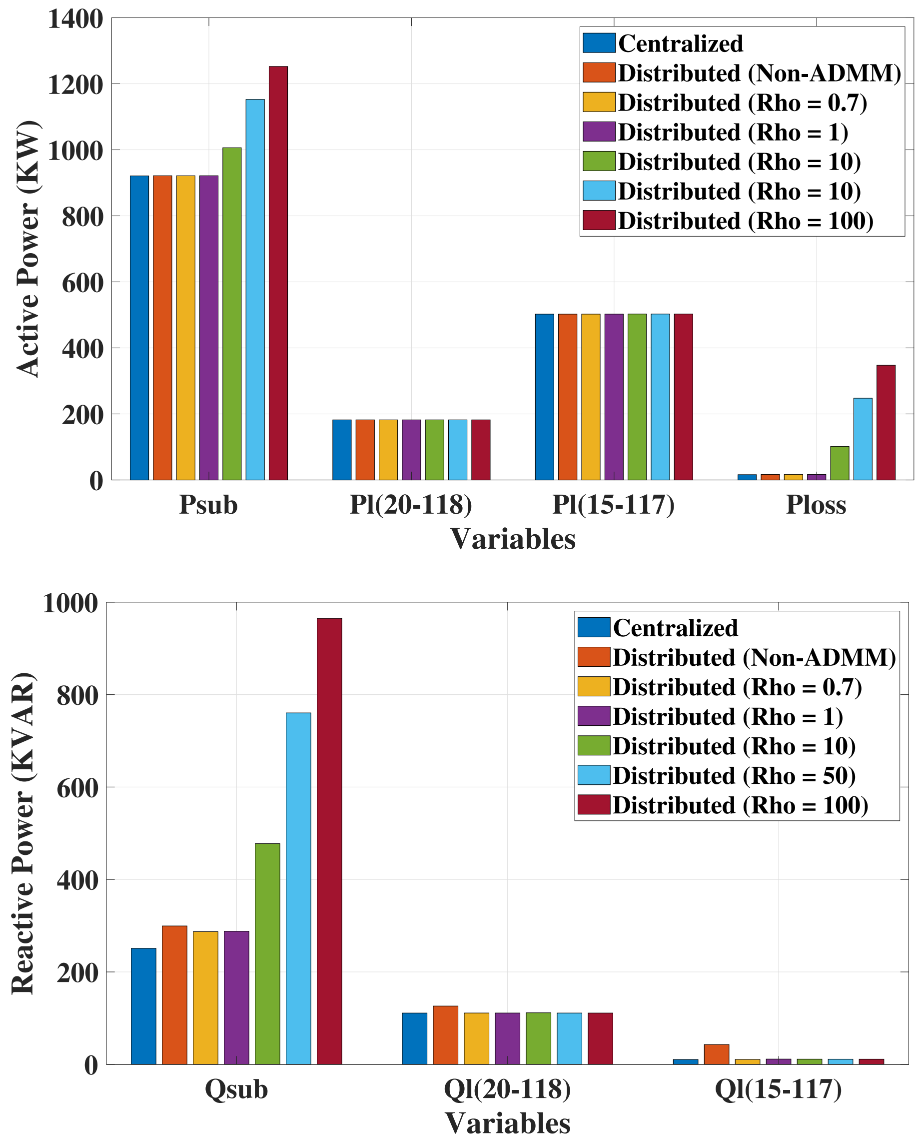

Figure 6.3: Comparison of substation active and reactive power, line power through connecting lines, and active power loss for different scenarios.

penalty factors. Here we ran the simulation for different values of ρ such as, $\rho = 0.7, 1.0, 10, 50, 100$. The change in the number of iterations for convergence with the change of penalty factor is observed. We can see in Fig.6.6 that, as the penalty factor value increases, the value of dual residual increases. Though with a higher value of penalty parameter, the gap between primal and dual residual decreases faster, the solution for the lower value of ρ is more optimal. That statement can be proved

Table 6.1: OPF solution comparison

Units KW/Kvar	Centralized BFM-SDP	Distributed Non-ADMM	Distributed ($\rho =$)			
			0.7	1	10	50
P_sub	921.0474	921.5347	921.4553	921.5349	1006.326	1152.632
Q_sub	251.0378	299.4837	287.1654	288.0038	477.5972	760.4315
P_loss	16.0574	16.5447	16.4653	16.5449	101.3359	247.6421
P_{20-118}	182.0654	182.1052	182.0667	182.0667	182.0837	182.0843
Q_{20-118}	111.0626	126.2216	111.1589	111.149	111.6502	111.1006
P_{15-117}	502.3250	502.3033	502.3359	502.4029	502.6494	502.6225
Q_{15-117}	10.61	42.9596	16.4653	11.4644	11.3007	11.1947
Time (s)	0.31	0.35	0.32	0.34	0.31	0.30

by the numerical results showcased in Table 6.1. The performance of the proposed approach is also compared with another distributed OPF method proposed in [115] which is noted as "Distributed (Non-ADMM) in the Table and figures. To compare the solution of the proposed approach with the centralized OPF solution, the active and reactive power generation from the substation, the total active power loss in the system, and the node voltage profile are compared in Fig. 6.3. It can be seen in Table 6.1 that, with the decrease of the value of ρ, the number of iterations increases, albeit the resultant voltage profile is closer to the centralized OPF solution's profile. The comparison of the voltage profiles is shown in Fig. 6.5. It is also evident the significance of choosing an appropriate penalty parameter. Since the formulation fails to converge for a lower value as $\rho = 0.1$. The percentage optimality of the solution from different values of the penalty factor can also be realized using the % error with respect to the solution from the centralized approach. The % error in substation active and reactive power is shown in Fig. 6.7.

6.4.1 Performance Analysis of D-SDP ADMM OPF

The proposed methodology is implemented on the following two IEEE test systems, real-life feeders of power distribution systems. They are a) modified IEEE 123 bus system as shown in Fig 6.8 and b) modified IEEE 8500 bus system as shown in Fig

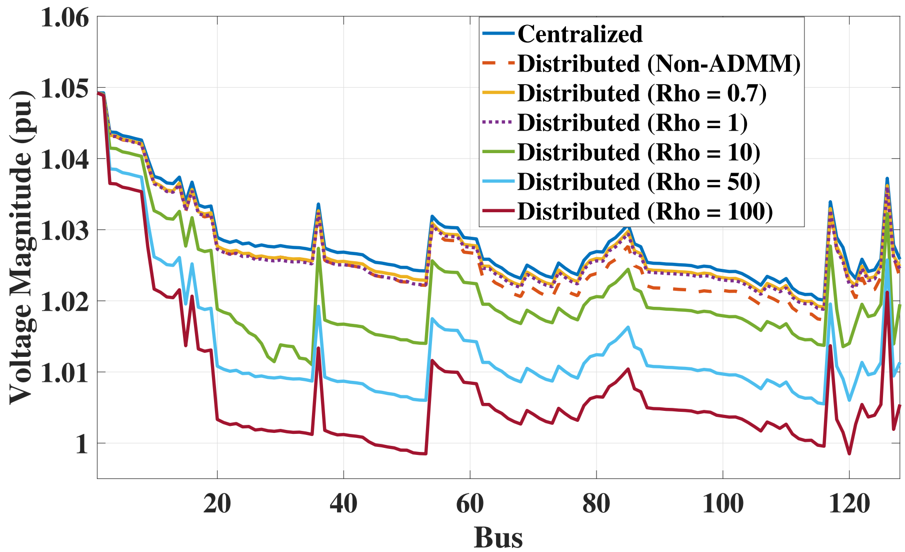

Figure 6.4: Voltage profile comparison among centralized OPF solution and proposed distributed approach for different penalty factor values.

6.8

The IEEE-123 bus system is a heavily loaded feeder with one three-phase and 3 single-phase voltage regulator and four shunt capacitors. This power grid model has been used to prove the applicability of the proposed OPF algorithm on a system with more number of regulators. For this purpose, the converted single-phase network is considered for OPF modeling using the OpenDSS software. First, a single-phase representation of the $Ybus$ is performed using a positive sequence representation of the three-phase $Ybus$. Then from the Y bus matrix, the line impedance values are extracted. The connected loads are also converted similarly. Table. 6.2 represents the power grid loading.

Table 6.2: Test systems description

Sl No	Test System	Volt. Reg.	Trans.	Shunt Caps	Avg R/X	Total Load
1	IEEE 123	4	1	4	0.2645	1.1633 MW 0.64 MVAR
2	IEEE 8500	4	1177	4	0.2145	3.3252 MW 0.8335 MVAR

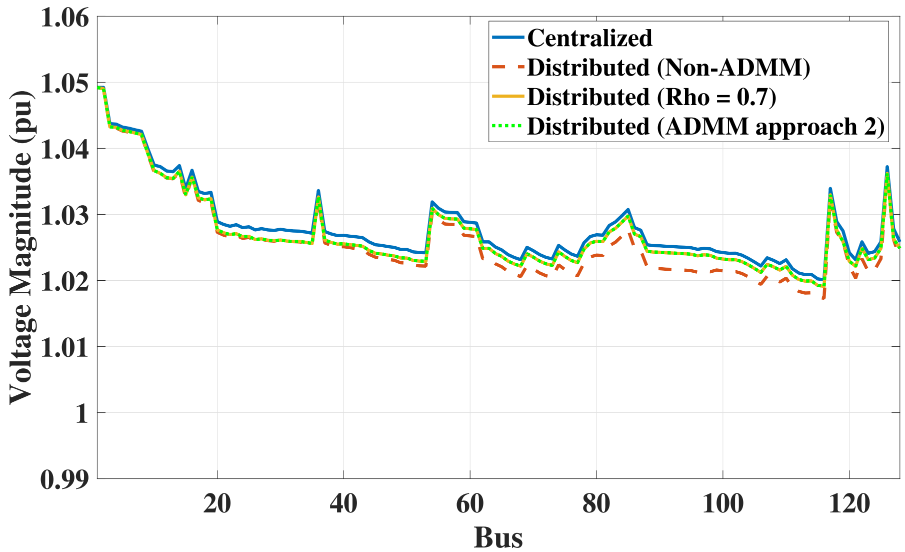

Figure 6.5: Voltage profile comparison among centralized OPF solution and proposed distributed approach for different penalty factor values.

The 8500-node test feeder consists of multiple feeder regulators, capacitor banks, split-phase service transformers, and feeder secondaries. The circuit has a $115kV$ source, $12.47kV$ medium voltage feeder sections, and a $120V$ low voltage feeder section. There are 4876 three-phase, two-phase, and single-phase medium-voltage nodes. The single-phase nodes are connected to 1177 split phase transformers. The two secondaries of these transformers are connected to load nodes using triplex lines. There are 3041 A phase nodes, $2830B$ phase nodes, and $2660C$ phase nodes. Table. 6.2 represents the power grid loading.

For evaluating the performance of the proposed approach on the power grid with DER, a 10%, 30%, and 50%, DER penetration is considered by placing DERs randomly at different locations on the feeder. The capacity of the DERs is considered equal to the loads connected to that bus. The reference bus voltage is considered as 1.05 pu. The upper and lower bound of voltage magnitude are set as 1.05 pu and 0.95 pu. For the IEEE 123 bus system, the base MVA is 5MVA; for the IEEE 8500 bus, the base MVA is set as 1MVA. The details of the DERs, including the location (bus number), size, and total number, are illustrated in Table. Table. 6.3 and Table. 6.4

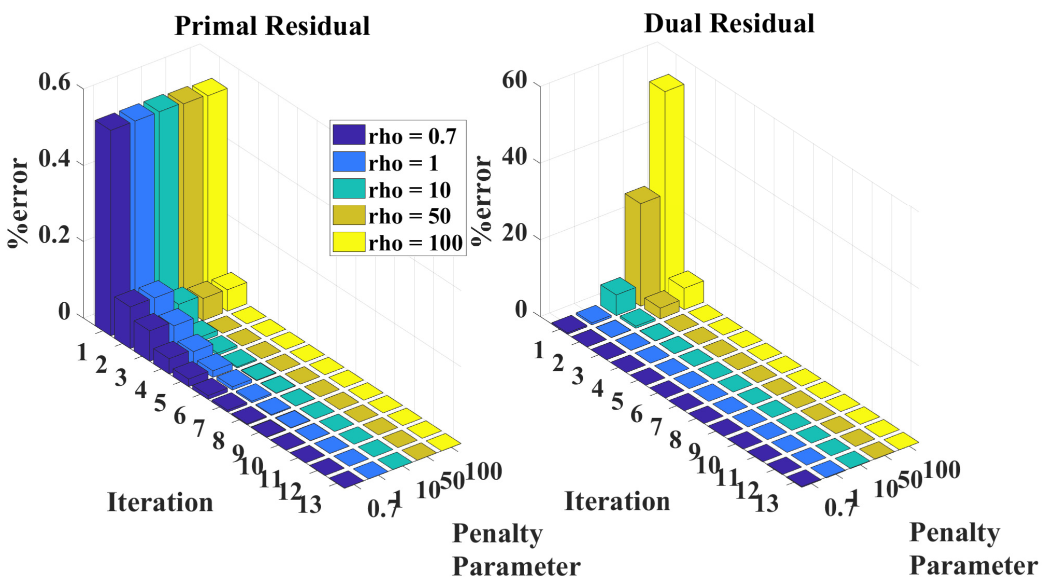

Figure 6.6: Primal and Dual residual values for the different magnitude of penalty parameters.

for IEEE 123 and IEEE 8500 node system. The active power generation of the DERs is considered equal to the bus's active power demand. The solution of the proposed decentralized method is compared with other state-of-the-art, including centralized OPF, consensus ADMM-based OPF, residual balanced ADMM-based OPF, Accelerated ADMM OPF, and Decentralized ADMM-based SDP-OPF. All the coding was done in the MATLAB platform using the YALMIP optimization toolbox and MOSEK solver.

6.4.2 The IEEE 123 node system:

First, the accuracy of the proposed method is analyzed on the base case (without any DERs). The analysis is when compared to other centralized and distributed methods. As the Nonlinear Programming (NLP) formulation provides a globally optimal solution (for near equilibrium conditions), the proposed approach is compared with the NLP. The comparisons are with four distributed optimal power flow algorithms viz. consensus ADMM (C-ADMM), residual balanced ADMM (RB-ADMM), Accelerated ADMM (A-ADMM), and decentralized ADMM (D-ADMM), one cen-

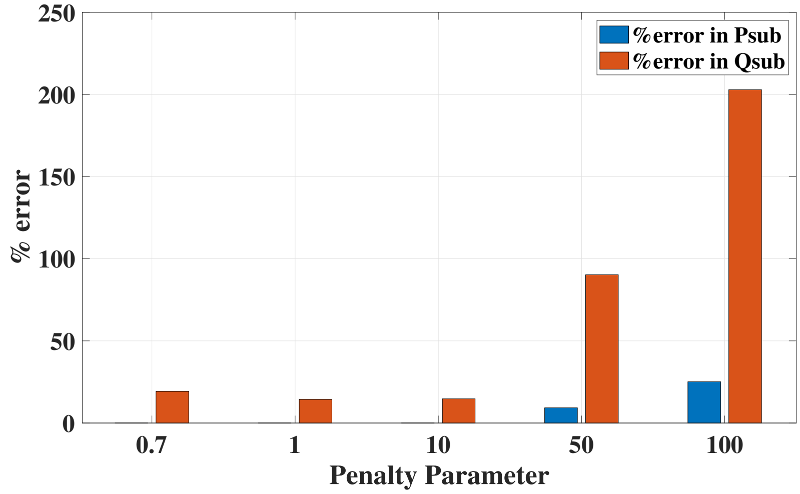

Figure 6.7: The percentage error in substation active and reactive power for different values of ρ with respect to centralized OPF dispatch.

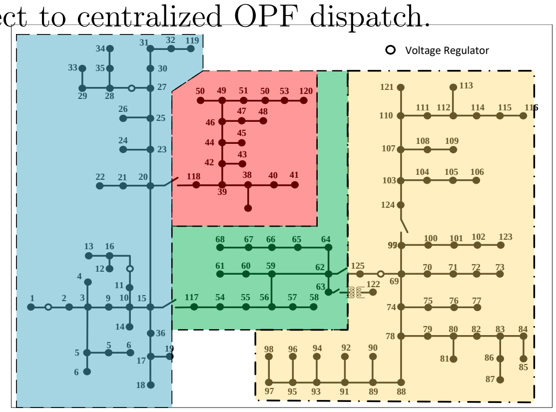

Figure 6.8: Modified IEEE 123 bus system with IBR Based DERs.

tralized approach based on NLP and the proposed D-SDP ADMM. Fig. 6.10 shows the comparisons; It can be seen that the proposed approach provides an immediate optimal solution when compared with NLP. It can also be seen that the solutions from other approaches are not accurate when compared to NLP.

In Fig 6.10, the comparison of voltage profiles from different approaches is shown. It can be observed that the distributed approaches such as A-ADMM, RB-ADMM, D-ADMM, and C-ADMM are deviating from the global optimal solution. As illustrated, the proposed approach can provide the closest solution to the globally optimal values in the NLP. Further comparisons for higher levels of DER penetrations are performed. From Fig.6.11 it can see that the solution from A-ADMM deviates most from the NLP

Table 6.3: DER location and rating for different penetration levels in IEEE 123 bus system

DER %	DER Location	DER Power Capacity (KW)	DER Power Capacity (KVA)
10%	11,30,89,102	13.33	16
	50	70	84
	60	6.667	8
	67	46.667	56
	78	81.66	98
30%	8,11,18,2130,32,37,45, 64,77,89,101,102,106,109	13.33	16
	53,57,60,86,98,113,116	6.667	8
	50	70	84
	67	46.667	56
	78	81.66	98
50%	8,11,18,21,24,26,30,32,35, 37,45,55,64,71,77,81,84,89, 92,96,101,102,106,109,111	13.33	16
	4,14,19,34,40,43,47,53,57,60, 86,98,113,116	6.667	8
	50	70	84
	67	46.667	56
	68	25	30
	78	81.66	98

solution and the voltage profile is very close to the lower bound for most buses. To get a better comparison Fig. 6.12 is provided where all other profiles except A-ADMM are compared. It can be seen that the profiles are close, but there are gaps among NLP solutions and other approaches, while the proposed approach was able to be the most accurate method.

Fig. 6.13 and Fig.6.14 shows a similar trend of the solution from the A-ADMM approach. In Fig. 6.14, it can be seen that as the level of penetration increased, the gap among the distributed ADMM profiles when compared to the central solutions while the proposed method still gives the most accurate solution. Results showed Fig. 6.15, and Fig. 6.16 validate the claim that the A-ADMM fails to provide the

Table 6.4: DER location and active power rating for 10% DER penetration in 8500 bus system

DER %	DER Location	DER Active Power Rating (KW)	DER Capacity (KVAR)
10%	1102,1183,1274,1368,1408, 1502,1642,1669,1674,1691, 1740,1816,1868,1883,2018, 1928,1969,1992,2043,2054, 2081,2092,2112,2139,2149, 2167,2180,2209,2299,2340, 2355,2364,2404,2420,2456, 2462,2516	2.9570	3.5484
	34,43,59,62,66,69,102,120, 149,151,162,194,200,213,224, 230,239,247,252,267,284,329, 363,372,384,402,409,432,486, 502,607,612,621,690,761,794, 800,823,833,850,885,899,928, 951,995,1038,1138,1146,1239, 1304,1313,1321,1416,1466,1473, 1647,1713,1723,1809,1860,1907, 1911,1938,2066,2097,2188,2194, 2311,2321,2326,2429,2468	3.3900	4.068
	23,40	5.0870	6.1044
	2520	5.9130	7.0956
	2485	29.560	35.472

global optimal solution while the proposed D-SDP ADMM approach still guaranty the exact solution for any level of DER penetration.

The consensus ADMM-based OPF converged to the optimal solution with a minor gap compared with the global optimal solution from centralized OPF. Similar convergence was achieved using the residual balanced ADMM-based OPF. Since the residual balanced approach updates the penalty parameter after each iteration, it shows a faster convergence speed. This is evident from data provided in Table6.5. In the accelerated ADMM-based distributed OPF, the global variable and Lagrangian multiplier are updated in additional steps. It is noted that this approach does not

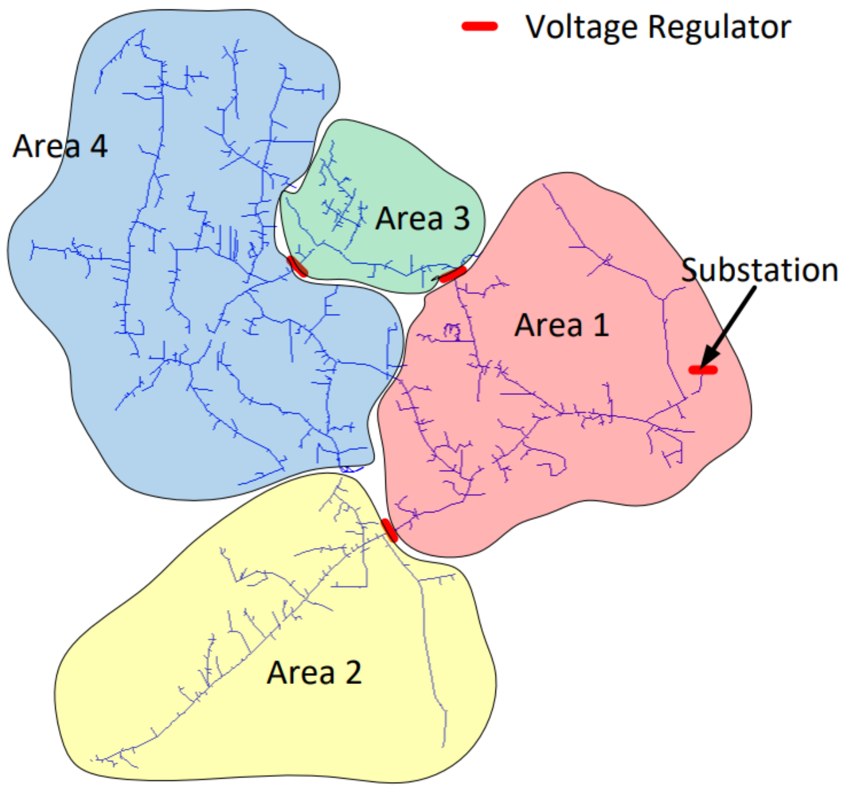

Figure 6.9: Modified IEEE 8500 bus one line diagram IBR Based DERs location.

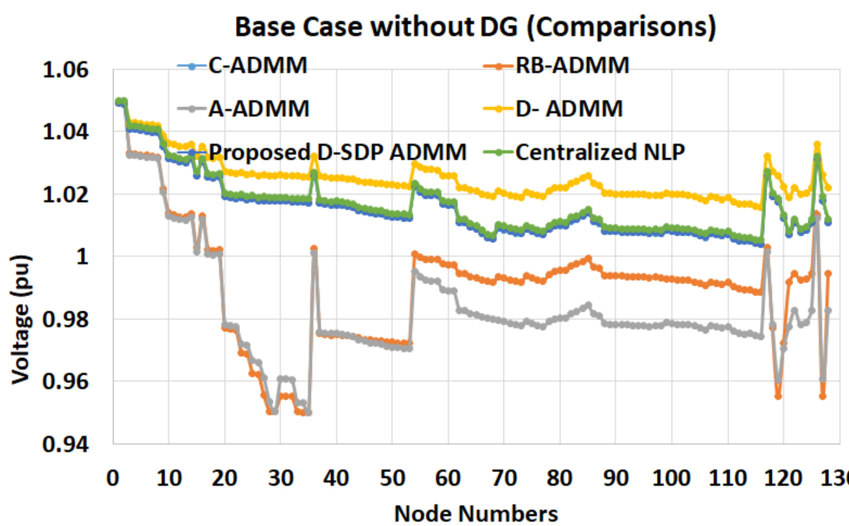

Figure 6.10: Voltage profile comparison of modified IEEE 123 bus system with no DG penetration.

guarantee faster convergence and globally optimal solutions all the time. The solution from the decentralized ADMM was closest to the global optimal solution, although it takes more iterations to achieve convergence. In the proposed approach, the penalty

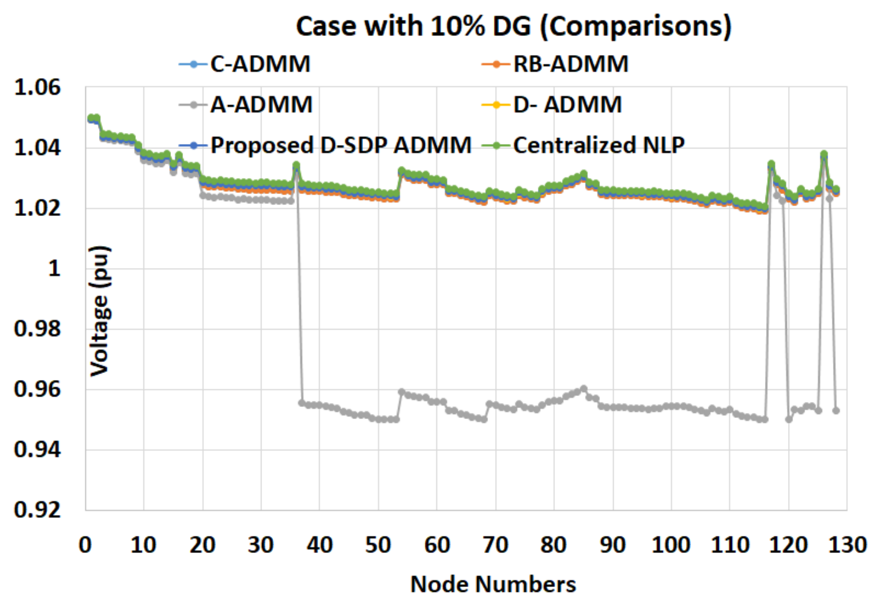

Figure 6.11: Voltage profile comparison of modified IEEE 123 bus system with 10% DER penetration.

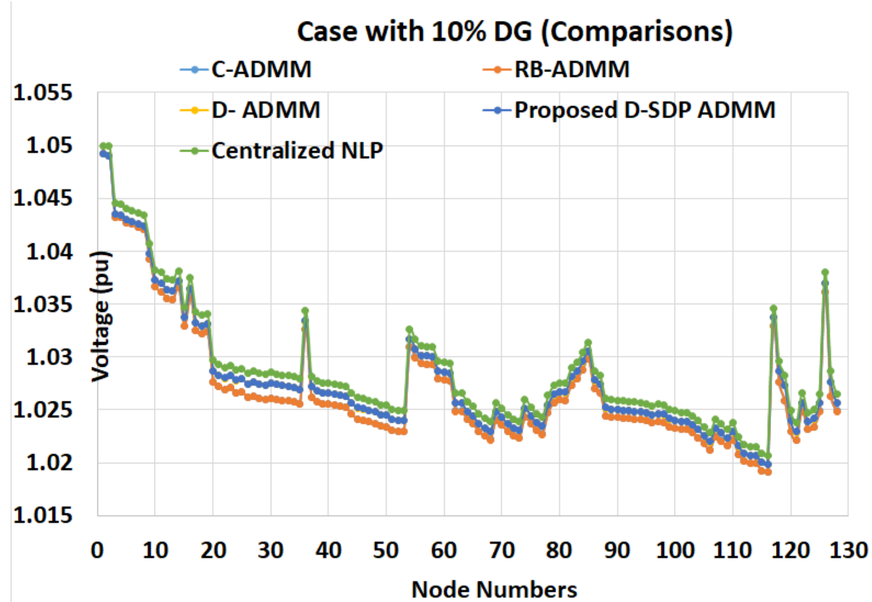

Figure 6.12: Voltage profile comparison of modified IEEE 123 bus system with 10% DER penetration.

parameter auto-tuning helps speed up the convergence.

The exactness of the solution from the proposed D-SDP ADMM method is further illustrated from the information provided in Table. 6.7. In Table. 6.7 substation active and reactive power dispatch, along with the number of iterations and total

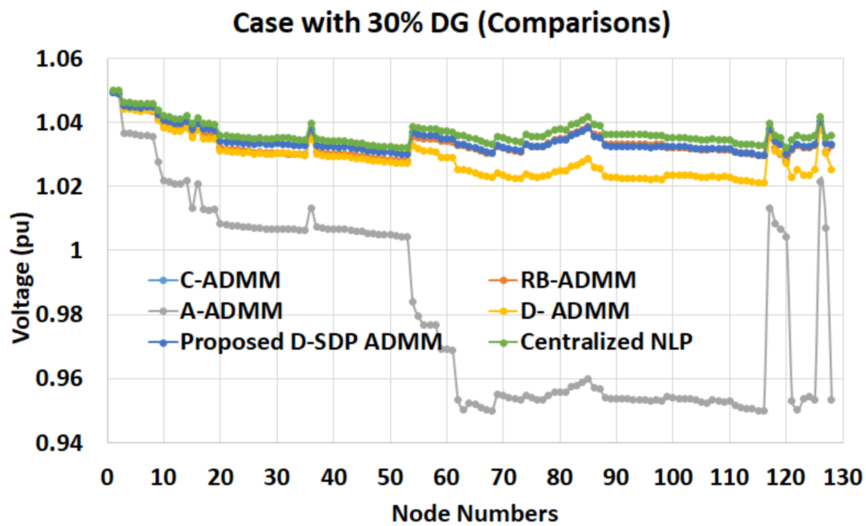

Figure 6.13: Voltage profile comparison of modified IEEE 123 bus system with 30% DER penetration.

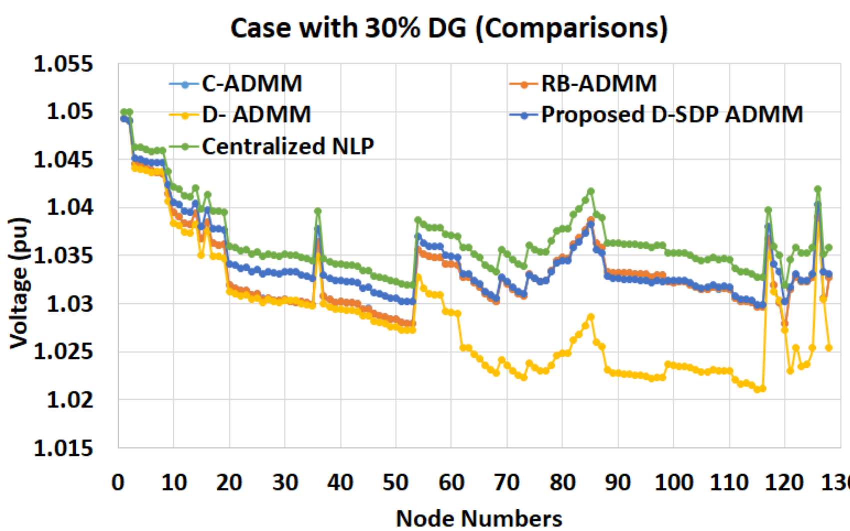

Figure 6.14: Voltage profile comparison of modified IEEE 123 bus system with 30% DER penetration.

computational time to converge from different distributed methods, i.e., centralized NLP, C-ADMM, RB-ADMM, A-ADMM, D-ADMM, and proposed D-SDP ADMM for base system and 10%, 30% and 50% DER penetration cases are compiled. The speed of the convergence for different methods can also be visualized from the plotting of residuals. Fig 6.17-Fig 6.19 shows the residual profiles from different approaches for different test system cases. In chronological order, the figures represent the base system, 10%, and 30% DER penetration cases. It can be seen that the profiles from

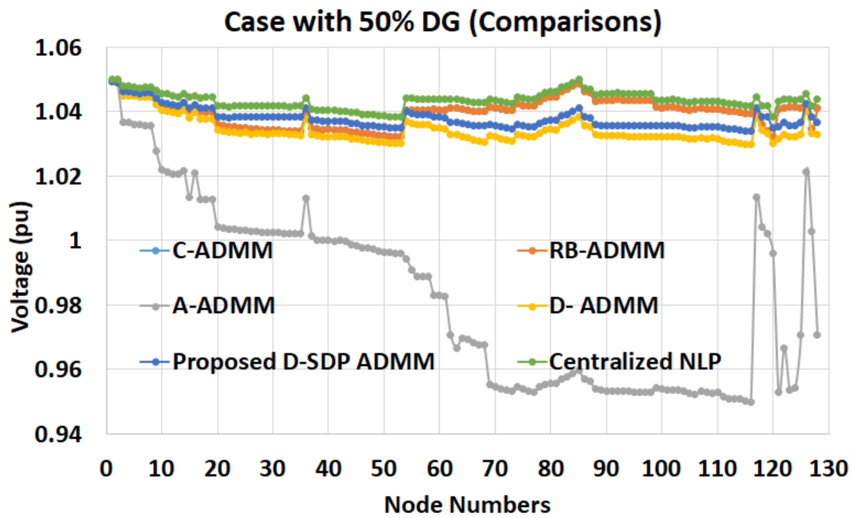

Figure 6.15: Voltage profile comparison of modified IEEE 123 bus system with 50% DER penetration.

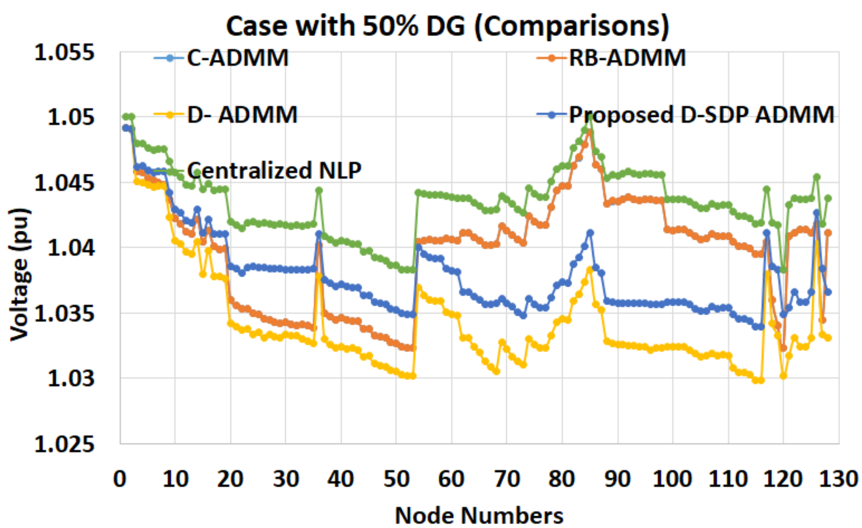

Figure 6.16: Voltage profile comparison of modified IEEE 123 bus system with 50% DER penetration.

C-ADMM and RB-ADMM have similar slop while A-ADMM has the steepest slope among the profiles. However, in the earlier discussion, it has been shown that A-ADMM fails to provide the global optimal solution. The proposed D-SDP ADMM method doesn't have the fastest convergence property but is faster than the C-ADMM, and RB-ADMM approaches and ensures the global optimal point. Please note that residue for 50% DER penetration case is similar to that of 20% DER penetration case, thus been omitted.

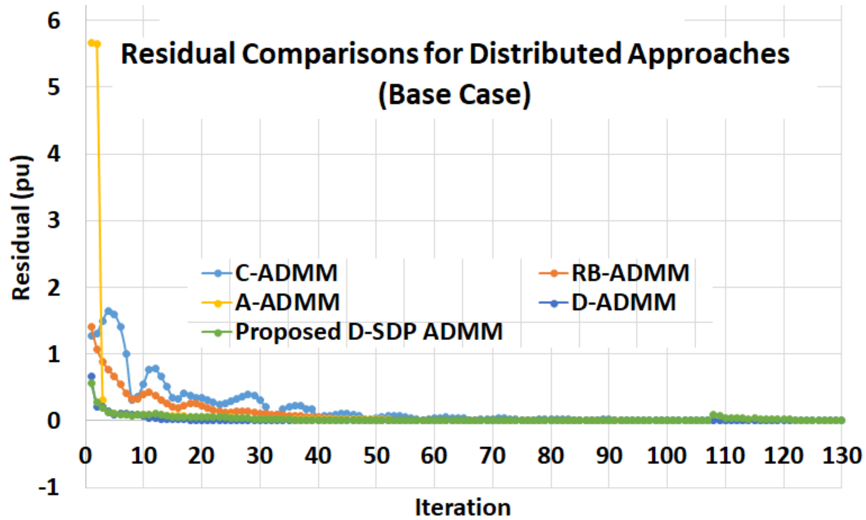

Figure 6.17: Residual comparison of modified IEEE 123 bus system base case.

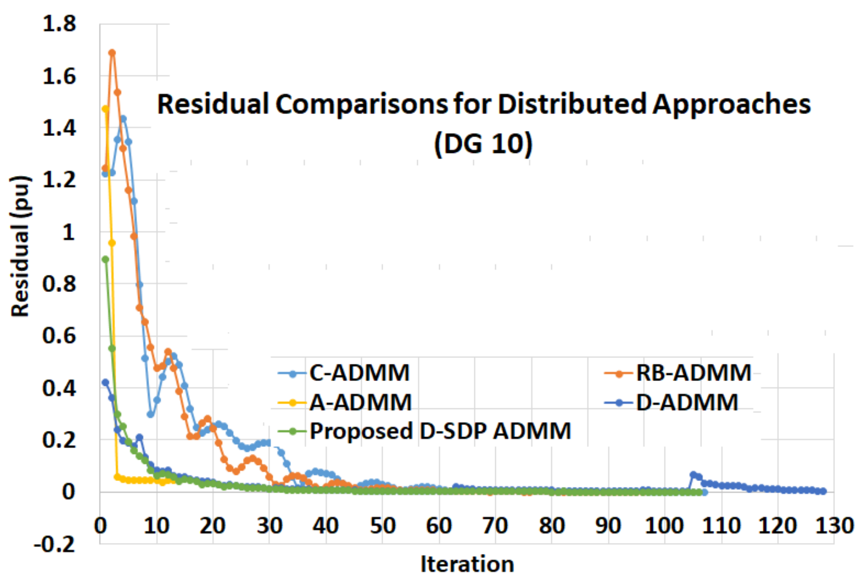

Figure 6.18: Residual comparison of modified IEEE 123 bus system with 10% DER penetration.

6.4.3 Scalability Analysis (IEEE 8500 node system):

Once the proposed model could provide satisfactory results for the modified IEEE 123 bus system, it was tested on another real-world test network, the modified IEEE 8500 node system. In this case, 10% DER penetration was considered. The whole network was partitioned into four interconnected subsystems. The numerical comparison of the solution for different approaches is showcased in Table. 6.7. Although few

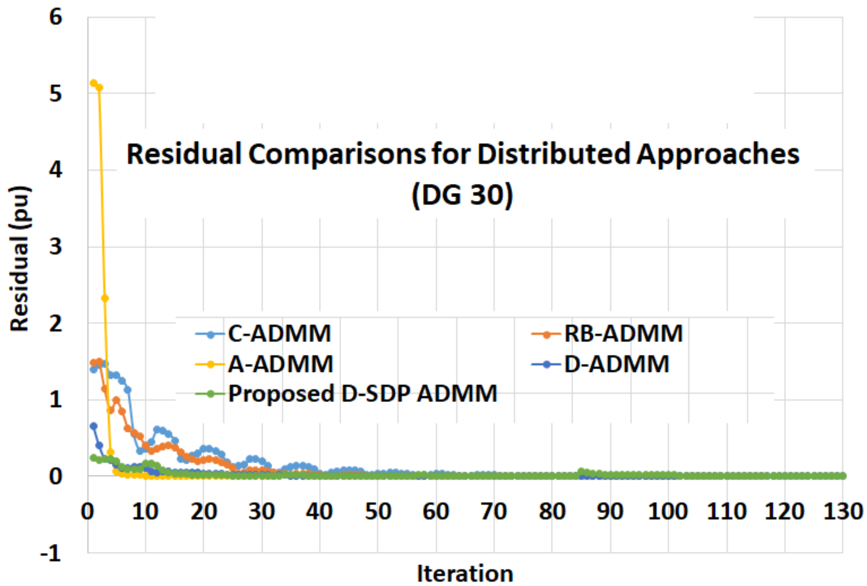

Figure 6.19: Residual comparison of modified IEEE 123 bus system with 30% DER penetration.

of the methods, i.e., residual balanced ADMM, accelerated ADMM, and decentralized SDP ADMM, could not converge to an optimal solution for the given threshold value. As shown before, the proposed method shows similar convergence properties compared with the consensus ADMM method. The number of iterations and convergence time is higher in the proposed method, but the solution is the closest to the global optimal point. From Fig.**??** it can be seen that there is a significant gap in the consensus ADMM while the profile from the proposed approach is almost similar to the centralized solution. Fig.6.20 shows the maximum residual profile in each iteration while solving the 8500 bus system using the proposed method. It is evident from the slope of the plot that the auto-tuning of the penalty parameter significantly improved the speed of convergence.

6.4.4 Validation Through Real-time Simulation

The numerical solution comparison from Table 6.7shows that the proposed distributed approach can converge at the global optimal solution with conclusive tightness compared to the centralized and non-linear approaches. For further validation and real-time applicability of the proposed method, the solution was validated using

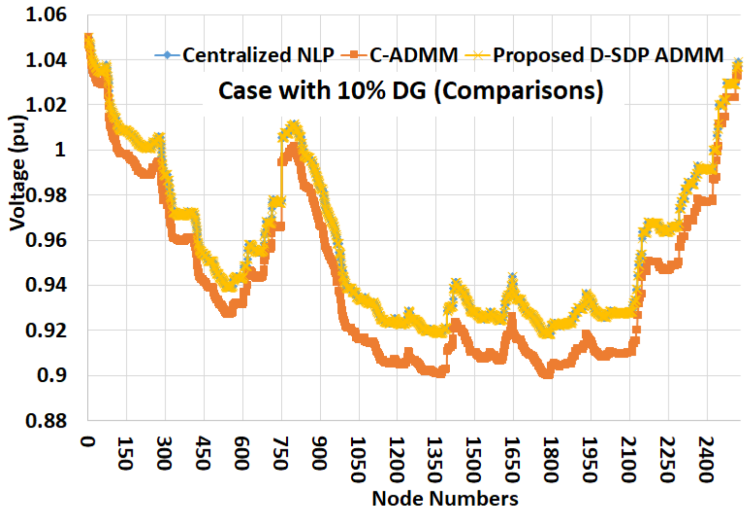

Figure 6.20: Residual comparison of modified IEEE 8500 bus system with 10% DG penetration.

a real-time power system simulator Opal-RT. The real-time simulation and validation setup is shown in Fig 6.21. The DER setpoints, such as active and reactive power dispatches for each DER inverter, are transmitted to a similar model built inside the Opar-RT simulator, and power flow was solved. Once done, the active and reactive power dispatches from the Opal-RT simulation substation and the proposed method's similarities are very conclusive. These steps are simulated for a load profile over 12 hours. The % error of the voltage profile from these two approaches is shown in Fig 6.22. We can see that the maximum error is around 1.3%, which indicates that the solutions are very similar. Also, the substation active and reactive power dispatches from Oplar-RT simulations and the same from the OPF solution are compared in Table6.9. From the Table, we can see that the solutions are almost similar, thus conclusive. Since the objective function selected was to minimize the line active power losses, thus, by comparing the substation active power dispatch, we can confirm that the proposed approach's solution is conclusive. Also, in the Opal-RT platform, each simulation takes around 60ms, while the proposed approach consumes around 25.41s. In real-world DSO, the operators usually perform the real-time dispatch on a 5 min time resolution. Since the computational time of our proposed approach is well below the 300s mark, it can be confirmed that the proposed approach can also be implemented in actual world operations.

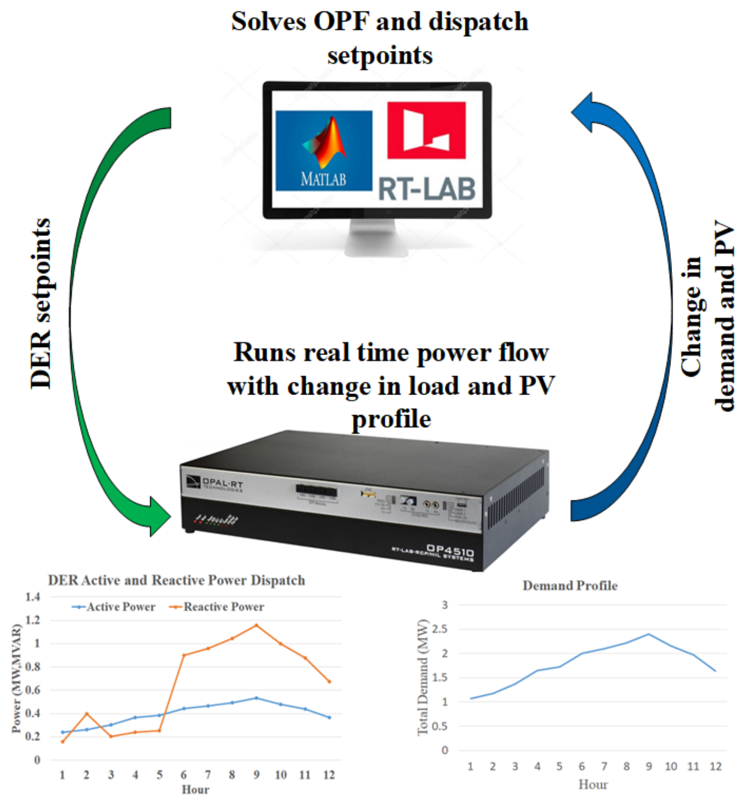

Figure 6.21: setup used for real-time simulation and validation using Opal-RT.

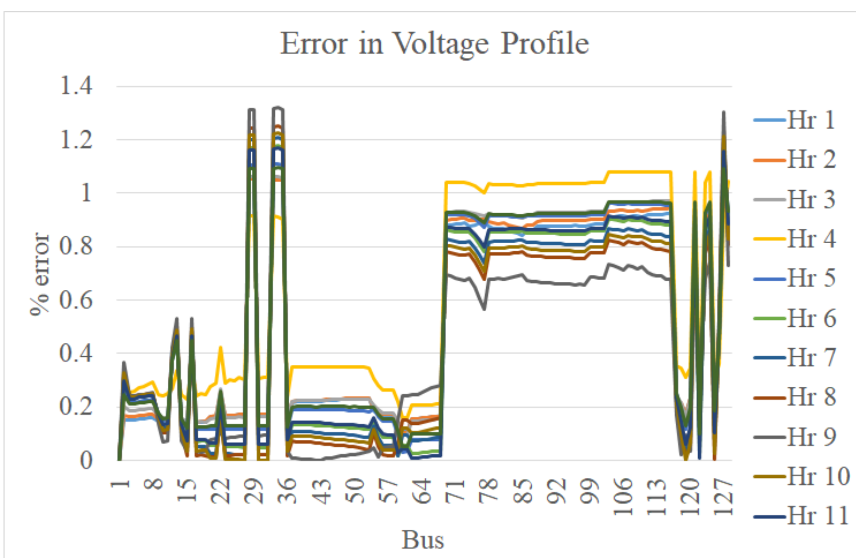

Figure 6.22: % Error of bus voltage magnitudes from proposed approach and OpalRT simulation.

6.5 Decentralized and Distributed Approach for Unbalanced System OPF Problem

The numerical complexity of the optimal power flow problem for unbalanced networks significantly scales up with the networks' size and the levels of DER penetration. An alternative to solving such a complex problem in a centralized order is to follow the distributed approach. Similar to the algorithm of ADMM-based distributed OPF models for single-phase networks, a distributed approach for the three-phase unbalanced network will be discussed in this section.

Let us consider that several small local networks are connected through tie lines. And all the local areas have access to the information of the adjoining buses to their adjacent networks. Similar to the objective functions stated in **??**, let's assume $\mathbf{x} = [v_i^{\phi_i}, S_{ij}^{\phi_{ij}}]$ is the set of control variables and $\mathbf{y}$ is the set of global consensus variable. Also, let us denote β and ϕ as the Lagrange multiplier and penalty parameter for the augmented lagrangian equation. Then the expression of the augmented lagrangian equation will be as follows:

$$L_\rho(x, y, \beta) = \sum_{i=1}^{N}(f(x_i)) + \beta^T(x_i^\phi - y^\phi) + \frac{\phi}{2}||x_i^\phi - y||_2^2 \tag{6.41}$$

Although the actual expression in the modeling will not be as simple as shown here. Since the voltage of a bus of an unbalanced network, V is a $3 * 3$ complex matrix, the product of VV^* will also be a complex matrix of dimension $3 * 3$. If an objective function contains complex entities in an optimization model, it cannot be considered a convex optimization problem. That's why all the variable matrices will be separated by their real and imaginary counterparts and included in the objective function. The next concern is that the 2-norm of a matrix is a non-linear term, which is not convex. The matrices will be reshaped as a vector before the norm is calculated. Two approaches were compared for the distributed OPF formulation of an unbalanced network. The consensus ADMM and proposed decentralized ADMM. They are briefly discussed here.

6.5.1 Consensus ADMM Based Distributed OPF for Unbalanced Network

Let us consider the same network shown in Fig 6.1 where 3 sub-networks are interconnected through tie lines. Area 1 is connected to area 2 through tie line (4-6) and area 3 through tie line (5-9). Area 1 has access to bus 5 and 9 information such as voltages. Thus extended portion of area 1 will also include buses 5 and 9 while solving the local OPF problem. Similarly, areas 2 and 3 will consist of buses 4 and 5 while solving their local OPF. The control or primal variable update objective function will take the form as shown below:

$$\text{Area 1:} \quad x_1^{k+1} := \arg\min_x \{f(x_i) + (\beta_1^k)^T([Re(x_1); Im(x_1)] - [Re(y_1^k); Im(y_1^k)]) + \frac{\rho}{2}||Reshape(Re(x_1) - Re(y_1^k))||_2^2 + \frac{\rho}{2}||Reshape(Im(x_1) - Im(y_1^k))||_2^2\} \tag{6.42}$$

$$\text{Area 2:} \quad x_2^{k+1} := \arg\min_x \{f(x_i) + (\beta_2^k)^T([Re(x_2); Im(x_2)] - [Re(y_2^k); Im(y_2^k)]) + \frac{\rho}{2}||Reshape(Re(x_2) - Re(y_2^k))||_2^2 + \frac{\rho}{2}||Reshape(Im(x_2) - Im(y_2^k))||_2^2\} \tag{6.43}$$

$$\text{Area 3:} \quad x_3^{k+1} := \arg\min_x \{f(x_i) + (\beta_3^k)^T([Re(x_3); Im(x_3)] - [Re(y_3^k); Im(y_3^k)]) + \frac{\rho}{2}||Reshape(Re(x_3) - Re(y_3^k))||_2^2 + \frac{\rho}{2}||Reshape(Im(x_3) - Im(y_3^k))||_2^2\} \tag{6.44}$$

The set of constraints will be the same as those used for BFM-SDP OPF in unbalanced networks in chapter 5.

$$
\begin{aligned}
& v_j = v_i^{\phi_{ij}} - (S_{ij} z_{ij}^H + z_{ij} S_{ij}^H) + z_{ij} l_{ij} z_{ij}^H \\
& \sum_{i:i \to j} diag(S_{ij} - z_{ij} l_{ij})^{\phi_j} + s_j = \sum_{k:j \to k} diag(S_{jk})^{\phi_j} \\
& v_1 = V_1^{ref} (V_1^{ref})^H \\
& V_i^{min} \leq diag(v_i) \leq V_i^{max} \\
& s_i^{min} \leq s_i \leq s_i^{max} \\
& \begin{bmatrix} v_i^{\phi_{ij}} & S_{ij} \\ S_{ij}^H & l_{ij} \end{bmatrix} \succcurlyeq 0
\end{aligned}
\tag{6.45}
$$

Once the primal variable is updated, next the global variables will be updated using the information gathered in the central coordinator as shown below:

$$
\text{Area 1}: \; y_1^{k+1} = \frac{x_1^{k+1} + [x_2^{k+1}; x_3^{k+1}]}{2} \tag{6.46}
$$

And finally, the Lagrange multiplier will be updated as

$$
\text{Area 1}: \; \beta_1^{k+1} := \beta_1^k + \rho(x_1^{k+1} - y_1^{k+1}) \tag{6.47}
$$

Next, the residuals will be calculated for all the areas, and until the maximum of the primal and dual residual stays higher than the threshold value, the algorithm iterates. Proposed Decentralized Approach for Unbalanced System A distributed approach consists of a central coordinator, the communication setup required to collect data from all the local areas, and transmitting back the global consensus variable values may cause traffic congestion sometimes. As a remedy to this issue, the proposed decentralized approach was motivated. As described in section 6.3.6.3, in this framework, only the adjacent areas communicate with each other removing the necessity of a central coordinator. The control variable update takes place as:

$$Area1 : x_1^{k+1} := \arg\min_x\{f(x_i) + \frac{\rho}{2}||Reshape(Re(x_1) - Re(w_1^k))||_2^2 + \frac{\rho}{2}||Reshape(Im(x_1) - Im(w_1^k))||_2^2\} \tag{6.48}$$

The constraints for the power balance will be the same as they are in 6.45. Next, the local auxiliary control variables will be updated as

$$Area1 : w_1^{k+1} := w_1^k + x_1^{k+1} - \frac{x_1^k + x_2^k}{2} \tag{6.49}$$

Then the primal and dual residual values will be calculated and compared for the convergence test.

6.5.2 Implementation of Distributed Approach for Unbalanced Network

Once the proposed decentralized distributed approach was validated for the single-phase networks, it was further extended to the unbalanced multi-phase networks. A modified portion of the IEEE 123 bus network is considered for the test system. It consists of 74 buses, one OLTC near the substation, and 2 voltage regulators. The total load connected to 3 phases is 855KW, 465KVAR at phase A, 505KW, 295KVAR at phase B, and 705KW, 395kVAR at phase C. There are DERs connected at buses 11, 30, 50, 60, and 67. The active power capacity of the DERs is considered equal to the load connected to that specific bus. The apparent power capacity of the inverters is 120% of the active power capacity. This network is then partitioned into three local areas based on the position of switches. The threshold value for the convergence of the primal and dual residuals was considered as $1e^{-3}$. The value of μ and τ were selected as 0.1 and 1.0. In the consensus ADMM approach, the value of the consensus variable was considered 0 and 1 as a flat start. The initial value of the Lagrange multiplier was set as random numbers. The performance of the two methods was compared with the help of the maximum residual value and objective function value throughout the iterations. They are shown in Fig. 6.24. The first figure shows how the value of residuals changed in iterations. We can see that the consensus ADMM reached the cutoff value of $1e^{-2}$ before the proposed D-SDP ADMM approach because, at that point of iteration, the proposed method started to slow down in reducing the residual value. A similar characteristic is also seen in the next figure showing the plot of objective function values. This figure shows that the value of the objective function, line losses, in this case, follows almost the same path as it did in the consensus ADMM method. Although in the case of single-phase models, we have seen that the proposed method showed better performance in the accuracy of the solution, in this case, it didn't perform as much better as anticipated. Since in the proposed method, the penalty parameter is tuned and two weighting factors μ and τ play an important role in convergence, thus it requires careful tuning of those two parameters' values for faster convergence.

6.6 Summary

This chapter has formulated a fully distributed approach to solving the convexified OPF problem for a radial power system. The scalability of the formulation has been tested on a modified IEEE 123 bus system with 10% DG penetration. This formulation can also apply to larger networks. The significance of choosing a proper penalty factor is shown by simulating different case scenarios. This formulation can improve the time of convergence for realistic large networks by splitting the system into small regions and solving the problem in parallel while ensuring inter-regional coordination. The proposed decentralized distributed approach with auto-tuning of penalty parameter helps to speed up the convergence as well as maintain high accuracy of the solution. Both of these methods are adaptable for real-time simulation which has been tested implementing in OPAL-RT. Finally, the distributed and de-

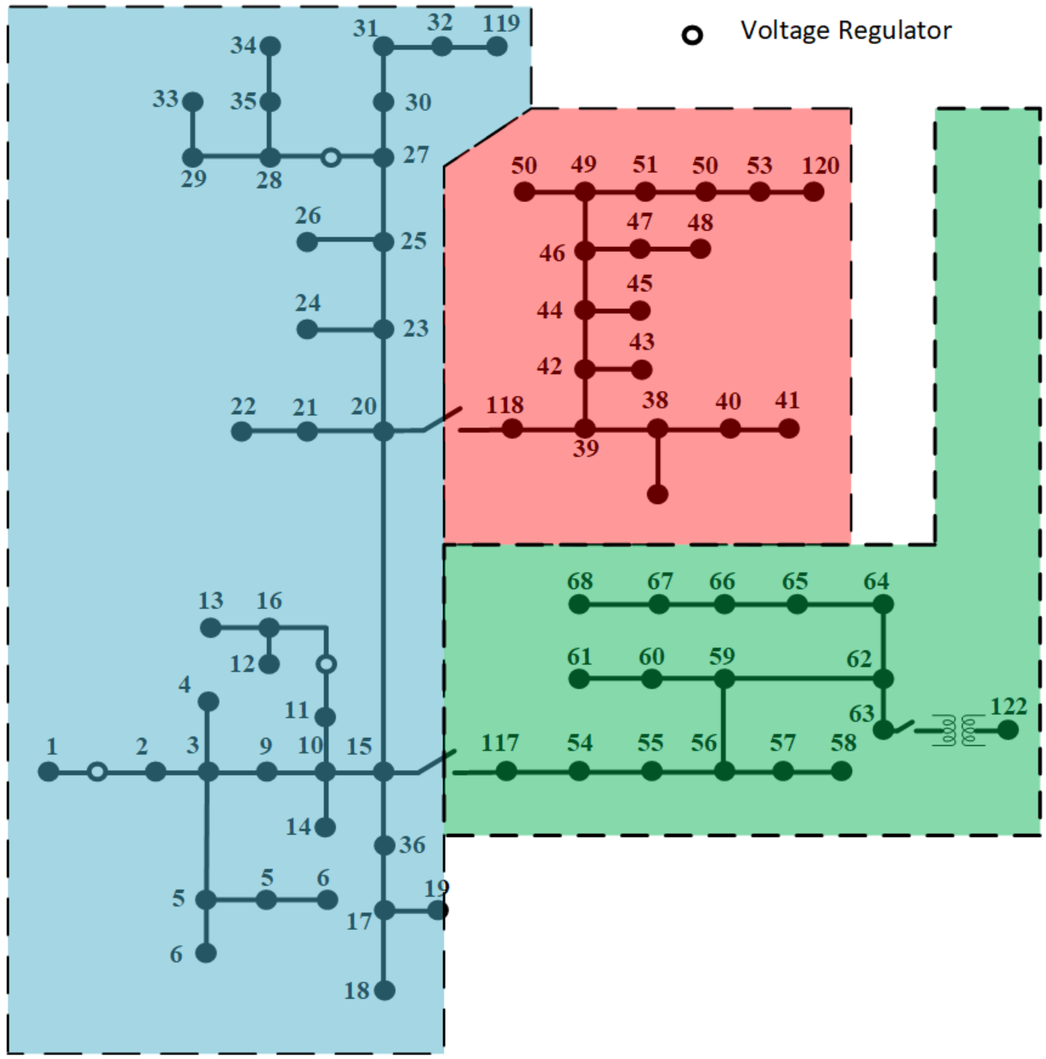

Figure 6.23: Test system for distributed OPF algorithms for unbalanced networks.

centralized approaches are scaled up for the unbalanced networks and case studies shown conclusive performance of the approaches.

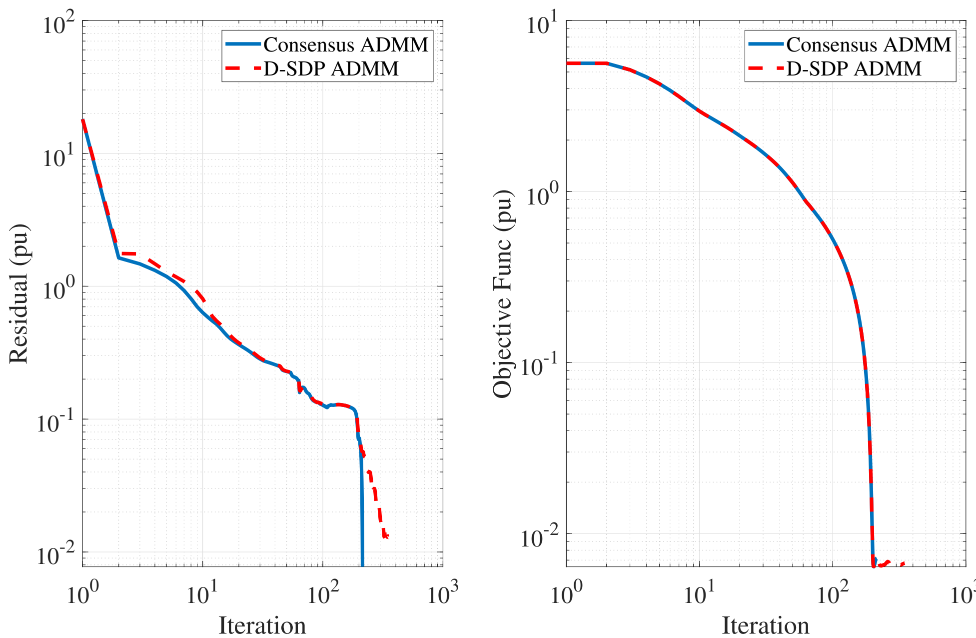

Figure 6.24: Residual and objective function value comparison between consensus ADMM and proposed D-SDP ADMM OPF for unbalanced networks.

Table 6.5: Comparison of Convergence Properties of Different Distributed Optimization Methods

	Centralized NLP		Consensus ADMM (C-ADMM)		Residual Balanced ADMM (RB-ADMM)		Accelerated ADMM (A-ADMM)		D-ADMM		Proposed D-SDP ADMM	
	Iter	Time (s)	Iter	Time (s)	Iter	Time (s)	Iter	Time (s)	Iter	Time (s)	Iter	Time (s)
123 Bus 4 Partitions	N/A	48.10	108	25.57	97	23.45	88	20.76	173	41.29	107	25.41
8500 Bus 4 Partitions	N/A	192.38	154	136.65	N/A	N/A	N/A	N/A	N/A	N/A	189	178.71

Table 6.6: Comparison of Substation Power of Different Distributed Optimization Methods

	Centralized NLP		Consensus ADMM (C-ADMM)		Residual Balanced ADMM (RB-ADMM)		Accelerated ADMM (A-ADMM)		D-ADMM		Proposed D-SDP ADMM	
	Psub (KW)	Qsub (KVAR)	Psub (KW)	Qsub (KVAR)	Psub (KW)	Qsub (KVAR)	Psub (KW)	Qsub (KVAR)	Psub (KW)	Qsub (KVAR)	Psub (KW)	Qsub (KVAR)
123 Bus 4 Partitions	921.07	251.081	921.5	287.1	921.4	287.1	1.3931	1.3319	921.2	251.3	921.2	251.14
8500 Bus 4 Partitions	3150.79	576.734	3255.8	1051.6	N/A	N/A	N/A	N/A	N/A	N/A	3150.8	576.8

Table 6.7: Comparison of substation power and number of iterations of Distributed Optimization Methods

IEEE 123 Bus System with base case and different DG Penetration All proposed methods are compared with 4 partitions					
Comparisons	Sub. Power	Base	10% DG	30% DG	50% DG
Centralized NLP	Psub (KW)	1192.136	921.07	728.471	518.527
	Qsub (KVAR)	447.85	251.081	146.675	91.66
	Iteration	N/A	N/A	N/A	N/A
	Time (s)	0.4781	0.4772	0.4851	0.4869
Consensus ADMM (C-ADMM)	Psub (KW)	1192.38	921.5	729.017	519.819
	Qsub (KVAR)	448.146	287.1	222.618	166.464
	Iteration	166	108	130	179
	Time (s)	38.3792	25.5744	31.213	42.1903
Residual Balanced ADMM (RB-ADMM)	Psub (KW)	1390.77	921.4	729.122	519.795
	Qsub (KVAR)	1327.48	287.1	222.662	166.502
	Iteration	94	97	117	134
	Time (s)	22.5885	23.4449	28.3374	32.264
Accelerated ADMM (A-ADMM)	Psub (KW)	1152.40	922.847	607.636	581.744
	Qsub (KVAR)	1499.73	1266.08	1110.347	490.63
	Iteration	52	14	32	54
	Time (s)	12.2044	3.3418	7.5776	12.6954
D-ADMM	Psub (KW)	921.536	921.2	729.112	518.746
	Qsub (KVAR)	309.92	251.3	274.48	24.256
	Iteration	200+	173	129	200+
	Time (s)	47.84+	41.2951	31.1019	47.76+
Proposed Approach	Psub (KW)	1192.362	921.2	725.548	518.507
	Qsub (KVAR)	448.024	251.144	153.271	114.81
	Iteration	187	107	200+	180
	Time (s)	44.2442	25.4125	48.36+	42.876

Table 6.8: Summary of Observations

Objective Function- Loss Minimization				
Methods	**Feasibility**	**Optimality**	**Accuracy**	**Scalability**
Centralized NLP	Feasible	Global Optimal	Most Accurate	No
C-ADMM	Feasible	Global/Local optimal	Accurate	Scalable
RB-ADMM	Feasible	Global/Local optimal	less accurate	Scalable
A-ADMM	Feasible	Local optimal	Inaccurate	Scalable
D-ADMM	Feasible	Local optimal	less accurate	Scalable
Proposed D-SDP ADMM	Feasible	Global optimal	Very accurate	Scalable

Table 6.9: Substation Active and Reactive Power Comparison between D-SDP OPF and Realtime Simulation

	D-SDP OPF		Opal-RT PF	
Hr	Psub (MW)	Qsub (MVAR)	Psub (MW)	Qsub (MVAR)
1	0.8462	0.2088	0.8508	0.1682
2	0.9305	0.2564	0.9341	0.2501
3	1.0907	0.3487	1.0913	0.3225
4	1.2627	0.4537	1.3132	0.4498
5	1.3764	0.5179	1.3687	0.5152
6	1.6080	0.6594	1.5907	0.6601
7	1.6860	0.7080	1.6647	0.6866
8	1.7936	0.7756	1.7665	0.7608
9	1.9413	0.8700	1.9051	0.8632
10	1.7348	0.7387	1.7111	0.7286
11	1.5790	0.6414	1.5799	0.6324
12	1.3094	0.4778	1.3183	0.4659

Table 6.10: Numerical Solution Comparison for Different Distributed Approaches

Substation Power		Power Flow	Centralized OPF	Consensus ADMM	D-SDP ADMM
Active Power (KW)	Phase A	870.79	870.84	939.93	883.36
	Phase B	507.17	507.17	465.30	524.89
	Phase C	720.28	720.10	718.46	740.5
Reactive Power (KVAR)	Phase A	500.76	501.16	197.65	535.82
	Phase B	303.81	304.07	272.69	331.1
	Phase C	408.88	409.18	490.56	450.31

CHAPTER 7: Discrete Control of the Legacy Devices in Three-phase Distribution Network

7.1 Introduction

In this chapter, a practical approach is proposed to solve the optimal power flow problem for the power distribution network, which includes the discrete control of the legacy devices such as voltage regulators and capacitor banks. In chapters 3 and 5, the convex optimal power flow problem has been formulated using the semidefinite relaxation method for branch flow models. In those formulations, the status of the discrete devices was considered known parameters. Due to the intermittency in renewable generation resources, the DSO faces severe challenges in maintaining a smooth voltage profile. In earlier chapters, it's already been shown that the reactive power support from the DER inverters can improve the voltage profile significantly and thus minimize the system-wide line loss. The motivation of this chapter is to explore the scope of integrating the discrete device control with the optimal power flow to minimize system loss further. Due to the lack of performance of the available MISDP solvers, the proposed approach decomposes the whole problem and is implemented in a two-step way. Firstly, a linearized OPF problem will be formulated for the unbalanced network. Then the integer control will be incorporated with the LP-OPF, making it a non-linear problem. That problem will be linearized using the big-M method, and the approximated MILP OPF problem will be completed. After solving the MILP-OPF with initialized line loss values, the tap positions for the voltage regulators will be used to solve the proposed BFM-SDP OPF for an unbalanced network. This process will continue in iteration, where in the next cycle, the line loss values will be updated from the solution of BFM-SDP OPF. The iteration will continue until the losses from the successive iteration become equal, representing the optimal tap position for the minimum line loss of the network.

7.2 Proposed Two-step Method for Discrete BFM-SDP OPF

This section will discuss the formulation of the LP-OPF, followed by the incorporation of integer control and linearization. Next, the BFM-SDP OPF formulation will be discussed. Finally, the combined algorithm will be presented.

7.2.1 Linear Approximation of OPF

The original Optimal Power Flow is a non-linear problem. For the formulation of the LP-OPF, the Distflow model is considered here. The distflow equations of the power distribution network can be written as shown below:

$$v_j = v_i^{\phi_{ij}} - (S_{ij} z_{ij}^H + z_{ij} S_{ij}^H) + z_{ij} l_{ij} z_{ij}^H \tag{7.1}$$

$$\sum_{i:i \to j} diag(S_{ij} - z_{ij} l_{ij}) + s_j = \sum_{j:j \to k} diag(S_{jk})^{\phi_j} \tag{7.2}$$

$$S_{ij} S_{ij}^H = v_i^{\phi_{ij}} l_{ij} \tag{7.3}$$

Here, $v_i^{\phi_i}$ denotes the voltage magnitude squared matrix of bus i and contains ϕ phases, $\phi = \{a, b, c\}$, l_{ij} denotes the current magnitude squared matrix of branch between buses i and j, S_{ij} represents the apparent power flow through the branch and s_i denotes the injected power at bus i. To linearize the problem, two major assumptions are considered.

- The line losses are negligible, $z_{ij} l_{ij} \ll S_{ij}$ for $i \to j$
- The phase voltages are nearly balanced, i.e.,

$$\frac{V_i^a}{V_i^b} \approx \frac{V_i^b}{V_i^c} \approx \frac{V_i^c}{V_i^a} \approx e^{j2\pi/3}$$

With the first assumption, the $z_{ij}l_{ij}$ term can be neglected from the distflow equations. Thus, equations 7.1 and 7.2 takes the form as shown below

$$v_j = v_i^{\phi_{ij}} - (S_{ij}z_{ij}^H + z_{ij}S_{ij}^H) \tag{7.4}$$

$$\sum_{i:i\to j} diag(S_{ij}) + s_j = \sum_{j:j\to k} diag(S_{jk})^{\phi_j} \tag{7.5}$$

But, these form of the two equations creates a conflict. As it can be seen, 7.5 gives us a feasible value for the diagonal entries of the branch apparent power S_{ij}, but not the off-diagonal entries. In this regard, from the second assumption, the off-diagonal entries can be approximated using the following matrices,

$$\alpha = e^{-j2\pi/3}$$

$$\gamma = \begin{bmatrix} 1 & \alpha^2 & \alpha \\ \alpha & 1 & \alpha^2 \\ \alpha^2 & \alpha & 1 \end{bmatrix}$$

If we assume the phase voltages to be balanced, then by introducing a new expression Ω, such as

$$S_{ij} = \gamma^{\phi_{ij}}\Omega_{ij} \tag{7.6}$$

where, $\Omega_{ij} = diag(S_{ij})$ for the branch between buses i and j. Also, a loss term will be initialized at the beginning of the formulation and included in the power balance constraint as a parameter. Let's denote the loss term as η. And with this approximation, the LP-OPF can be formulated as,

$$\text{Minimize } f(x) \tag{7.7}$$

Subject to,

$$v_j = v_i^{\phi_{ij}} - (S_{ij} z_{ij}^H + z_{ij} S_{ij}^H) \tag{7.8}$$

$$S_{ij} = \gamma^{\phi_{ij}} \Omega_{ij} \tag{7.9}$$

$$\sum_{i:i \to j} (\Omega_{ij} - \eta_{ij}) + s_j = \sum_{j:j \to k} \Omega_{jk}^{\phi_j} \tag{7.10}$$

$$v_0 = v_{ref} \tag{7.11}$$

$$v_{min} \leq v_i^{\phi_i} \leq v_{max} \tag{7.12}$$

$$s_{min} \leq s_i^{\phi_i} \leq s_{max} \tag{7.13}$$

7.2.2 Including Discrete Control and Linearizing to MILP

Once the LP-OPF formulation is prepared, the regulator integer control is included. Let's assume the branch between bus i and j consists of a voltage regulator. Now, the primary and secondary voltage relation can be depicted as

$$v_{reg} = t_{ij}^2 * v_j \tag{7.14}$$

where v_{reg} is the primary node and v_j is the secondary node of the regulator. t_{ij} is the tap ratio of the regulator, which can be written as

$$t_{ij}^{\phi_{ij}} = t_{ij}^{min} + T_{ij} \Delta t_{ij} \tag{7.15}$$

$$\Delta t_{ij} = (t_{ij}^{max} - t_{ij}^{min}) / K_{ij} \tag{7.16}$$

here, t^{min} and t^{max} are the minimum and maximum ratios for the regulator. Now, we can write the T_{ij} in terms of a binary variable $p_{ij,n}$ as shown below:

$$t_{ij} = t_{ij}^{min} + \Delta t_{ij} \sum_{n=0}^{N_{ij}} 2^n p_{ij,n}^{\phi_{ij}} \tag{7.17}$$

$$\sum_{n=0}^{N_{ij}} 2^n p_{ij,n}^{\phi_{ij}} \leq K_{ij} \tag{7.18}$$

Here, N_{ij} is the length of a binary representation of K_{ij}. Multiplying both side of 3.24 with v_j and defining new variables $m_{ij} = t_{ij}v_j$ and $x_{ij}^{\phi_{ij}} = p_{ij,n}^{\phi_{ij}} u_j$ hereby obtained

$$m_{ij} = t_{ij}^{min} v_j + \Delta t_{ij} \sum_{n=0}^{N_{ij}} 2^n x_{ij,n}^{\phi_{ij}} \tag{7.19}$$

Now, $x_{ij}^{\phi_{ij}} = p_{ij,n}^{\phi_{ij}} u_j$ can be equivalently replaced with the help of big-M method using the following equations

$$0 \leq v_j - x_{ij,n}^{\phi_{ij}} \leq (1 - p_{ij,n}^{\phi_{ij}})M \tag{7.20}$$

$$0 \leq x_{ij,n}^{\phi_{ij}} \leq p_{ij,n}^{\phi_{ij}} M \tag{7.21}$$

Applying the similar procedure to form $v_{reg} = t_{ij}m_{ij}$ and defining a new variable $y_{ij,n}^{\phi_{ij}} = p_{ij,n}^{\phi_{ij}} m_{ij}$

$$v_{reg} = t_{ij}^{min} + \Delta t_{ij} \sum_{n=0}^{N_{ij}} 2^n y_{ij,n}^{\phi_{ij}} \tag{7.22}$$

$$0 \leq m_{ij} - y_{ij,n}^{\phi_{ij}} \leq (1 - p_{ij,n}^{\phi_{ij}})M \tag{7.23}$$

$$0 \leq y_{ij,n}^{\phi_{ij}} \leq p_{ij,n}^{\phi_{ij}} M \tag{7.24}$$

Now, combining these equations with the LP-OPF model, the MILP-OPF formulation will be completed as shown below,

$$
\begin{aligned}
&\text{Minimize } f(x) \qquad (7.25)\\
&\text{Subject to,}\\
&v_j = v_i^{\phi_{ij}} - (S_{ij} z_{ij}^H + z_{ij} S_{ij}^H)\\
&S_{ij} = \gamma^{\phi_{ij}} \Omega_{ij}\\
&\sum_{i:i\to j} (\Omega_{ij} - \eta_{ij}) + s_j = \sum_{j:j\to k} \Omega_{jk}^{\phi_j}\\
&v_0 = v_{ref}\\
&v_{min} \le v_i^{\phi_i} \le v_{max}\\
&s_{min} \le s_i^{\phi_i} \le s_{max}\\
&(7.18) - (7.24)
\end{aligned}
$$

7.2.3 BFM-SDP OPF for Unbalanced Network

The same formulation will be used to solve the convex optimal power flow for the unbalanced network, which is proposed in chapter 5. The model is stated below,

$$\text{Minimize} \sum_{j:i\sim j} (z_{ij} l_{ij}) \tag{7.26}$$

Subject to,

$$v_j = v_i^{\phi_{ij}} - (S_{ij} z_{ij}^H + z_{ij} S_{ij}^H) + z_{ij} l_{ij} z_{ij}^H$$

$$\sum_{i:i\to j} diag(S_{ij} - z_{ij} l_{ij})^{\phi_j} + s_j = \sum_{k:j\to k} diag(S_{jk})^{\phi_j}$$

$$v_1 = V_1^{ref} (V_1^{ref})^H$$

$$V_i^{min} \le diag(v_i) \le V_i^{max}$$

$$s_i^{min} \le s_i \le s_i^{max}$$

$$\begin{bmatrix} v_i^{\phi_{ij}} & S_{ij} \\ S_{ij}^H & l_{ij} \end{bmatrix} \succcurlyeq 0$$

In this BFM-SDP OPF model, the tap position is considered a parameter that will be provided from the solution of the proposed MILP-OPF.

7.2.4 Combined Two-Step Formulation

As indicated earlier, the complete discrete control is decomposed into two steps and solved iteratively until the gap in the loss term converges.

7.3 Result and Analysis

The proposed MILP and SDP optimization models have been developed in YALMIP and MATLAB, where the algorithms used appropriate solvers such as Gurobi and Mosek for individual problems. All the tests are conducted on a Dell machine with a 2.5GHz Core i5 processor and 16GB memory.

The proposed model is tested in a small network of 5 buses, a small portion of the

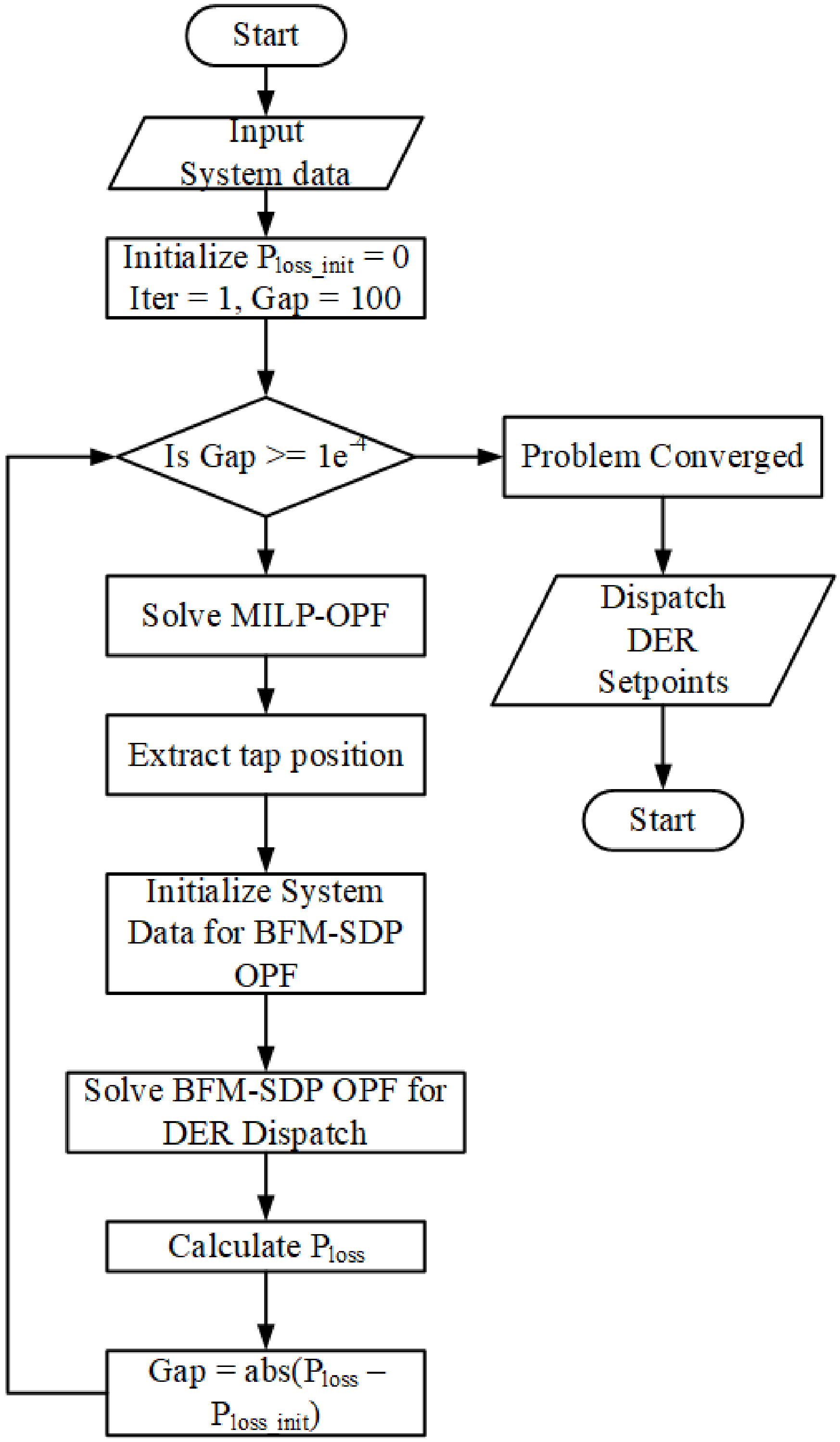

Figure 7.1: Flowchart of two staged MILP-SDP OPF framework

Algorithm 4 Combined MILP-SDP OPF

input network parameters
initialize line losses $P_{loss\_init} \leftarrow 1e^{-4}$
$iter \leftarrow 1$
while $Gap \geq 0$ **do**
  Solve the MILP-OPF using (7.25)
  Recover the tap position from solution
  Initialize the tap setting for BFM-SDP OPF
  Solve BFM-SDP OPF using (7.26)
  $Gap = abs(P_{loss\_init} - P_{loss})$
  if $Gap \geq 1e^{-4}$ **then**
    $P_{loss\_init} \leftarrow P_{loss}$
    $iter \leftarrow iter + 1$
  end if
end while

IEEE 123 bus system. It contains an OLTC in the first line after the substation node. Three loads are connected in the system, and all are considered constant PQ loads. There is a three-phase balanced load connected to bus 3, a single-phase load on bus 4, and a two-phase load connected to bus 5. Total connected load 220 KW/ 110 KVAR. The tap of the OLTC can change from {-16 to 16}. The numerical solution of the proposed method for the small 5-bus system is compared to the power flow solution for the exact tap position of the voltage regulator. Since we had no access to other MISOCP or MINLP algorithms at the point of testing, it was impossible to compare the solution of the similar problem from different approaches. In the test study, the substation voltage was considered at 1.0 p.u. The objective was to minimize the line loss. After the sub-problems converged, the tap position of the regulators found was $0, 0, -6$. Then, the system's power flow was solved using the same tap position. The total time consumed by the solver to converge in the MILP-SDP-OPF method was. First, the voltage magnitude profiles from both the OPF and power flow were compared. The Comparison is shown in Fig. 7.2. We notice a minimum mismatch in the voltages in phase C due to the mismatch in the reactive power injection in that phase. The numerical solutions containing substation active and reactive power dispatch and

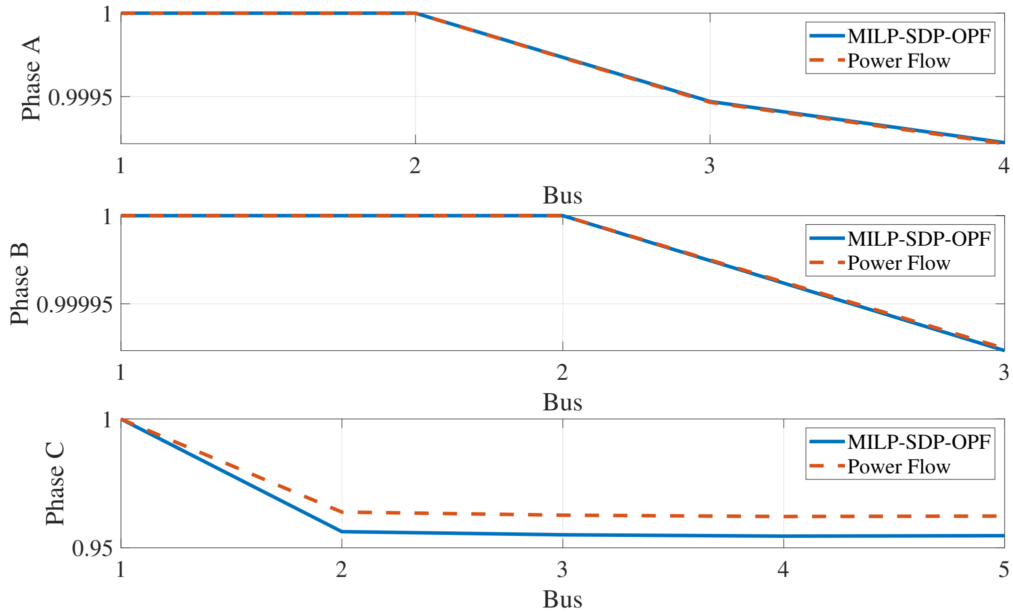

Figure 7.2: Voltage profile comparison of MILP-SDP OPF and Power flow for 5 bus networks.

the total line losses are summarized in Table 7.1. From that table also, we can see that the gap in the active and reactive power injection in phase C is marginally more than in the other two buses. Albeit, the maximum %error for all those values is less than 1%, which indicates that the solution is conclusive.

Table 7.1: Numerical Solution Comparison

		MILP-SDP OPF		Power Flow	
		Active Power (KW)	Reactive Power (KVAR)	Active Power (KW)	Reactive Power (KVAR)
Substation Power	Phase A	80.0111	40.108	80.011	40.103
	Phase B	40.005	19.997	40.005	19.994
	Phase C	100.111	50.167	100.971	50.081
Total Loss	(KW)	0.1277		0.9880	

7.4 Summary

The proposed two-step method is an initiative to solve the MISDP problem in a decomposed manner. It is tested on a small network to validate the accuracy of the solution. To scale up the network, the MILP approach can be solved for IEEE 123 bus network. The part left is formulating a generic approach to synchronize the branch losses updated from the BFM-SDP-OPF solution. Once the generic incorporation is done, then the scalability of the approach can be tested. Also, if any other MINLP or MISOCP solution becomes available, then the comparison of the proposed method can be tested for its performance with different approaches.

CHAPTER 8: CONCLUSIONS AND FUTURE WORK

In this dissertation, we have proposed Optimal Power flow, and Unit Commitment approaches for transmission and power distribution networks with and without Distributed Energy Resources (DER) based on Semi Definite Programming (SDP) variant of convex optimization. The OPF formulation also extended to the unbalanced multi-phase networks, including legacy devices such as voltage regulators, transformers, capacitor banks, and the mutual coupling of the branches. Finally, we have presented distributed and decentralized approaches for solving OPF in partitioned networks.

8.1 Conclusions

First, an alternative bus injection model-based SDP relaxed OPF formulation for the distribution system is proposed, which reduces the computational complexity by using the matrix entries for constraint formulation rather than the whole matrix. An SDP relaxed OPF formulation is also presented using a branch flow model, including integer control. It has been observed that

- This alternative BIM-SDP OPF formulation is exact and provides the global optimal solution for the system.
- This formulation is scalable and can be implemented on larger power distribution systems.
- The BFM-SDP OPF provides a solution with a minimum optimality gap and is scalable for large networks. The integer control can be combined with the OPF formulation, and solutions are the global optimal solution after a conclusive comparison with the original non-linear OPF solution.

Second, a two-staged formulation of the combined UC-OPF problem is proposed. The unit commitment problem is solved in a MILP manner, and the OPF is solved in a BIM model-based SDP relaxed approach. Both the problem is solved in iteration until convergence is achieved. The other observations are

- The unified Mixed Integer Semi Definite Program(MISDP) formulation is exact and provides a global solution for larger systems.
- It includes the power loss term in the power balance constraint, which was neglected in the original UC problem.
- It does not leverage the rounding operation of the integer variable. Thus the solution is more accurate.
- The proposed branch and bound approach can provide the most economic solution for small networks but the performance starts to deteriorate as the system size increases.

Next, a branch flow model-based SDP relaxed OPF is formulated for multi-phase unbalanced radial distribution systems. The OPF problem formulation for multi-phase networks is always complex. Following are the aspects observed in the formulation

- This formulation includes voltage regulator modeling of the network. That's why the formulation is more exact.
- The formulation considers the mutual coupling of the branch impedance matrix, which makes the solution more tight and accurate.
- This formulation is scalable and tested for large distribution networks which are radial and unbalanced in topology.
- The proposed method can be adapted for receding horizon control which can include inter-temporal constraints.

Later, a distributed formulation of OPF is proposed. It is formulated based on the alternating direction method of multipliers(ADMM), and the underlying OPF formulation is based on BFM-SDP. The distributed OPF is proven effective for large power networks with higher DG penetration, and the solutions of the distributed approach are found to be conclusive when compared with the solution to the centralized OPF problem. The key observations are

- The distributed formulation is exact and tight and provides an accurate solution compared with the centralized approach.
- This formulation reduces the computational stress of solvers for the larger networks.
- ADMM ensures the convergence of the iterative process, and BFM-SDP guarantees the global optimal solution of the problem.
- This approach is scalable and implemented on large distribution networks.
- Next, a decentralized approach is proposed with the auto-tuning of penalty parameters, which improves the convergence speed and solution accuracy.
- The purposed methods can be implemented for real-time simulation.
- Later, the distributed and decentralized approaches are formulated for the unbalanced networks.

Finally, the integer control of the legacy devices is included in the multi-phase BFM-SDP OPF by adopting a two-stage approach. The main outcomes of the formulation are,

- The two-staged approach is formulated by combining a MILP and BFM-SDP OPF approaches.

- Both the MILP and BFM-SDP methods are scalable for larger networks, thus validating the scalability of the proposed approach.

8.2 Future Works

Future work that needs to be completed is as follows.

- Leverage the sparsity property of the large PSD matrix for the formulation, reducing the consumed memory and, consequently, the solver time to converge.
- Formulate a novel branch-and-bound methodology for the combined UC-OPF problem, which will not require rounding the integer variable and ensuring the global optimal solution.
- Formulate an automated partitioning of the distribution networks based on the geographical position or location of the voltage regulators.

LIST OF PUBLICATIONS

[C1]. B. D. Biswas and S. Kamalasadan, "Semidefinite Program Based Optimal Power Flow Formulation With Voltage Regulators in Multiphase Distribution Networks", 2022 IEEE PES General Meeting.

[C2]. Biswas, B. D., S., Kamalasadan. (2021, October). Distributed Convex Optimal Power Flow Model Based on Alternating Direction Method of Multipliers for Power Distribution System. In 2021 IEEE IAS Annual Meeting (IAS AM) (pp. 1-6). IEEE.

[C3]. Biswas, B. D., Moghadasi, S., Kamalasadan, S., Paudyal, S. (2019, October). Integrated transmission systems convex optimal power flow considering security constraints. In 2019 North American Power Symposium (NAPS) (pp. 1-6). IEEE.

[C4]. Biswas, B. D., Kamalasadan, S., Paudyal, S. (2021, February). A Two-Stage Combined UC-OPF Model Using Mixed Integer and Semi-Definite Programming. In 2021 IEEE Power Energy Society Innovative Smart Grid Technologies Conference (ISGT) (pp. 1-5). IEEE.

[C5]. B. D. Biswas and S. Kamalasadan, "Alternative SDP Relaxed Optimal Power Flow Formulation for Radial Distribution Networks," 2022 IEEE International Conference on Power Electronics, Smart Grid, and Renewable Energy (PESGRE), 2022, pp. 1-6, doi: 10.1109/PESGRE52268.2022.9715879.

[J1]. Biswas, B. D., Hasan, Md., S., Kamalasadan, S. (2022). Decentralized Distributed Convex Optimal Power Flow Model For Power Distribution System Based on Alternating Direction Method of Multipliers. IEEE Transactions on Industry Applications (Under Review) .

[J2] Jha, R.R., Inaolaji, A., Biswas, B. D., Suresh, A., Dubey, A., Paudyal, S., Kamalasadan, S. (2022), Distribution Grid Optimal Power Flow (D-OPF) Modeling, Analysis, and Benchmarking. IEEE Transactions on Power Systems (Accepted).

[J3]. Hossain, S. J., Biswas, B. D., Bhattarai, R., Ahmed, M., Abdelrazek, S., Kamalasadan, S. (2019). Operational value-based energy storage management for photovoltaic (PV) integrated active power distribution systems. IEEE Transactions on Industry Applications, 55(5), 5320-5330.

[J4]. Thakallapelli, A., Nair, A. R., Biswas, B. D., Kamalasadan, S. (2020). Frequency regulation and control of grid-connected wind farms based on online reduced-order modeling and adaptive control. IEEE Transactions on Industry Applications, 56(2), 1980-1989.

REFERENCES

[1] R. Faranda and S. Leva, “Energy comparison of mppt techniques for pv systems,” *J. Electromagn. Anal. Appl.*, vol. 3, 01 2008.

[2] B. Kocuk, S. S. Dey, and X. A. Sun, “Strong socp relaxations for the optimal power flow problem,” *Operations Research*, vol. 64, no. 6, pp. 1177–1196, 2016.

[3] J. Carpentier, “Contribution a lâetude du dispatching economique,” *Bulletin de la Societe Francaise des Electriciens*, vol. 3, no. 1, pp. 431–447, 1962.

[4] M. Huneault and F. D. Galiana, “A survey of the optimal power flow literature,” *IEEE Transactions on Power Systems*, vol. 6, pp. 762–770, May 1991.

[5] J. A. Momoh, R. Adapa, and M. E. El-Hawary, “A review of selected optimal power flow literature to 1993. i. nonlinear and quadratic programming approaches,” *IEEE Transactions on Power Systems*, vol. 14, pp. 96–104, Feb 1999.

[6] J. A. Momoh, M. E. El-Hawary, and R. Adapa, “A review of selected optimal power flow literature to 1993. ii. newton, linear programming and interior point methods,” *IEEE Transactions on Power Systems*, vol. 14, pp. 105–111, Feb 1999.

[7] K. Pandya and S. Joshi, “A survey of optimal power flow methods,” *Journal of Theoretical and Applied Information Technology*, vol. 4, p. 450â458, 01 2008.

[8] S. Frank, I. SteponaviÄÄ, and S. Rebennack, “Optimal power flow: a bibliographic survey i,” *Energy Systems*, vol. 3, 09 2012.

[9] S. Frank, I. SteponaviÄÄ, and S. Rebennack, “Optimal power flow: a bibliographic survey ii,” *Energy Systems*, vol. 3, 09 2012.

[10] A. Mary, B. Cain, and R. OâNeill, “History of optimal power flow and formulations,” *Fed. Energy Regul. Comm.*, vol. 1, pp. 1–36, 01 2012.

[11] R. P. OâNeill, A. Castillo, and M. B. Cain, “The iv formulation and linear approximations of the ac optimal power flow problem,” *Published online at http://www. ferc. gov/industries/electric/indus-act/market-planning/opf-papers/acopf-2-iv-linearization. pdf*, 2012.

[12] A. Castillo and R. P. OâNeill, “Survey of approaches to solving the acopf (opf paper 4),” *US Federal Energy Regulatory Commission, Tech. Rep*, 2013.

[13] A. Castillo and R. P. OâNeill, “Computational performance of solution techniques applied to the acopf (opf paper 5),” *US Federal Energy Regulatory Commission, Tech. Rep*, 2013.

[14] B. Stott and O. Alsac, “Fast decoupled load flow,” *IEEE Transactions on Power Apparatus and Systems*, vol. PAS-93, pp. 859–869, May 1974.

[15] O. Alsac, J. Bright, M. Prais, and B. Stott, “Further developments in lp-based optimal power flow,” *IEEE Transactions on Power Systems*, vol. 5, pp. 697–711, Aug 1990.

[16] K. Purchala, L. Meeus, D. Dommelen, and R. Belmans, “Usefulness of dc power flow for active power flow analysis,” vol. 1, pp. 454 – 459 Vol. 1, 07 2005.

[17] B. Stott, J. Jardim, and O. Alsac, “Dc power flow revisited,” *Power Systems, IEEE Transactions on*, vol. 24, pp. 1290 – 1300, 09 2009.

[18] C. Coffrin and P. Van Hentenryck, “A linear-programming approximation of ac power flows,” *INFORMS Journal on Computing*, vol. 26, 06 2012.

[19] R. A. Jabr, “Radial distribution load flow using conic programming,” *IEEE Transactions on Power Systems*, vol. 21, pp. 1458–1459, Aug 2006.

[20] X. Bai, H. Weihua, K. Fujisawa, and Y. Wang, “Semidefinite programming for optimal power flow problems,” *International Journal of Electrical Power Energy Systems*, vol. 30, pp. 383–392, 07 2008.

[21] M. Farivar and S. H. Low, “Branch flow model: Relaxations and convexificationâpart i,” *IEEE Transactions on Power Systems*, vol. 28, pp. 2554–2564, Aug 2013.

[22] M. E. Baran and F. F. Wu, “Optimal capacitor placement on radial distribution systems,” *IEEE Transactions on Power Delivery*, vol. 4, pp. 725–734, Jan 1989.

[23] M. Baran and F. F. Wu, “Optimal sizing of capacitors placed on a radial distribution system,” *IEEE Transactions on Power Delivery*, vol. 4, pp. 735–743, Jan 1989.

[24] J. Lavaei and S. H. Low, “Zero duality gap in optimal power flow problem,” *IEEE Transactions on Power Systems*, vol. 27, pp. 92–107, Feb 2012.

[25] X. Bai and H. Weihua, “A semidefinite programming method with graph partitioning technique for optimal power flow problems,” *International Journal of Electrical Power Energy Systems - INT J ELEC POWER ENERG SYST*, vol. 33, pp. 1309–1314, 09 2011.

[26] R. A. Jabr, “Exploiting sparsity in sdp relaxations of the opf problem,” *IEEE Transactions on Power Systems*, vol. 27, pp. 1138–1139, May 2012.

[27] D. Molzahn, J. Holzer, B. Lesieutre, and C. Demarco, “Implementation of a large-scale optimal power flow solver based on semidefinite programming,” *Power Systems, IEEE Transactions on*, vol. 28, pp. 3987–3998, 11 2013.

[28] S. Bose, S. Low, T. Teeraratkul, and B. Hassibi, "Equivalent relaxations of optimal power flow," *IEEE Transactions on Automatic Control*, vol. 60, 01 2014.

[29] J. Carpentier, "Optimal power flows: uses, methods and developments," *IFAC Proceedings Volumes*, vol. 18, no. 7, pp. 11–21, 1985.

[30] W. Rosehart, C. Canizares, and V. Quintana, "Costs of voltage security in electricity markets," in *2000 Power Engineering Society Summer Meeting (Cat. No.00CH37134)*, vol. 4, pp. 2115–2120 vol. 4, July 2000.

[31] M. B. Maskar, A. R. Thorat, and I. Korachgaon, "A review on optimal power flow problem and solution methodologies," in *2017 International Conference on Data Management, Analytics and Innovation (ICDMAI)*, pp. 64–70, Feb 2017.

[32] H. W. Dommel and W. F. Tinney, "Optimal power flow solutions," *IEEE Transactions on power apparatus and systems*, no. 10, pp. 1866–1876, 1968.

[33] C. M. Shen and M. A. Laughton, "Determination of optimum power-system operating conditions under constraints," *Proceedings of the Institution of Electrical Engineers*, vol. 116, pp. 225–239, February 1969.

[34] O. Alsac and B. Stott, "Optimal load flow with steady-state security," *IEEE transactions on power apparatus and systems*, no. 3, pp. 745–751, 1974.

[35] A. M. H. Rashed and D. H. Kelly, "Optimal load flow solution using lagrangian multipliers and the hessian matrix," *IEEE Transactions on Power Apparatus and Systems*, vol. PAS-93, pp. 1292–1297, Sep. 1974.

[36] H. Happ, "Optimal power dispatch," *IEEE Transactions on Power Apparatus and Systems*, no. 3, pp. 820–830, 1974.

[37] D. Wells, "Method for economic secure loading of a power system," in *Proceedings of the Institution of Electrical Engineers*, vol. 115, pp. 1190–1194, IET, 1968.

[38] R. Mota-Palomino and V. Quintana, "A penalty function-linear programming method for solving power system constrained economic operation problems," *IEEE transactions on power apparatus and systems*, no. 6, pp. 1414–1422, 1984.

[39] E. Lobato, L. Rouco, M. Navarrete, R. Casanova, and G. Lopez, "An lp-based optimal power flow for transmission losses and generator reactive margins minimization," in *2001 IEEE Porto Power Tech Proceedings (Cat. No. 01EX502)*, vol. 3, pp. 5–pp, IEEE, 2001.

[40] G. F. Reid and L. Hasdorff, "Economic dispatch using quadratic programming," *IEEE Transactions on Power Apparatus and Systems*, no. 6, pp. 2015–2023, 1973.

[41] S. N. Talukdar and T. C. Giras, "A fast and robust variable metric method for optimum power flows," *IEEE Transactions on Power Apparatus and Systems*, no. 2, pp. 415–420, 1982.

[42] A. Berizzi, M. Delfanti, P. Marannino, M. S. Pasquadibisceglie, and A. Silvestri, "Enhanced security-constrained opf with facts devices," *IEEE Transactions on Power Systems*, vol. 20, pp. 1597–1605, Aug 2005.

[43] J. A. Momoh, S. Guo, E. Ogbuobiri, and R. Adapa, "The quadratic interior point method solving power system optimization problems," *IEEE Transactions on Power Systems*, vol. 9, no. 3, pp. 1327–1336, 1994.

[44] Ding Xiaoying, Wang Xifan, Song Yonghua, and Geng Jian, "The interior point branch and cut method for optimal power flow," in *Proceedings. International Conference on Power System Technology*, vol. 1, pp. 651–655 vol.1, Oct 2002.

[45] W. Yan, J. Yu, D. Yu, and K. Bhattarai, "A new optimal reactive power flow model in rectangular form and its solution by predictor corrector primal dual interior point method," *IEEE transactions on power systems*, vol. 21, no. 1, pp. 61–67, 2006.

[46] A. Bakirtzis, V. Petridis, and S. Kazarlis, "Genetic algorithm solution to the economic dispatch problem," *IEE proceedings-generation, transmission and distribution*, vol. 141, no. 4, pp. 377–382, 1994.

[47] M. U. Aslam, M. U. Cheema, M. Samran, and M. B. Cheema, "Optimal power flow based upon genetic algorithm deploying optimum mutation and elitism," in *2014 The 1st International Conference on Information Technology, Computer, and Electrical Engineering*, pp. 334–338, IEEE, 2014.

[48] H. Yoshida, K. Kawata, and Y. Fukuyama, "Member," *IEEE, Shinichi Takayama, and Yosuke Nakanishi, Member, IEEE A âParticle Swarm Optimization for Reactive Power and Voltage Control Considering Voltage Security Assessmentâ IEEE Transactions On Power Systems*, vol. 15, no. 4, 2000.

[49] L. Lai, T. Nieh, D. Vujatovic, Y. Ma, Y. Lu, Y. Wang, and H. Braun, "Particle swarm optimization for economic dispatch of units with non-smooth input-output characteristic functions," in *Proceedings of the 13th International Conference on, Intelligent Systems Application to Power Systems*, pp. 5–pp, IEEE, 2005.

[50] B. Yang, Y. Chen, Z. Zhao, and Q. Han, "Solving optimal power flow problems with improved particle swarm optimization," in *2006 6th World Congress on Intelligent Control and Automation*, vol. 2, pp. 7457–7461, IEEE, 2006.

[51] P. E. Onate and J. M. Ramirez, "Optimal power flow solution with security constraints by a modified pso," in *2007 IEEE Power Engineering Society General Meeting*, pp. 1–6, IEEE, 2007.

[52] G. Chen and J. Yang, “A new particle swarm optimization solution to optimal reactive power flow problems,” in *2009 Asia-Pacific Power and Energy Engineering Conference*, pp. 1–4, IEEE, 2009.

[53] H. Leung and D. D.-C. Lu, “Particle swarm optimization for opf with consideration of facts devices,” in *IECON 2011-37th Annual Conference of the IEEE Industrial Electronics Society*, pp. 2406–2410, IEEE, 2011.

[54] D. K. Molzahn and I. A. Hiskens, *A Survey of Relaxations and Approximations of the Power Flow Equations.* now, 2019.

[55] J. Nie, K. Ranestad, and B. Sturmfels, “The algebraic degree of semidefinite programming,” *Mathematical Programming*, vol. 122, no. 2, pp. 379–405, 2010.

[56] P. A. Parrilo and S. Lall, “Semidefinite programming relaxations and algebraic optimization in control,” *European Journal of Control*, vol. 9, no. 2-3, pp. 307–321, 2003.

[57] R. Madani, S. Sojoudi, and J. Lavaei, “Convex relaxation for optimal power flow problem: Mesh networks,” *IEEE Transactions on Power Systems*, vol. 30, pp. 199–211, Jan 2015.

[58] M. Fukuda, M. Kojima, K. Murota, and K. Nakata, “Exploiting sparsity in semidefinite programming via matrix completion i: General framework,” *SIAM Journal on Optimization*, vol. 11, no. 3, pp. 647–674, 2001.

[59] R. A. Jabr, “Exploiting sparsity in sdp relaxations of the opf problem,” *IEEE Transactions on Power Systems*, vol. 27, no. 2, pp. 1138–1139, 2011.

[60] B. C. Lesieutre, D. K. Molzahn, A. R. Borden, and C. L. DeMarco, “Examining the limits of the application of semidefinite programming to power flow problems,” in *2011 49th annual Allerton conference on communication, control, and computing (Allerton)*, pp. 1492–1499, IEEE, 2011.

[61] L. Gan and S. H. Low, “Convex relaxations and linear approximation for optimal power flow in multiphase radial networks,” in *2014 Power Systems Computation Conference*, pp. 1–9, IEEE, 2014.

[62] C. Coffrin, H. L. Hijazi, and P. Van Hentenryck, “The qc relaxation: A theoretical and computational study on optimal power flow,” *IEEE Transactions on Power Systems*, vol. 31, no. 4, pp. 3008–3018, 2015.

[63] J. B. Lasserre, “Global optimization with polynomials and the problem of moments,” *SIAM Journal on optimization*, vol. 11, no. 3, pp. 796–817, 2001.

[64] J.-B. Lasserre, *Moments, positive polynomials and their applications*, vol. 1. World Scientific, 2010.

[65] R. A. Jabr, "Radial distribution load flow using conic programming," *IEEE transactions on power systems*, vol. 21, no. 3, pp. 1458–1459, 2006.

[66] H. Hijazi, C. Coffrin, and P. Van Hentenryck, "Convex quadratic relaxations for mixed-integer nonlinear programs in power systems," *Mathematical Programming Computation*, vol. 9, no. 3, pp. 321–367, 2017.

[67] D. Bienstock and G. Munoz, "On linear relaxations of opf problems," *arXiv preprint arXiv:1411.1120*, 2014.

[68] D. Bienstock and G. Muñoz, "Approximate method for ac transmission switching based on a simple relaxation for acopf problems," in *2015 IEEE Power & Energy Society General Meeting*, pp. 1–5, IEEE, 2015.

[69] C. Coffrin, H. Hijazi, and P. Van Hentenryck, "Network flow and copper plate relaxations for ac transmission systems," in *2016 Power Systems Computation Conference (PSCC)*, pp. 1–8, IEEE, 2016.

[70] X. Bai and H. Wei, "A semidefinite programming method with graph partitioning technique for optimal power flow problems," *International Journal of Electrical Power & Energy Systems*, vol. 33, no. 7, pp. 1309–1314, 2011.

[71] J. Lavaei and S. H. Low, "Zero duality gap in optimal power flow problem," *IEEE Transactions on Power Systems*, vol. 27, no. 1, pp. 92–107, 2011.

[72] B. Zhang and D. Tse, "Geometry of feasible injection region of power networks," in *2011 49th Annual Allerton Conference on Communication, Control, and Computing (Allerton)*, pp. 1508–1515, IEEE, 2011.

[73] D. K. Molzahn, J. T. Holzer, B. C. Lesieutre, and C. L. DeMarco, "Implementation of a large-scale optimal power flow solver based on semidefinite programming," *IEEE Transactions on Power Systems*, vol. 28, no. 4, pp. 3987–3998, 2013.

[74] S. Bose, S. H. Low, T. Teeraratkul, and B. Hassibi, "Equivalent relaxations of optimal power flow," *IEEE Transactions on Automatic Control*, vol. 60, no. 3, pp. 729–742, 2014.

[75] F. Capitanescu, I. Bilibin, and E. R. Ramos, "A comprehensive centralized approach for voltage constraints management in active distribution grid," *IEEE Transactions on Power Systems*, vol. 29, no. 2, pp. 933–942, 2013.

[76] S. Paudyal, C. A. Canizares, and K. Bhattacharya, "Optimal operation of distribution feeders in smart grids," *IEEE Transactions on Industrial Electronics*, vol. 58, no. 10, pp. 4495–4503, 2011.

[77] F. Capitanescu and L. Wehenkel, "Sensitivity-based approaches for handling discrete variables in optimal power flow computations," *IEEE Transactions on Power Systems*, vol. 25, no. 4, pp. 1780–1789, 2010.

[78] A. Mohapatra, P. R. Bijwe, and B. K. Panigrahi, "An efficient hybrid approach for volt/var control in distribution systems," *IEEE transactions on power delivery*, vol. 29, no. 4, pp. 1780–1788, 2014.

[79] D. K. Molzahn and I. A. Hiskens, "Convex relaxations of optimal power flow problems: An illustrative example," *IEEE Transactions on Circuits and Systems I: Regular Papers*, vol. 63, no. 5, pp. 650–660, 2016.

[80] E. Dall'Anese, H. Zhu, and G. B. Giannakis, "Distributed optimal power flow for smart microgrids," *IEEE Transactions on Smart Grid*, vol. 4, no. 3, pp. 1464–1475, 2013.

[81] S. H. Low, "Convex relaxation of optimal power flowâpart ii: Exactness," *IEEE Transactions on Control of Network Systems*, vol. 1, no. 2, pp. 177–189, 2014.

[82] W. Wang and N. Yu, "Chordal conversion based convex iteration algorithm for three-phase optimal power flow problems," *IEEE Transactions on Power Systems*, vol. 33, no. 2, pp. 1603–1613, 2017.

[83] L. Gan, N. Li, U. Topcu, and S. H. Low, "Exact convex relaxation of optimal power flow in radial networks," *IEEE Transactions on Automatic Control*, vol. 60, no. 1, pp. 72–87, 2014.

[84] M. Baran and F. F. Wu, "Optimal sizing of capacitors placed on a radial distribution system," *IEEE Transactions on power Delivery*, vol. 4, no. 1, pp. 735–743, 1989.

[85] L. L. Garver, "Power generation scheduling by integer programming-development of theory," *Transactions of the American Institute of Electrical Engineers. Part III: Power Apparatus and Systems*, vol. 81, no. 3, pp. 730–734, 1962.

[86] S. Atakan, G. Lulli, and S. Sen, "An improved mip formulation for the unit commitment problem," *Optimization Online, 2015*, 2015.

[87] J. Ostrowski, M. F. Anjos, and A. Vannelli, "Tight mixed integer linear programming formulations for the unit commitment problem," *IEEE Transactions on Power Systems*, vol. 27, no. 1, pp. 39–46, 2011.

[88] R. Jabr, "Tight polyhedral approximation for mixed-integer linear programming unit commitment formulations," *IET Generation, Transmission & Distribution*, vol. 6, no. 11, pp. 1104–1111, 2012.

[89] J. M. Morales, A. J. Conejo, and J. Pérez-Ruiz, "Economic valuation of reserves in power systems with high penetration of wind power," *IEEE Transactions on Power Systems*, vol. 24, no. 2, pp. 900–910, 2009.

[90] M. J. Feizollahi, M. Costley, S. Ahmed, and S. Grijalva, "Large-scale decentralized unit commitment," *International Journal of Electrical Power & Energy Systems*, vol. 73, pp. 97–106, 2015.

[91] J. D. Guy, "Security constrained unit commitment," *IEEE Transactions on Power apparatus and Systems*, no. 3, pp. 1385–1390, 1971.

[92] W.-C. Chu, B.-K. Chen, and C.-K. Fu, "Scheduling of direct load control to minimize load reduction for a utility suffering from generation shortage," *IEEE Transactions on Power Systems*, vol. 8, no. 4, pp. 1525–1530, 1993.

[93] K.-Y. Huang, H.-T. Yang, and C.-L. Huang, "A new thermal unit commitment approach using constraint logic programming," in *Proceedings of the 20th International Conference on Power Industry Computer Applications*, pp. 176–185, IEEE, 1997.

[94] F. Zhuang and F. D. Galiana, "Towards a more rigorous and practical unit commitment by lagrangian relaxation," *IEEE Transactions on Power Systems*, vol. 3, no. 2, pp. 763–773, 1988.

[95] A. Verma, *Power grid security analysis: An optimization approach.* Columbia University, 2010.

[96] K. Lehmann, A. Grastien, and P. Van Hentenryck, "Ac-feasibility on tree networks is np-hard," *IEEE Transactions on Power Systems*, vol. 31, no. 1, pp. 798–801, 2015.

[97] M. R. Bussieck, A. Pruessner, *et al.*, "Mixed-integer nonlinear programming," *SIAG/OPT Newsletter: Views & News*, vol. 14, no. 1, pp. 19–22, 2003.

[98] C. Murillo-Sanchez and R. Thomas, "Thermal unit commitment with nonlinear power flow constraints," in *IEEE Power Engineering Society. 1999 Winter Meeting (Cat. No. 99CH36233)*, vol. 1, pp. 484–489, IEEE, 1999.

[99] Y. Fu, M. Shahidehpour, and Z. Li, "Security-constrained unit commitment with ac constraints," *IEEE transactions on power systems*, vol. 20, no. 2, pp. 1001–1013, 2005.

[100] H. Ma and S. Shahidehpour, "Unit commitment with transmission security and voltage constraints," *IEEE transactions on power systems*, vol. 14, no. 2, pp. 757–764, 1999.

[101] A. Nasri, S. J. Kazempour, A. J. Conejo, and M. Ghandhari, "Network-constrained ac unit commitment under uncertainty: A bendersâ decomposition approach," *IEEE transactions on power systems*, vol. 31, no. 1, pp. 412–422, 2015.

[102] B. D. Biswas, S. Moghadasi, S. Kamalasadan, and S. Paudyal, "Integrated transmission systems convex optimal power flow considering security constraints," in *2019 North American Power Symposium (NAPS)*, pp. 1–6, 2019.

[103] D. Rajan, S. Takriti, *et al.*, "Minimum up/down polytopes of the unit commitment problem with start-up costs," *IBM Res. Rep*, vol. 23628, pp. 1–14, 2005.

[104] F. Magnago, J. Alemany, and J. Lin, "Impact of demand response resources on unit commitment and dispatch in a day-ahead electricity market," *International Journal of Electrical Power & Energy Systems*, vol. 68, pp. 142–149, 2015.

[105] X. Bai, H. Wei, K. Fujisawa, and Y. Wang, "Semidefinite programming for optimal power flow problems," *International Journal of Electrical Power & Energy Systems*, vol. 30, no. 6-7, pp. 383–392, 2008.

[106] S. H. Low, "Convex relaxation of optimal power flowâpart ii: Exactness," *IEEE Transactions on Control of Network Systems*, vol. 1, no. 2, pp. 177–189, 2014.

[107] C. Zhao, E. Dall-Anese, and S. H. Low, "Optimal power flow in multiphase radial networks with delta connections," tech. rep., National Renewable Energy Lab.(NREL), Golden, CO (United States), 2017.

[108] S. Moghadasi and S. Kamalasadan, "An architecture for voltage stability constrained optimal power flow using convex semi-definite programming," in *2015 North American Power Symposium (NAPS)*, pp. 1–6, 2015.

[109] M. Farivar, C. R. Clarke, S. H. Low, and K. M. Chandy, "Inverter var control for distribution systems with renewables," in *2011 IEEE international conference on smart grid communications (SmartGridComm)*, pp. 457–462, IEEE, 2011.

[110] M. Farivar and S. H. Low, "Branch flow model: Relaxations and convexificationâpart i," *IEEE Transactions on Power Systems*, vol. 28, no. 3, pp. 2554–2564, 2013.

[111] M. Khanabadi and S. Kamalasadan, "Day ahead scheduling of distribution system with distributed energy resources considering demand response and energy storage," in *2013 North American Power Symposium (NAPS)*, pp. 1–6, IEEE, 2013.

[112] B. H. Kim and R. Baldick, "Coarse-grained distributed optimal power flow," *IEEE Transactions on Power Systems*, vol. 12, no. 2, pp. 932–939, 1997.

[113] R. Baldick, B. H. Kim, C. Chase, and Y. Luo, "A fast distributed implementation of optimal power flow," *IEEE Transactions on Power Systems*, vol. 14, no. 3, pp. 858–864, 1999.

[114] S. Boyd, N. Parikh, and E. Chu, *Distributed optimization and statistical learning via the alternating direction method of multipliers*. Now Publishers Inc, 2011.

[115] R. Sadnan and A. Dubey, "Distributed optimization using reduced network equivalents for radial power distribution systems," *IEEE Transactions on Power Systems*, 2021.